creative commons

COMMONS DEED

저작자표시-비영리-변경금지 2.0 대한민국

이용자는 아래의 조건을 따르는 경우에 한하여 자유롭게

- 이 저작물을 복제, 배포, 전송, 전시, 공연 및 방송할 수 있습니다.

다음과 같은 조건을 따라야 합니다:

저작자표시. 귀하는 원저작자를 표시하여야 합니다.

비영리. 귀하는 이 저작물을 영리 목적으로 이용할 수 없습니다.

변경금지. 귀하는 이 저작물을 개작, 변형 또는 가공할 수 없습니다.

- 귀하는, 이 저작물의 재이용이나 배포의 경우, 이 저작물에 적용된 이용허락조건을 명확하게 나타내어야 합니다.
- 저작권자로부터 별도의 허가를 받으면 이러한 조건들은 적용되지 않습니다.

저작권법에 따른 이용자의 권리는 위의 내용에 의하여 영향을 받지 않습니다.

이것은 이용허락규약(Legal Code)을 이해하기 쉽게 요약한 것입니다.

Disclaimer

dCollection

공학석사 학위논문

파랑 중 원통형 세장체 운동에 대한 이론 및 실험적 연구

Theoretical and Experimental studies on Behavior of Slender Cylinder on Both Waves and Currents

지도교수 조 효 제

2014년 2월

한국해양대학교 대학원

조선해양시스템공학과

Maige Mwigulu Masanja

본 논문을 Maige Mwigulu Masanja의
공학석사 학위논문으로 인준함

위원장 손 경 호 (인)

위 원 이 승 재 (인)

위 원 조 효 제 (인)

2014년 2월

한국해양대학교 대학원

dCollection

CONTENTS

Collection

Collection

Collection

Collection

List of Tables

Collection

Collection

List of Figures

Collection

Collection

Collection

KOREA MARITIME UNIVERSITY 1945 한국해양대학교

Collection

Collection

Collection

List of Photos

Collection

파랑 중 원통형 세장체의 운동에 관한 이론 및 실험적 연구

Maige Mwigulu Masanja

Department of MARINE SYSTEM

Graduate School of Korea Maritime University

Abstract

원통형 세장체 구조물은 현존하는 수많은 해양구조물을 이루는 매우 중요한 요소 중 하나로 라이져 (risers), 케이블 (cables), 송전선 (umbilical's) 및 전력공급선 (wires)과 같이 다양한 해양시스템에서 각각 중요한 용도로 널리 분포되어있다. 파랑과 조류가 가지는 유체의 힘이 진동과 복원력을 발생시키며 이들 세장체 구조물에게 직접적인 영향을 준다. 이 때 구조물이 받는 힘은 유체의 속성과 유동의 상태 그리고 세장체의 기하하적 형태와 규격에 의해 정해진다. 지속적인 유동이 정지 상태에 이르러도 유체의 운동이 세장체 구조물을 움직이며 계속적으로 복원력의 영향을 받게 된다. 유체 진동과 복원력은 복잡한 비선형적 유체현상으로

Collection

심해역 환경의 세장체 구조물 설계에 있어 여러 가지의 도전과제를 야기하며 플랫폼과 유정을 잇는 극히 긴 라이저에 (Riser) 기인하는 몇 가지 문제점을 그 예로 들 수 있다. 본 논문에서는 수심이 깊어질수록 세장체 구조물은 더욱 가늘어지고 유연해짐에 따라 세장체 구조물이 가지는 두 가지 문제점에 관한 연구를 수록하였으며 1) 세장체 구조물의 운동과 해양의 복잡한 유체의 흐름 간의 상호작용 및 2) 유체의 흐름에 놓인 원통형 세장체 구조물 주위에서 발생하는 변동와류로 인한 진동에 (VIV, Vortex Induced Vibration) 관한 연구를 논하고자 한다. VIV를 통하여 레이놀즈수의 범위 내에서 발생하는 유체와 세장체 구조물의 진동을 관찰할 수 있으며 유체가 세장체 구조물을 통과할 때 생기는 주기적인 와류는 양력에 인한 진동을 유발한다. 따라서 유체와 세장체 구조물간의 공진을 피하기 위해 유체의 복원력과 세장체 구조물이 가지는 고유주기를 달리 해야 한다. 본 논문에서는 복잡한 유체의 흐름으로 인한 원통형 세장체 구조물의 운동을 이론과 2차원 조파수조를 이용한 모형실험을 통해 기술하였다.

KEY WORDS: VIV (Vortex Induced Vibration) 와유기진동; Reynolds number 레이놀즈수

KOREA MARITIME UNIVERSITY 1945 한국해양대학교
dCollection

Nomenclatures

Hs	: Significant Wave Height.
Ts	: Significant Wave Period.
d	: Water depth.
Tp	: Peak Period.
Tz	: Zero Crossing Period.
S	: Wave Steepness.
H / WH	: Wave Height.
g	: Acceleration due to gravity.
λ	: Wavelength.
μ	: Wave shallowness.
Φ	: Velocity potential.
ω	: Circular frequency.
k	: Wave number.
z	: Depth below SWL.
η	: Surface profile.
V	: Wave celerity/current velocity.
u	: Horizontal velocity of water particle/flow velocity.
w	: Vertical velocity of water particle.

Collection

a_x	: Horizontal acceleration of water particle.
a_y	: Vertical velocity of water particle.
Re	: Reynolds number.
D	: Diameter of a cylinder.
υ	: Kinematic Viscosity.
f_s	: Vortex shedding frequency.
S_t/S	: Strouhal number.
ρ	: Density of water.
C_M	: Inertia coefficient.
C_D	: Drag coefficient.
$\dot{U}$	: Water particle acceleration.
U_b	: Velocity of a body.
$\dot{U}_b$	: Acceleration of a body.
X	: Oscillating cylinder displacement.
$\dot{X}$	: Oscillating cylinder velocity.
$\ddot{X}$	: Oscillating cylinder velocity.
KC	: Keulegan-Carpenter Number.
β	: Frequency parameter.
F_y	: Lift force.

Collection

C_L	: Lift force Coefficient.
T_w / WT	: Wave period.
T_o	: Oscillation Period.
f_n	: Natural frequency of Tensioned beam/string.
E	: Modulus of elasticity.
M	: Mass per unit length.
L	: Length.
I	: Moment of inertia.
δ_r	: Reduced damping.
A_y	: Cross flow amplitude.
γ	: Mode factor.
$C_{d_{uv}}$	: Drag coefficient due to velocity v and u.
$C_{d_{uu}}$	: Drag coefficient of velocity u^2.
C_{DM}	: Mean drag Coefficient.
C_{Dr}	: Oscillating drag coefficient in relative model.
MT	: Motion period.

Collection

CHAPTER ONE

1.0 INTRODUCTION.

As offshore structures are installed in deeper water and more severe environmental condition an improved understanding of the interaction of the waves and current with these structures remains important as:

- Theoretical calculations become more advanced requiring better data and models.

-Costs are to be reduced and one way of achieving that is through the application of better technology.

Analysis for design of these structures requires integration of hydrodynamics and structural mechanics and innovative use of theoretical and experimental techniques. Offshore structures are usually composed of cylinders, in particular slender cylinders are essential elements in a great variety of offshore application and systems. They are found as structural elements in fixed steel offshore structures and Jack up platforms, as pipe (conduits) protecting gas and oil well from the environment, as conduit for fluid and gas transfer (risers). With a fixed and floating production systems and offshore mining installations as line(anchors) for positioning of floating vessels, As electrical or hydraulic lines (cables, umbilical's) for transmission of power and data.

The behavior of slender cylinders in marine environments depends on three factors these are:

-The hydrodynamic interaction between the cylinder and the ambient flow.

Collection

-The properties of mechanical systems that is formed by the cylinder.

-The boundary conditions at both ends- the structure at which it is connected or from which it is suspended. Tests have been carried out to study flow-structure interaction experimentally by oscillating a vertical cylinder inline direction with steady flow and waves.

1.1 PROBLEM SURVEY.

A cylinder experiences excitation hydrodynamic forces in a direction perpendicular to its longitudinal axis due to action of current, wave or current and waves. The forces depend on the fluid properties and flow conditions in the ambient environment as well as the geometry of orientation of a cylinder itself. Even when the ambient environment is at rest the cylinder will nonetheless experience hydrodynamic reaction forces when moves through the fluids. The excitation and reaction forces constitute a complex nonlinear hydrodynamic problem. The dynamic behavior of the long and slender cylinder is a complex nonlinear problem, even when the time varying excitation is fully known. It is influenced by factors such as the large displacements involved, the internal and external fluid pressure, and the variable mass of flow through the pipe and the coupling between axial and torsional deflections. The structure response of the cylinder (i.e. its motions) to the loading experienced interacts with the forcing mechanisms to change the loading and thereby change the cylinder motion.

Collection

1.2 RESEARCH OBJECTIVES.

The overall objectives of the research reported here is to predict the behavior of flexible slender cylindrical models oscillating in complex flow (towing motion of cylinder model, current and waves). Using the method of recording the displacement of markers located along the model, the 3D displacements were recorded using high speed cameras and MCU 24 unit, the system record x-displacement, y-displacement and z-displacement of the markers located along the model of flexible slender cylinder. The specific objectives of this thesis are:

(1) To investigate the flow pattern around the cylinder in flow involving both currents and waves.
(2) To investigate behavior of a cylinder (motion) in a complex flow
(3) To estimate the hydrodynamic forces on a cylinder in a complex flow (lift force and inline hydrodynamic forces).

1.3 THESIS OUTLINE.

This thesis has been organized into two main parts:

Part one deal with theoretical studies of slender cylinder in both waves and currents.

Part two deal with experimental studies of slender cylinder in both waves and currents

-Chapter two, deal with ocean wave theories , this chapter deal with, the main types of wave in ocean environments, essential wave parameters , hydrodynamic wave theory .

Collection

-Chapter three, deal with interaction of the slender cylinder with both current and wave flow, the main focus of this chapter is to identify the main flow pattern around a cylinder under various values of KC and Reynolds number and estimation of hydrodynamic forces (inline force and cross flow force) on a cylinder

-Chapter four, deal with the Vortex Induced Vibrations (VIV) of a slender cylindrical structures in complex flow conditions, this chapter addresses issue like "how and under what conditions Vortex Induced Vibrations occur", "what are the methods used to overcome and control Vortex Induced Vibrations of slender cylinders".

-Chapter five deal with the experimental description on the model test, experimental data collection, data analysis, Discussion of results and Conclusions.

CHAPTER TWO

2.0 OCEAN WAVE THEORIES.

2.1 OCEAN ENVIRONMENTS.

Environmental conditions play a predominant role in design of almost all offshore structures. These conditions are site specific and extreme events are often encountered with long return periods. In order to incorporate environmental loads accurately into design process long term data describing the expected environment at the location of the structure needs to be available. Wave data are recorded and evaluated thoroughly and the amount of information available varies significantly from each site. In order to interpret the available information correctly it is important to have a general understanding of the procedure which is used to obtain the data. In general, oceanographic data is collected through the use of submerged

Collection

floating and airbone recorder. Of these options, floating device in particular wave rider buoys are most commonly used method. The data provided by the records of these devices describe the wave climate as the sequence of time and generally characterizes it as a series of different sea states. When data is collected at a certain location in the sea, three hour sea states are assumed for recording. In other words, it is assumed that the energy in the sea state does not change significantly within three hour period time period. Collecting data to characterize the wave climate at a certain location in sea is usually a process which usually takes multiple years. In order to reduce the amount of data which accumulates over the course of recording, data is in practice, only collected for a duration of 20 minutes intervals and assumed to be constant for rest of each individual three hour sea state. In general there are two basic approaches that can be taken when obtaining data to model a sea state, these are through an actual wave analysis and by converting wind data into wave information. Although a wave analysis will provide a more accurate description, it is often difficult together large scale wave data required to perform this calculations. In this case the more readily available wind information may be used to model the wave.

2.2 TYPES OF WAVES.

In order to define load cases for a particular offshore structure, a sea model which describes the water motion at specific site must be established, such model describes the sea elevation process as a sequence of waves. Depending on the model which is chosen for the simulation, different types of waves are encountered .The waves can be categorized based on their characteristics. Waves can be generally defined as being “REGULAR” or “IRREGULAR”.

Collection

Regular waves consist of heights and periods, such as a wave that is approximated by sine function, on the other hand, both heights and periods vary for irregular waves.

Figure 1: Regular wave profile.

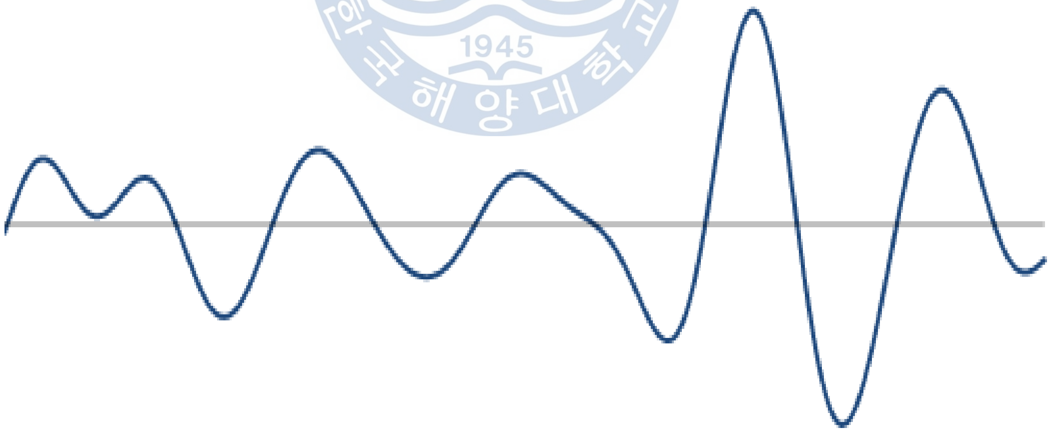

Figure 2: Irregular wave profile.

KOREA MARITIME UNIVERSITY 1945 한국해양대학교

Collection

It is also possible to distinguish between “LINEAR” and “NONLINEAR” waves. The main difference between these two types of waves lies in the assumptions under the underlying theory was derived. In regards to the ocean waves, the profile of nonlinear waves is long crested, meaning that it consists of higher, sharper crest and longer, rounded trough, while the wave profile of a regular linear wave is symmetrical with respect to still water level. Both linear and nonlinear wave theory can be used to describe a regular as well as an irregular wave environment, although it is significantly more difficult to obtain nonlinear irregular wave models. This is due to fact that it is possible to attain an irregular sea state by summing up various regular waves when using linear wave theory, while the principle of superposition does not apply to nonlinear wave theories.

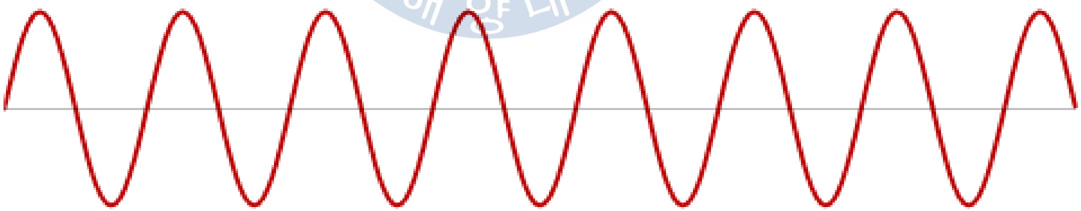

Figure 3: Linear wave profile.

dCollection

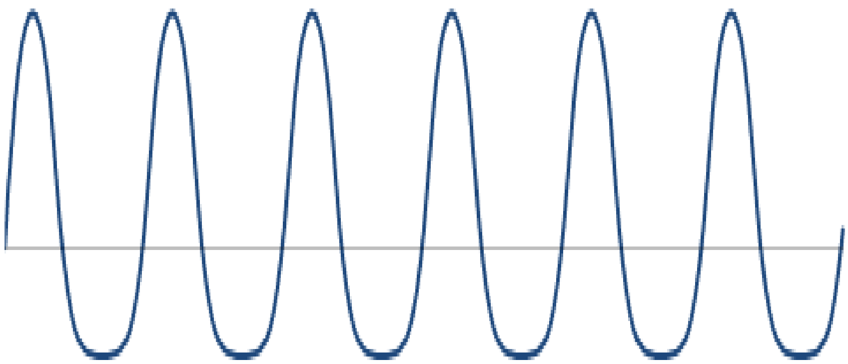

Figure 4: Nonlinear wave profile.

Wave models can be divided into two types “DETERMINISTIC” and “STOCHASTIC” model .The base assumption made in the deterministic approach is that the characteristics of the waves are known exactly and there is no randomness involved in the process. Such a model will produce the same results anytime when used. Since a wave state is highly irregular and in general cannot be characterized by specific constant values, This approach is only valid to analyze particular extreme loads. When analyzing long term effects a stochastic model need to be considered which accurately depicts the irregularities of the sea. Rather than relying on simple deterministic values, a whole spectrum is introduced to define the parameters. This approach requires some fundamental knowledge of spectral analysis.

Collection

2.3 ESSENTIAL WAVE PARAMETERS.

Depending on the approach taken to model a sea state, different parameters are required as impact data. However all models require certain information from the location of offshore structures, regardless of the theory which is selected during design process. In particular knowledge about the height of the waves (the vertical distance between the crest and trough of a wave), the wave period (the duration of one cycle of the wave) and water depth are essential. Not only are these parameters fundamental for modeling the sea, but they also give an indication of which theory is applicable to a certain site. The most important offshore parameters are:

-Significant Wave Height H_s-Four times the root mean square of water levels relative to mean water level. For particular reason H_s is often assumed to be approximately equal to the average height of the highest one third of the waves.

-Significant Wave Period T_s-The average period of the highest one third of all recorded waves.

-Water depth d-The distance measured between the mean sea level (MSL) and seabed.

The significant Wave Height is widely used parameter, it should be noted that several definitions are commonly used to describe the period of waves. In particular the peak period and zero up crossing period are often used as alternatives to the significant wave period to characterize a sea elevation process. The peak period is of particular interest when using wave spectrum to define a model, and is commonly used when describing

Collection

irregular random sea states. Often standard offshore literature also refers to the zero up crossing period, since it can be obtained quite easily from wave records, regardless of its shape; while it is sometimes difficult to define a clear beginning and end of a single wave in a highly random elevation process, the zero up crossing period is always clearly defined.

-Peak period T_p-The period of the wave containing the most power.

-Zero up crossing period T_z-The average time between successive movements of the water surface through mean position in the upward direction.

2.4 WAVE PARAMETERS TO DETERMINE AN APPLICABLE WAVE THEORY.

Although there are different theories been developed which can theoretically be used to formulate wave models, only few are widely used and even less have found application in practical engineering procedure. Regardless of the wave theory, fundamental assumptions are made which, depending in the location, only hold true to a certain degree. In order to decide whether the theory is still applicable, it is important to understand the errors which occur when certain conditions do not apply. To simply the matter of selecting an appropriate theory for engineering applications, some general rules have been established based on the knowledge of only few fundamental parameters at a specific site. The validity of a wave theory can generally be defined by graph shown below. It is a widely accepted presentation of the applicability of wave theories and commonly used in Coastal and Ocean Engineering Codes. With this graph, it is possible to select a wave theory based on three parameters, the wave height H, the

Collection

wave period T and water depth d. The three parameters define the wave steepness S and wave shallowness μ.

$$S=\frac{2\pi H}{gT^2}=\frac{H}{\lambda} \tag{2.1}$$

$$\mu=\frac{2\pi d}{gT^2} \tag{2.2}$$

These parameters are of particular interest, as they quantify the potential significance of nonlinear effects. Waves in shallow water tends to have higher crests and flatter troughs an effect which can generally not be taken into account using linear wave theory. This behavior is amplified for higher wave steepness and lower water depths. Not all wave theories are capable of accurately taking these effects into account. In order to simplify using figure 5 below, the constant value of $\frac{2\pi}{g}$ has been incorporated into the scale of the graph. The scale is given in imperial units.

Collection

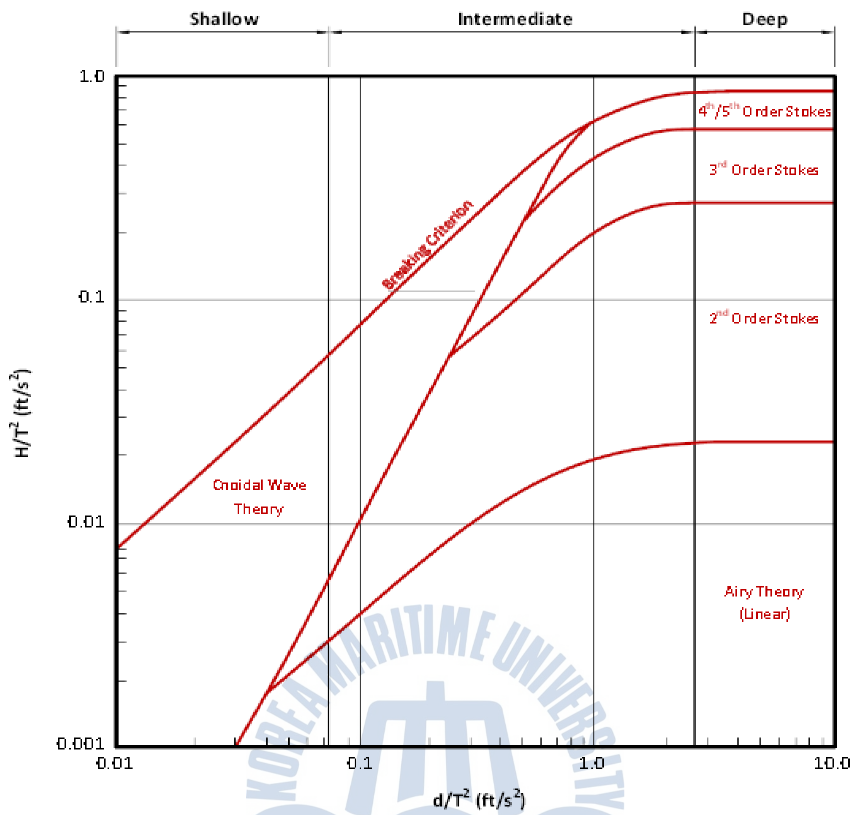

Figure 5: Ranges of Validity of wave theories.

2.5 LINEAR WAVE THEORY.

The linear wave theory is valid in the range of small wave steepness S, linear wave theory assume that the waves consist of small amplitudes in comparison to wavelengths, because of this reason linear wave theory is also called small amplitude wave theory. The graph shows that in deepwater, linear wave theory can be used up to a wave steepness of 0.02ft/s^2, while its application become increasingly limited as the water depth.

Collection

2.6 STOKES WAVE THEORY.

Stokes wave theory refer to a nonlinear and periodic surface wave on inviscid fluid layer of constant mean depth. This type of modeling was introduced by Sir George Stokes in mid of 19^{th} century; Using a perturbation series approach known as Stokes expansion, obtained approximate solution for nonlinear wave motion. Stokes wave theory is of limit of practical use for waves on intermediate and deepwater. It is used in design of Coastal and offshore structures, in order to determine the wave kinematics (free surface elevation and flow velocities). The wave kinematics are needed in the design process to determine wave loads on a structure.

2.7 APPLICABILITY OF STOKES WAVE THEORY.

Stokes wave theory, when using a low order of the perturbation expansion (e.g. up to second, third or fifth order) is valid for nonlinear waves on intermediate and deepwater, that is for wavelengths (λ) not larger compared to mean depth. In shallow water, the lower order stokes expansion breakdown (give unrealistic results) for appreciable wave amplitude (as compared to water depth).

For engineering use, the fifth order formulations of Fenton are convenient, applicable to Stokes first and second. The demarcation between when fifth order Stokes theory is preferable over fifth order cnoidal theory is for Ursell parameter below about 40. In Stokes wave theory, as the order increases,

Collection

the steepness of the crest obtained from resulting wave is also increased compared to lower order solution, with increasing wave height, and decreasing water depth, this characteristic of wave become more pronounced and even higher order solutions need to be determined to establish an accurate model for extreme wave scenarios. In common practice,Stokes theory is applied up to a fifth order for which wave kinematics have been derived by Skjelbreia and Hendrickson(1961). It is found that even this higher order theory is not accurate for steeper waves, which are commonly in shallow water. This is because the higher order term begin to distort the results unrealistically when the wave steepness is high. So the applicability of Stokes wave theory to offshore structures is then limited. So Stokes theory is suitable for waves which are not very long relative to water depth.

The main restriction of the wave theories were caused by deficiencies in providing satisfactory results for waves of high steepness or limitations in relative water depth.

In additions all theories were purely analytical, resulting in extremely complex equations. Dean introduced an alternative approach by developing purely numerical procedure to solve the boundary value problem for nonlinear wave called the stream function theory. The range of this theory is broader than the other theories. The major advantage of the theory is that it simplifies satisfying the boundary conditions of nonlinear wave problems, so using Dean's approach; it is possible to obtain a steady stream line at the free surface and with it a constant value of a stream function. Thus the free surface becomes streamline itself and it follows the

Collection

kinematic free surface boundary conditions, which demands a smooth motion of water particles at the surface . The only condition which is not easily satisfied in stream function theory is the dynamic free surface condition. Here the pressure throughout the free surface must be equal to constant value namely the atmospheric pressure. Dean applies this condition numerically through an iterative solution process. The surface is divided into “n” points equally spaced along the wave profile iteration are carried out until the boundary condition is sufficiently met. Dean’s stream function theory has the big advantage that it is applicable in much wider range of water depths than Stokes or Cnoidal theory. Furthermore the iterative solution process allows for a simultaneous calculation of the nonlinear equation, instead of solving the problem successively based on a previously calculated lower order theory. It is therefore significantly easier to obtain higher order solutions.

2.8 HYDRODYNAMIC WAVE THEORY.

This section is aimed at familiarizing at the basic principles and notation of water wave mechanics.

2.8:1WATER PARTICLE KINEMATICS.

Using small amplitude wave theory, it can be shown through the conservation of mass, the assumption of irrotational motion and incompressibility of fluid, that a velocity potential can be solved given the

Collection

set of boundary condition applicable. Thus using Laplace equations, it is possible to derive an expression for velocity potential (Dean et al 1991;Sorensen 1993)

$$\Phi=\frac{Hg\cosh k(d+z)}{2\omega \cosh kd}\sin(kx-\omega t) \tag{2.3}$$

There are several other important expressions that can be derived using the velocity potential. One is the surface profile for a wave, namely the instantaneous deviation from the SWL (z=0)

$$\eta=\frac{H}{2}\cos(kx-\omega t) \tag{2.4}$$

Another expression is the dispersion relation ω^2=gktanh(kd) (2.5)

The dispersion relation can be rearranged for the definition of wave celerity at any water depth

$$V=\frac{\omega}{k}=\sqrt{\left(\frac{g}{k}\tanh(kd)\right)} \tag{2.6}$$

The equation for the particle velocity components in horizontal and vertical directions can be derived over the water depth

$$u=\frac{\partial\Phi}{\partial x}=\frac{H\omega\cosh k(d+z)}{2\sinh kd}\cos(kx-\omega t) \tag{2.7}$$

$$W=\frac{\partial\Phi}{\partial z}=\frac{H\omega\sinh k(d+z)}{2\sinh kd}\sin(kx-\omega t) \tag{2.8}$$

The velocity potential can be differentiated to give particle accelerations

$$a_x=\frac{\partial u}{\partial t}=\frac{H\omega^2}{2}\frac{\cosh k(d+z)}{\sinh kd}\sin(kx-\omega t) \tag{2.9}$$

$$a_y=\frac{\partial w}{\partial t}= -\frac{H\omega^2}{2}\frac{sinhk(d+z)}{sinhkd}\cos(kx-\omega t) \quad (2.10)$$

CHAPTER THREE.

3 FLOWS AROUND CIRCULAR CYLINDERS.

3.1: Regimes of flow around a smooth, circular cylinder.

The non dimensional quantities' describing the flow around a smooth circular cylinder depends on the cylinder Reynolds number,

$$Re=\frac{UD}{\nu} \quad (3.1)$$

Where D is the diameter of the cylinder, U is the flow velocity and v is the Kinematic Viscosity. The flow undergoes tremendous change as the Reynolds number is increased from zero. The flow regimes experienced with increasing Reynolds number (Re) are summarized in Figure 6 and Table 1 shown below:

Collection

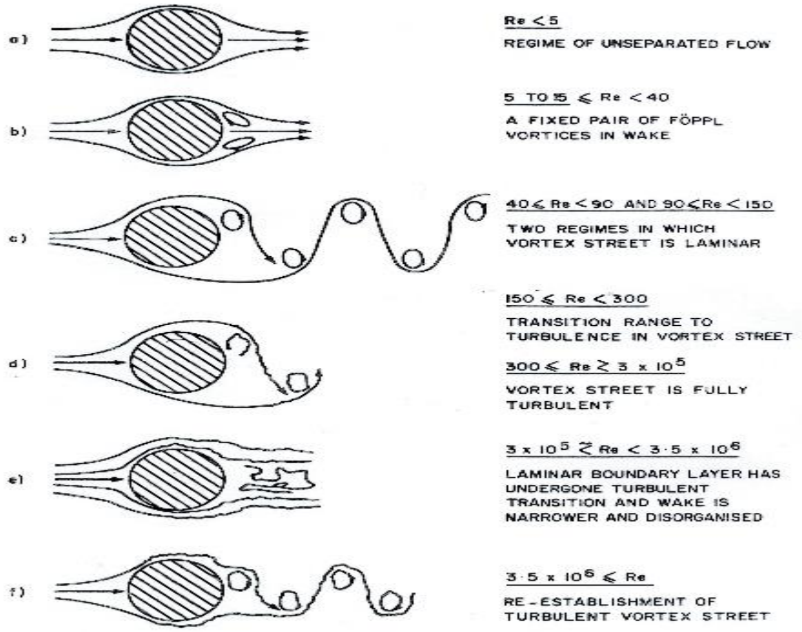

Figure 6: Flow regimes experienced with increasing Reynolds Number.

The table below shows the state of flow as compiled by Zdravkovich (1997).

Table 1: State of flow, From Zdravkovich (1997).

Laminar state	0<Re<4-5	Non separating regime
	4-5<Re<30-48	Steady separation regime
	30-48<Re<180-200	Periodic Laminar regime
Transition in wake state	180-200<Re<220-250	Far wake
	220-250<Re<350-400	Near wake
Transition in shear	350-400<Re<10^3-2x10^3	Lower

layers(Subcritical)	$10^3-2x10^3<Re<2x10^4-4x10^4$	Intermediate
	$2x10^4-4x10^4<Re<10^5-2x10^5$	Upper
Transition in boundary Layer	$10^5-2x10^5<Re<3x10^5-3.4x10^5$	Pre critical regime
	$3x10^5-3.4x10^5<Re<3.8x10^5-4x10^5$	One bubble regime(critical)
	$3.8x10^5-4x10^5<Re<5x10^5-10^6$	Two bubble regime(critical)
	$5x10^5-10^6<Re<3.4x10^6-6x10^6$	Supercritical regime
	$3.4x10^6-6x10^6<Re<$ Unknown	Post critical regime
Fully turbulent state	Unkown<Re< infinity	Invariable ultimate

For very small values of Re no separation occurs. The separation first appears when Re>5. For the range of Reynolds number 5<Re<40, a fixed pair of vortices forms in the wake of the cylinder. The length of this Vortex formation increases with Re (Batchelor,1967). When the Reynolds number is further increased, the wake becomes unstable, which eventually give birth to phenomenon called Vortex Shedding in which Vortices are shed alternately at either side of the cylinder at a certain frequency. Consequently, the wake has an appearance of a Vortex Street. For the range of the Reynolds number 40<Re<200, the vortex street is laminar. The shedding essentially two dimensional i.e it does not vary in span wise direction (Williamson,1989). With further increase in Reynolds number (Re), however transition to turbulence occurs in the wake region. The region of transition to turbulence move towards the cylinder, as Reynolds number increased in a range 200<Re<300 (Bloor,1964). Bloor(1964) reports that at Re=400, the vortices once formed are turbulent. Observations shows that the two dimensional features of the vortex shedding observed in a range 40<Re<200 becomes distinctly 3 dimensional in this range (Gerrard, 1978 and Williamson,1988), the vortices are shed in cells in the spanwise direction. For Re>300, the work is completely turbulent. The boundary layer over the cylinder surface remains laminar, however for increasing Re over a very wide range of Re namely 300<Re<3×10^5 the regime is known as the subcritical flow regime. With a further increase in Re, transition to turbulence occurs in boundary layer itself. The transition first take place at a point where the boundary layer separates, and then the region of transition to turbulence moves upstream over the cylinder surface towards the stagnation point as Re increased. In the narrow Re band 3×10^5<Re<3.5×10^5 the boundary layer become turbulent at the separation point, but this occurs only at one side of the cylinder. So the boundary layer separation is turbulent at one side of the cylinder and laminar at the other side. This regime is called critical (or lower transition) flow regime. The flow asymmetry causes a non zero mean lift on the cylinder. The side at which the separation is turbulent switches from one side to the other occasionally (schewe,1983). Therefore the lift changes direction as one sided transition to turbulence changes side, shifting from one side to the other (Schewe,1983). In 3.5×10^5<Re<1.5×10^6 this Reynolds number is called Supercritical flow regime, in this regime the boundary layer separation is turbulent on both sides of the cylinder. However,transition to turbulence in boundary layer has not been completed yet, the region of transition to

Collection

turbulence is located somewhere between the stagnation point and separation point. The boundary layer on one side becomes fully turbulent when Re reaches the value of about 1.5×10^6, in this flow regime, the boundary layer is completely turbulent on one side of the cylinder and partially laminar and partially turbulent on the other side. This type of flow regime, called upper transition flow regime, prevails over the range of Re, 1.5×10^6<Re<4.5×10^6. When Re is increased so that Re>4.5×10^6, the boundary layer over the cylinder surface is virtually turbulent everywhere. This flow regime is called the Transcritical flow regime.

3.2 Vortex Shedding.

The Vortex Shedding phenomenon is common to all the flow regimes for Re>40, For these values of Re the boundary layer over the cylinder surface will separate due to the adverse pressure gradient imposed by the divergent geometry of the flow environment at rear side of the cylinder. The boundary layer formed along the cylinder contains a significant amount of vorticity. This vorticity is fed into a shear layer formed downstream of the separation point and causes the shear layer to roll up into a vortex with the sign identical to that of the incoming vorticity.

Consider pair of vortex “A” and “B” formed on the opposite side of the cylinder, the two vortices are unstable when exposed to small disturbances for Reynolds number Re>40. Consequently one vortex will grow larger than the other if Re>40. The larger Vortex (vortex “A”) become stronger enough to draw the opposing vortex (Vortex “B”) across the wake. If the vorticity in

Collection

vortex “A” is in clockwise direction, then vorticity in vortex “B” is in anticlockwise direction. The approach of vorticity of the opposite sign will then cut off further supply of vorticity to vortex “A” from its boundary layer. This is the instant where vortex “A” is shed being free vortex, vortex “A” is then converted downstream by the flow. Following the shedding of vortex “A” a new vortex will be formed at the same side of the cylinder namely vortex “C”, Vortex “B” will now play the same role as vortex “A”, i.e it will grow in size and strength so that it will draw vortex “C” across the wake. This will lead to shedding of vortex “B”. This process will continue each time new vortex is shed at one side of the cylinder where the shedding will continue to occur in alternate manner between the sides of the cylinder.The vortex shedding occurs only when the two shear layers interact each other. If this interaction is inhibited in one way or another example by putting a splitter plate at the downstream side of the cylinder between the two shear layers, the shedding would be prevented and therefore no vortex shedding would occur in this case.

3.3 Vortex Shedding Frequency.

The vortex shedding frequency is the frequency at which the pair of vortices are shed from the cylinder and is calculated based on the following expression $f_s=\frac{SU}{D}$ (3.2)

Where f_s is the Vortex Shedding frequency, S is the Strouhal number and U is the flow velocity and D is the diameter of the cylinder.

dCollection

Strouhal Number is a dimensionless frequency of the Vortex shedding and is the function of the Reynolds number. Reynolds number Re is a dimensionless parameter representing the ratio of inertia force to Viscous force. Re=$\frac{UD}{\nu}$ where U is the flow velocity, D is the diameter of the cylinder and ν is the Kinematic Viscosity of water at 30°C =0.801× 10^{-6} m^2/s.

The variation of Strouhal number versus Reynolds number is shown below.

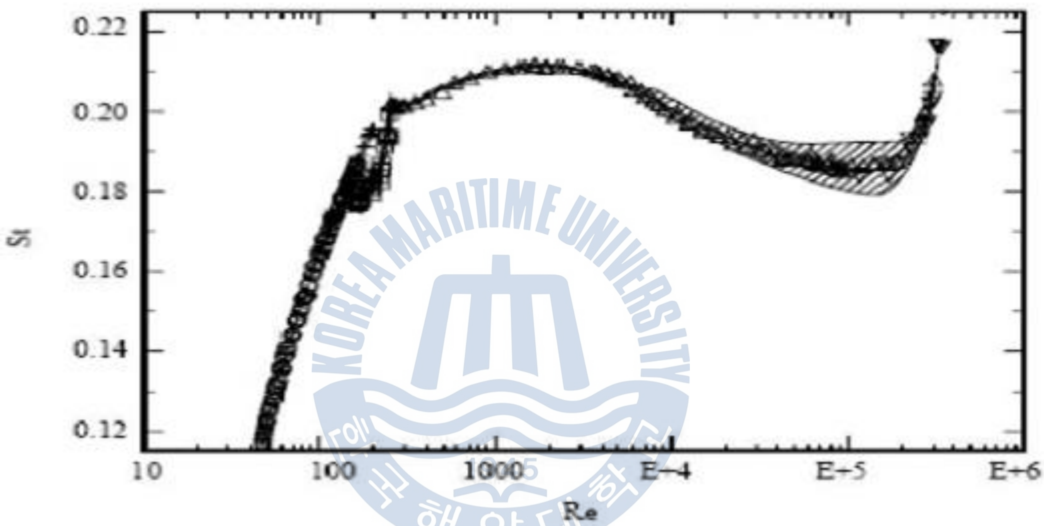

Figure 7: Variation of Strouhal Number versus Reynolds Number.

3.4 Estimation of Hydrodynamic Forces on the slender cylinder.

The estimation of hydrodynamic forces on a slender cylinder is the key consideration in the design of these slender cylindrical structures. The hydrodynamic force on a slender vertical cylinder is obtained from the Morison equation, first proposed by Morison et al (1950). This approach assumes that the structure is sufficiently small so as not to disturb the incident wave field. This it may be applied to conditions corresponding to

Collection

D<<λ where D is the cylinder diameter and λ is the wavelength. The definition sketch is given in Figure 8 below:

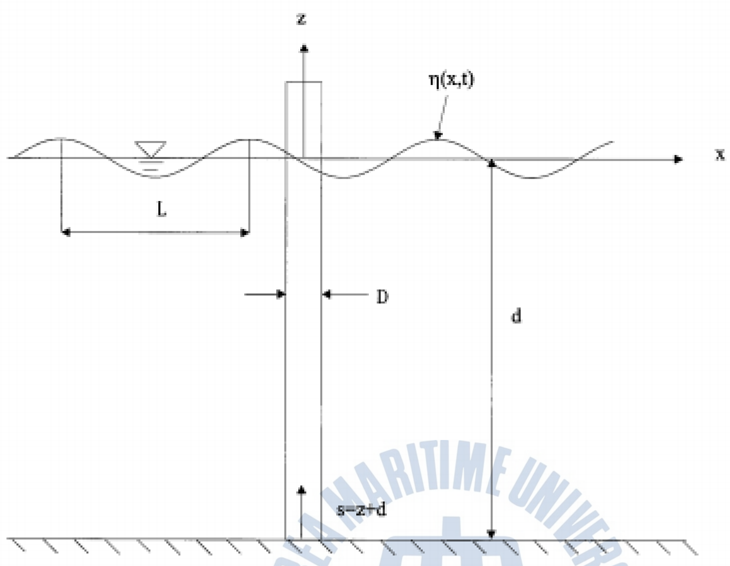

Figure 8: The definition sketch of slender cylinder.

The Morison equation expresses the horizontal force dF acting on a strip of height ds of a vertical circular cylinder as the sum of two force components, a drag force and inertia force and is given by dF=$\frac{1}{2}$ρD C_D U $|U|$ ds +$\frac{1}{4}$πρ$D^2 C_M \dot{U}$ds (3.3)

Where ρ is the density of water, U is the horizontal velocity of water, $\dot{U}$ is the horizontal acceleration of water particles, D is the diameter of the section, C_D is the drag force coefficient and C_M is the inertia force coefficient or mass coefficient. When the Morison equation is used in conjunction with linear wave theory, the horizontal particle velocity U and acceleration $\dot{U}$ based on linear wave theory may be applied. The corresponding expression for U and $\dot{U}$ are given respectively as:

Collection

$$U=\frac{\pi H\cosh(ks)}{T\sinh(kd)}\cos(kx-\omega t) \quad (3.4)$$

$$\mathring{U}=\frac{2\pi^2 H}{T^2}\frac{\cosh(ks)}{\sinh(kd)}s \quad (3.5)$$

Where H is the wave height, T is the wave period, k is the wave number, ω is the wave angular frequency, d is the water depth, t is time, x is the horizontal coordinate in the direction of wave propagation, the is the vertical coordinate measured upwards from the still water level and s= z+d is the vertical distance from seabed.

In steady currents, a cylinder subject to an oscillatory flow may experience two kind of forces these are : the inline force and lift force. The inline drag force is given by

$$F_{D}=\frac{1}{2}\rho C_D D U|U| \quad (3.6)$$

Where F_D is the force per unit length of the cylinder and U is the flow velocity, D is the diameter of a cylinder and C_D is the drag force coefficient. In case of oscillatory flow, there will be two additional contribution to the total inline force so the force will be

$$F=\frac{1}{2}\rho C_D D U|U| + m'\dot{U} + \rho V\dot{U} \quad (3.7)$$

In which $m'\dot{U}$ is the hydrodynamic mass force while $\rho V\dot{U}$ is the Froude Krylov force, V is the volume of a cylinder and m' is the hydrodynamic mass.

The hydrodynamic mass of a circular cylinder is given by

$$m'=C_M\frac{\pi D^2}{4}\rho \quad (3.8)$$

The hydrodynamic mass coefficient for a cylinder C_M=1, In the case when the body moves relative to the flow in the inline direction the Morison equation is modified as

$$F=\frac{1}{2}\rho C_D(U-U_b)|U-U_b| +\rho C_M A(\mathring{U}-\mathring{U}_b)+\rho A\dot{U} \qquad (3.9)$$

Where U_b is the velocity of the body in the inline direction. For more complicated flow conditions such as those involving inclined members, interference effect, flexible members and wave current interactions. In order to calculate the inline hydrodynamic forces under complicated flow conditions, one can use the alternative forms of modified Morison equations shown in Table 2 below:

Collection

Table 2: Modified forms of Morison equation under different flow condition.

S/No or Name	Equation Form
1.Relative velocity	F=$C_{dr}(\frac{1}{2}\rho D)(V+u)^2+C_{ar}(\frac{\pi D^2}{4}\rho)\mathring{u}$
2.Absolute velocity	F=$C_{DM}(\frac{1}{2}\rho D)V^2+C_{di}(\frac{1}{2}\rho D)u^2+C_{ai}(\frac{\pi D^2}{4}\rho)\mathring{u}$
3.	F=$\frac{1}{2}\rho DC_d(V+u)u+\frac{\pi D^2}{4}\rho C_a\mathring{u}$
4.	F=$\frac{1}{2}\rho DC_{DM}V^2+\frac{1}{2}\rho DC_d(V+u)u+\frac{\pi D^2}{4}\rho C_a\mathring{u}$
5.	F=$C_{DM}(\frac{1}{2}\rho D)V^2+C_{d_{uv}}(\frac{1}{2}\rho D)Vu+C_{d_{uu}}(\frac{1}{2}\rho D)u^2+C_a(\frac{\pi D^2}{4}\rho)\mathring{u}$
6.Linearized relative velocity	F=$\frac{1}{2}\rho DC_{DM}V^2+\frac{1}{2}\rho DC_{d\delta}\sqrt{\frac{8}{\pi}}\delta_u u+\frac{\pi D^2}{4}\rho C_{ai}\mathring{u}$
7.	F=$\frac{1}{2}\rho C_{d_7}(V+u)(V\beta+u_{max}\cos\beta)+\frac{\pi D^2}{4}\rho C_{ar}\mathring{u}$, where $\sin\beta=\frac{V}{u_{max}}$
8	F=$\frac{1}{2}\rho DC_{d_8}(V+u_{max})(V+u)+\frac{\pi D^2}{4}\rho C_{a_8}\mathring{u}$

3.5 Hydrodynamic Forces on oscillating cylinder.

If the cylinder is oscillating where the amplitude of oscillation is A and oscillating frequency is f_o, if the displacement of a cylinder is X, velocity $\dot{X}$ and acceleration $\ddot{X}$ at any time t are

X=Asin(2πf_ot)

Collection

$\dot{X}$=A(2πf_o)cos (2πf_ot)

$\ddot{X}$=-A$(2\pi f_o)^2$sin (2πf_ot) (3.10)

The hydrodynamic force on a cylinder due to interaction of the cylinder in still water is summarized in Table 3 below:

Table 3: Hydrodynamic model for oscillation of a cylinder in still water.

Hydrodynamic Model	Equation
Morison Equation	F=-$C_D(\frac{1}{2}\rho D)\lvert\dot{X}\rvert\dot{X}$-$C_A(\frac{\pi}{4}D^2)\ddot{X}$
Harmonic Model(drag form)	F=$\frac{1}{2}\rho D C_{DT}\dot{X}_m{}^2$ sin(2πf_ot+φ_o)
Harmonic Model(inertia form)	F=$\frac{1}{4}\rho\pi D^2 C_{AT}\ddot{X}_m$sin(2π$f_o$t+$\varphi_o$)
Linearized Morison equation	F=-$C_{Dl}(\frac{1}{2}\rho D)\frac{8}{3\pi}\dot{X}_m\dot{X}$-$C_{Al}(\rho\frac{\pi}{4}D^2)\ddot{X}$

C_A is added mass coefficient, C_D is the drag force coefficient ,C_{DT} is the total drag coefficient(From harmonic analysis), C_{AT} is the total added mass coefficient(From harmonic analysis), C_{Al} is the added mass coefficient(Linearized Morison equation), $\dot{X}_m$ is the maximum cylinder oscillatory velocity, $\ddot{X}_m$ is the max cylinder acceleration and φ_o is the phase angle due to oscillation.

3.6 Lift force on a cylinder.

Vortex Shedding causes additional force acting on the cylinder in direction perpendicular to the flow direction. This force component is called

Collection

Lift force (Transverse force). The lift force is strongly correlated to the development of the flow field around the cylinder and can induce substantial transverse vibrations. The lift force per unit length on a cylinder is given by $F_y=\frac{1}{2}U^2\rho D C_L \sin(2\pi f_s t)$

(3.11)

Where C_L is the Lift force coefficient, t time in second, U is the flow velocity, D is the diameter of cylinder, ρ is the density of water. The maximum lift force is given by:

$$F_y=\frac{1}{2}\rho {U_m}^2 D C_L \sin(2\pi f_s t) \tag{3.12}$$

Where U_m is the maximum flow velocity, where U=$U_m$sin $(2\pi f_o t)$ where f_o is the forced oscillation frequency.

3.7 Estimation of Reynolds Number and Keulegan-Carpenter Number for a given flow conditions.

The complex flow conditions is fully described by flow velocity U, this velocity is the function of wave velocity u, current velocity V and velocity of oscillating cylinder $\dot{X}$, the flow velocity is given as

$$U=(u \pm V \pm \dot{X}) \tag{3.13}$$

The components of flow velocity are:

-U= (u +V+$\dot{X}$), when wave, current and cylinder oscillation velocity act in the same direction.

Collection

-U= (u-V-$\dot{X}$), when current and cylinder oscillation velocity act in opposite direction to wave velocity.

-U= (u +V- $\dot{X}$), when wave and current move in the same direction and cylinder oscillation velocity move in opposite direction.

-U= (u- V +$\dot{X}$), when wave and cylinder move in the same direction and current move in opposite direction. Using the flow velocity it is possible to estimate the Reynolds numbers Re and Keulegan Carpenter can be obtained, once Re and KC are obtained from flow condition it is possible to obtain the values of hydrodynamic coefficients C_L, C_M and C_D from graphs plotted from experimental results which shows the Variations of these hydrodynamic coefficient for different values of Re, KC and frequency parameter β. The KC and Re definition for different flow conditions are given in Table 4 below:

Table 4: Definition of Re, KC and frequency parameter β for different flow condition.

Flow Type	Reynolds Number Re	Keulegan Carpenter Number KC
Cylinder motion in still water(Motion alone)	$\frac{\dot{X}D}{\nu}$	$\frac{\dot{X}T_o}{D}$
Cylinder motion in current(motion + current)	$\frac{(V \pm \dot{X})}{\nu}$	$\frac{(V \pm \dot{X})T_o}{D}$
Cylinder in wave (wave alone)	$\frac{uD}{\nu}$	$\frac{UT_w}{D}$
Cylinder motion in wave(motion + wave)	$\frac{(u + \dot{X})D}{\nu}$	$\frac{UT_w}{D} \pm \frac{\dot{X}T_o}{D}$
Cylinder in wave and current(wave +current)	$\frac{(u \pm V)D}{\nu}$	$\frac{(U \pm V)T_w}{D}$
Cylinder motion in both wave and current(motion+wave+current)	$\frac{(u \pm V \pm \dot{X})D}{\nu}$	$\frac{(u \pm V \pm \dot{X})T_w}{D}$
Frequency parameter β	β=$\frac{Re}{KC}$	β=$\frac{Re}{KC}$

3.7.1 Estimation of Lift force coefficientC_L, Drag force coefficients C_D and inertia force coefficientsC_M.

All hydrodynamic coefficients are estimated from experimental results. Using the flow condition available, the following parameters can be calculated : The Reynolds number Re, the Keulegan Carpenter number KC and frequency parameter β. The hydrodynamic coefficients depends on these parameters and therefore can be estimated from the following graphs which show the variation of these coefficients against Re, KC and β. The hydrodynamic coefficients can be estimated from the following graphs below:

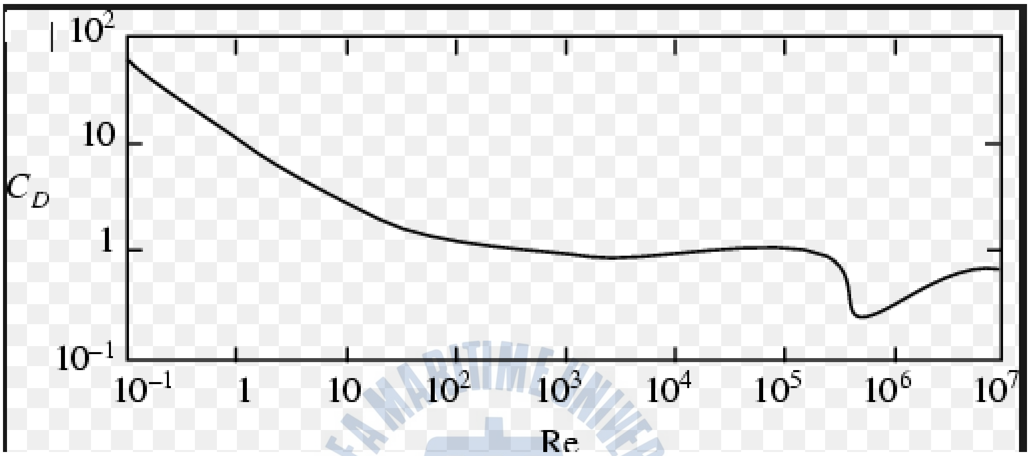

Figure 9: Drag coefficient of a smooth cylinder versus Reynolds number.

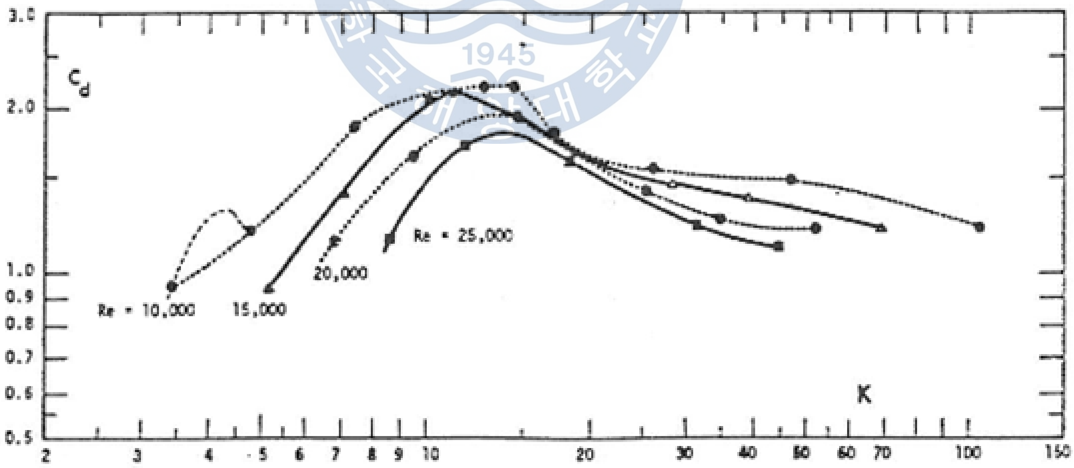

Figure10: Graph of drag force coefficient as a function of KC and Re.

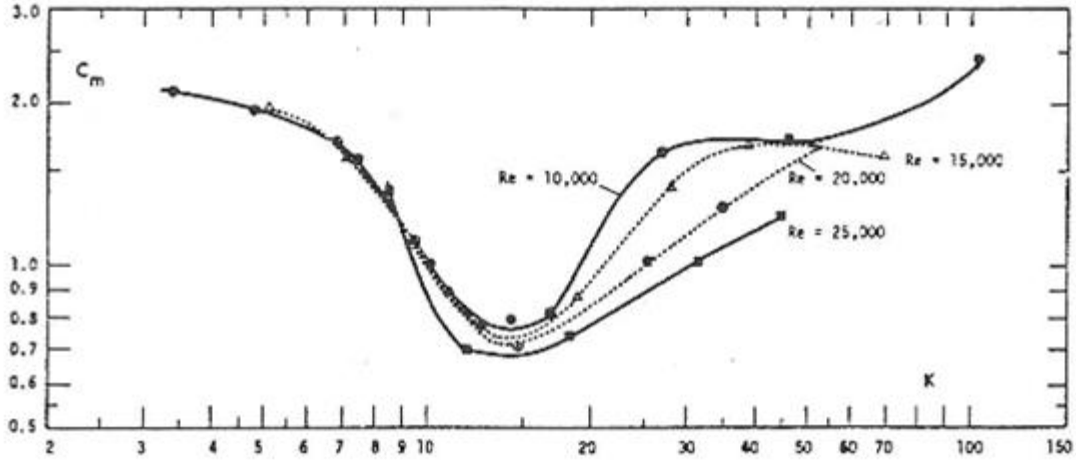

Figure 11: Graph of inertia coefficient as the function of Re and KC.

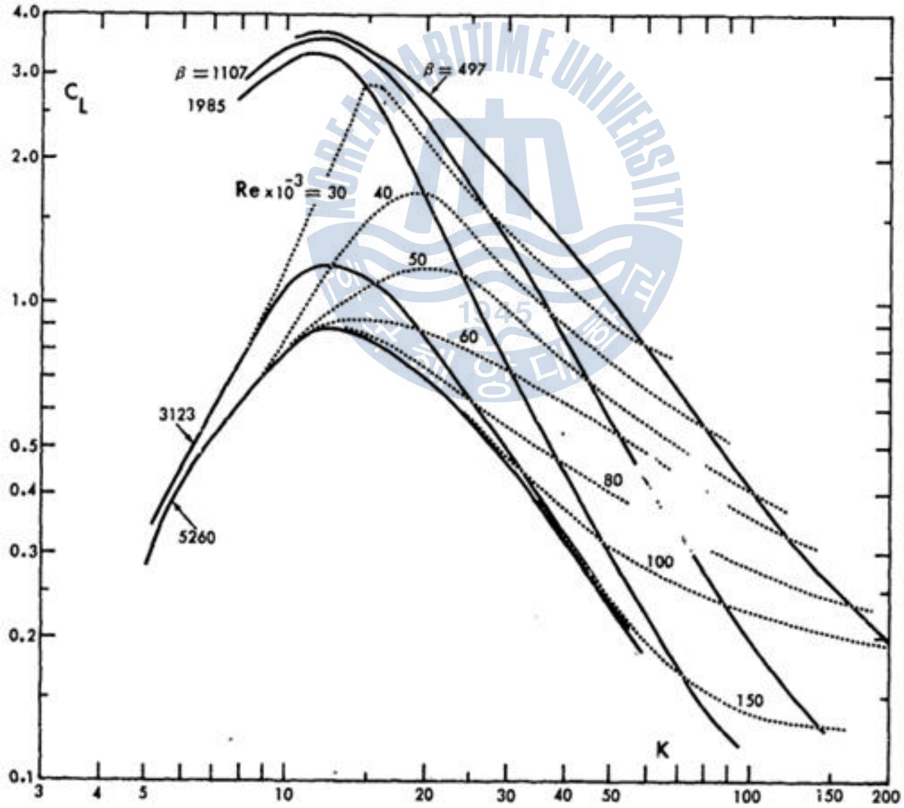

Figure 12: Graph of lift coefficient as the function of KC, Re and frequency parameter β

dCollection

CHAPTER FOUR

4.0 VORTEX INDUCED VIBRATIONS (VIV) OF CYLINDRICAL STRUCTURES.

Use of flexible cylinders has increased significantly in recent years since the drilling depth become deeper and deeper. The risers at deep sea oil fields are long and flexible and the eigenfrequencies are low. Low order eigenmodes are therefore expected to be excited even in shallow water. Another trend in offshore industry is to drill in region with extreme weather condition and high currents, Extreme conditions are critical , since higher eigenmode can be excited which results in reduced fatigue life. In offshore industry, Vortex Induced Vibrations is of particular interest since the drilling depth increases, Vortex induced Vibrations is probably the single most important design issue for steel catenary risers, particularly in the areas with high currents. This induces high frequency cyclic stresses in riser which can result in fatigue damage. Deepwater risers are especially susceptible to Vortex Induced Vibrations because:

(a) Currents are typically higher in deepwater areas than in shallower areas.
(b) The increased length of risers lower its natural frequency and thereby lowering the magnitude of current required to excite Vortex Induced Vibrations (VIV).
(c) Deepwater platforms are usually floating platforms so that the flexibility of the system is further increased.

Collection

At greater depths, the offshore riser is not rigid, but act like a tensioned string, the natural frequency of a string is dictated by the following equation (Blevins 1977)

$$f_n=\sqrt{\frac{EI}{ML^4}} \tag{4.1}$$

Where f_n is the Natural frequency, E is the Modulus of Elasticity, I is the moment of inertia, M is mass per unit length and L is the length.

As the length of riser increases, the frequency goes down the most because it is raised to fourth power. Increasing the mass also decreases the natural frequency. Increasing the Modulus of elasticity and moment of inertia increases the natural frequency. The shedding frequency is given by equation fs=$\frac{SU}{D}$ where fs is shedding frequency, D is the diameter of the cylinder and U is the in flow velocity. If the natural frequency of riser is close to the shedding frequency of the cylinder lock in condition occur and hence VIV occur and cause fatigue stress on the riser that can lead to failure.

4.1 Most important Parameters of Vortex Induced Vibrations.

The following are the most important parameters governing Vortex Induced Vibration of slender cylindrical structures:

(a) Geometry ($\frac{L}{D}$).

(b) Mass ratio (m^*).

(c) Damping ratio (ζ).

(d) Reynolds Number (Re).

Collection

(e) Reduced velocity (V_r).

(f) Flow Characteristics (flow profile, steady/oscillating flow, turbulence intensity).

The study of Vortex Induced Vibrations (VIV) involves understanding important concepts in fluid mechanics, structural dynamics, materials and statistics. Vortex Induced Vibration is encountered in many engineering applications such as vibration of bridges, aircraft structures and offshore structures. Because of its theoretical complexity and practical importance VIV has been extensively studied over the past 50 years. Through experimental studies and numerical simulations, especially tests conducted on short rigid cylinders in laboratory condition much progress related to VIV has been made such as gaining an understanding of synchronization conditions, maximum motion amplitudes, response modes, Vortex pattern etc. Details related to the studies are discussed in comprehensive reviews by Blevins, Sarpkaya, Bearman,Pantazopoulos, Khalak and Williamson, Williamson and Govardhan.

(a) **Geometry ($\frac{L}{D}$):** Is the relation between the length and diameter of the cylinder. The natural frequency of a cylindrical structure depends on the length of the cylinder, it decreases as the length of the cylinder increases. So Natural frequency of the cylinder decreases as the length of the cylinder increases, this effect lowering the magnitude of current required to excite Vortex Induced Vibrations. The diameter of the cylinder also effects the magnitude of shedding frequency fs=$\frac{S_t U}{D}$. When it happens that fs shedding frequency is almost close to

Collection

natural frequency of the cylinder then Vortex Induced Vibration will occur.

(b) **Mass ratio (m*):** It is the ratio of the mass of the cylinder per unit length to mass of displaced fluid. It is expressed as m*=$\frac{m}{\frac{1}{4}\pi D^2\rho} \leftrightarrow \frac{4m}{\pi D^2\rho}$ (4.2)

Where m mass per unit length, ρ is the density of fluid, and D is the diameter of the cylinder. The mass ratio is a measure of the susceptibility of the cylinder to Vortex Induced Vibrations. The range of reduced velocity values over which synchronization occur primarily controlled by mass ratio. A lower mass ratio indicates a wider synchronization range, while a larger mass ratio indicate a narrower synchronization range. This is because the effect of variation of added mass is more important for low mass ratio cylinders. The mass ratios of deep water drilling risers are relatively low, usually they are slightly above unity for steel risers and they may be even less than unit for composite risers. If the Vortex Shedding frequency is close to one of the natural frequency of a body, it causes resonance and the body start to vibrate with some frequency as the shedding frequency, this is called "LOCK IN". LOCK IN sometimes is called synchronization, critical and large damaging vibrations take place when the body becomes "LOCK IN". It is not obvious when the structure becomes LOCK IN and it can occur in a range of frequencies. The span of frequencies is strongly dependent on the mass ratio m^*. The lock in region is larger for small mass ratio and becomes critical as the mass ratio goes to unity.

(c) Mass damping parameter ($m_r\zeta$).

Collection

It is a combined parameter which is the product of mass ratio m_r and natural damping factor ζ. The mass damping parameter can be related directly to several other parameters the includes:

-Stability parameter $K_s=\pi^2 m_r \zeta$. (4.3)

-Scraton Number $S_c=\frac{\pi}{2} m_r \zeta$. (4.4)

-Skop-Griffin parameter $S_G=2\pi^3 {S_t}^2 m_r \zeta$. (4.5)

Where S_t is the Strouhal number. Among these, the Skop Griffin parameter might be the most widely used form that is related to mass –damping parameter. Under lock in conditions the mass damping parameter is thought to control the peak amplitude of VIV motion.

(d) Reynolds Number (Re).

A dimensionless number that measure the ratio of inertia forces to viscous forces for a given flow condition. Reynolds number is used to characterize whether a flow is laminar(typically when Re<2000) or turbulent (typically when Re>4000). The definition of Reynolds number is given by

$Re=\frac{UD\rho}{\mu}=\frac{UD}{\upsilon}$ (4.6)

Where U is the mean fluid velocity, D is the diameter of the cylinder cross section, ρ is the density of the fluid, μ is the dynamic Viscosity of the fluid and v is the Kinetic Viscosity of fluid which is given as

$v=\frac{\mu}{\rho}$ (4.7)

In various wake patterns behind a cylinder in different Reynolds number regimes. The Reynolds number range 300< Re<1.5X10^5 is referred to as the subcritical region, in this region, the cylinder

Collection

boundary layer becomes turbulent and the Vortex Shedding become irregular. In the supercritical Reynolds number range Re>3.5X10^6, the cylinder boundary layer is turbulent but the Vortex Shedding gain some more regularity again. Most engineering applications of VIV are associated with the upper subcritical and transitional Reynolds Number regimes.

(e) Reduced velocity V_r.

The ratio of the length of the stream path per cycle to the diameter of the cylinder

$$V_r=\frac{U}{fD} \tag{4.8}$$

Where U is the mean fluid velocity, f is the frequency of Vibrations and D is the diameter of the cylinder. During lock in condition, the Vortex shedding is trapped by the Vibration of the cylinder, and Vortex Shedding frequency is synchronized with the frequency of frequency i.e f_s =f. Recall that, under lock in conditions S_t=0.2, thus V_r =$\frac{1}{S_t}$ =5. Because of the interaction mechanism of VIV with the Variation in added mass, the actual reduced velocity range for lock in is much wider, usually we have 4<V_r <8. The bounds of the reduced velocity range for lock in depends on many factors, one of the most important of these is the mass ratio.

(f) **Added mass coefficient C_a** .

It is the ratio of effective added mass m_a to mass of displaced water $\frac{\pi D^2 \rho}{4}$ expressed as

$$C_a=\frac{m_a}{\frac{\pi D^2 \rho}{4}} \tag{4.9}$$

Collection

When a cylinder oscillate in a fluid, the movement of the cylinder causes the surrounding fluid particles accelerate from the original positions. The force exerted by the accelerated fluid particles on the cylinder which is in phase with the inertial force of the cylinder. The effective added mass force, consisting of these two components is represented by added mass m_a and added mass coefficient c_a. The added mass coefficient is not a constant. From forced oscillation experiments Sarpkaya presented the variation of the added mass coefficient with reduced velocity for different values of normalized vibration amplitudes, see figure 12 below

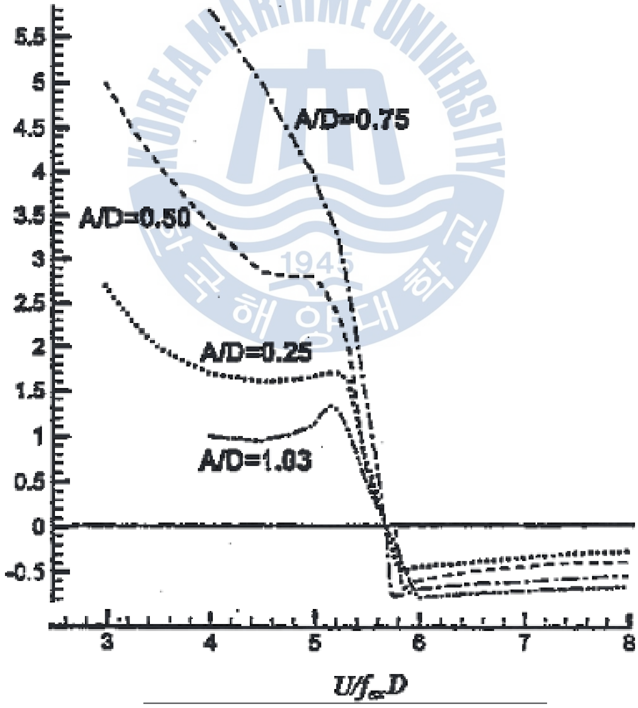

Figure13. Variation of the added mass coefficient with reduced velocity for different values of normalized vibration amplitude.

dCollection

The x-axis in the figure refers to reduced velocity and the y-axis show the added mass coefficient, the normalized vibration amplitude $\frac{A}{D}$ is the ratio of the amplitude of the cross flow vibration to diameter of the cylinder. Consider the curve for $\frac{A}{D}$=0.5 to illustrate the variation of c_a with reduced velocity. The value of c_a rapidly decreases from about 5 to -0.7 when the value of V_r increases from 3 to 5.8, then it increases slightly to about -0.4 as the value of V_r increases further to 8. The variation of C_a has more dominant effect on the cylinder with a low mass ratio. The virtual mass, whichis the sum of mass of the cylinder and added mass, may be expressed as:

$$m+m_a=(m_r + c_a)\frac{\pi D^2 \rho}{4} \tag{4.10}$$

For a cylinder with a low mass ratio, under lock in condition, the virtual mass is mass is much less than the mass of the cylinder itself, this explains why the actual VIV amplitude of a cylinder can be much larger than the amplitude that can be excited by relative small lift force exerted by Vortex Shedding. The variation of c_a also helps to explains possible wide synchronization range for VIV. With an increase in reduced velocity, the added mass decreases and the natural frequency of the cylinder increases, this causes synchronization to persist out to higher values of fluid speed.

4.2 METHODS USED TO REDUCE VORTEX INDUCED VIBRATIONS.

The amplitude of resonant Vortex Induced Vibration and the associated magnification of steady drag can be reduced by modifying either the structure or the flow as follows:

Collection

(a) Increasing reduced damping: If the reduced damping can be increased then the amplitude of vibration will be reduced as predicted by formulas given in table below:

Table 5: Expressions for maximum resonant Amplitude.

Investigator	Predicted displacement amplitude
Wake oscillator, Blevins (1977)	$\frac{A_y}{D}=\frac{0.07\gamma}{(1.9+\delta_r)S^2}(0.3+\frac{0.72}{(1.9+\delta_r)S})^{\frac{1}{2}}$
Griffin and Ramberg(1982)	$\frac{A_y}{D}=\frac{1.29\gamma}{(1+0.43(2\pi S^2\delta_r))\text{^}3.35}$
Sarpkaya (1979)	$\frac{A_y}{D}=\frac{0.32\gamma}{(0.6+(2\pi S^2\delta_r)^2)^{\frac{1}{2}}}$
Harmonic model	$\frac{A_y}{D}=\frac{C_L}{4\pi S^2\delta_r}$

Where A_y is the cross flow amplitude, D is the diameter of the cylinder, C_L is the lift coefficient, δ_r is reduced damping, γ is the mode factor and S is the Strouhal Number. If the reduced damping exceeds about 64, i.e $\frac{2m(2\pi\zeta)}{\rho D^2}$>64, then the peak amplitudes at resonance are ordinarily less than 1% of diameter and are negligible in comparison with the deflection induced by drag. Reduced damping can be increased by either increasing structural damping or increasing structural mass. Increased damping can be achieved by permitting scraping or banging between structural elements by using materials with high internal damping such as viscoelastic materials, rubber, wood or by using external dampers. The stock bridge damper has been used to reduce Vortex Induced Vibrations of power lines.

Collection

(b) **Avoid resonance**: If the reduced velocity is kept below 1, $\frac{U}{f_n D} < 1$ where f_n is the natural frequency of the structure in the mode of interest, the inline and transverse resonance are avoided. This is achieved by stiffening the structure. Stiffening is often most practical for smaller structures.

(c) **Streamline cross section**: If separation from the structure can be minimized, then Vortex shedding will be minimized and drag will be reduced. Streamlining the downstream side of the structure ordinarily require a taper of 6 longitudinal for each unit lateral, or an included angle of the taper no bigger than 8 to 10 degree to be effective. Hanko (1967) discusses the reduction of Vortex Induced Vibration of a pier by tapering. Gardner(1982) discussed streamlined oil pipe. Toebes and Eagleson(1961) found that the vortex induced vibrations of a plate were suppressed by streamlining the trailing edge.

(d) **Add a Vortex Suppression devices**.

Zdravkovich(1981), Wong and Kokkalis(1982), Hafen and Meggit(1971), Every et al (1982) and Rogers(1983) review add-on devices for suppression of Vortex Induced Vibration of cylindrical structures in marine applications. Seven devices of proven effectiveness which are: helical strake, shroud, axial slots, streamlined fairing, Splitter, ribboned cable, pivot guiding vane and spoiler plates. These devices act by disrupting or preventing the formation of an organized two dimensional vortex street.

Collection

PART TWO.

CHAPTER FIVE

EXPERIMENTAL STUDIES ON BEHAVIOR OF SLENDER CYLINDER ON BOTH WAVES AND CURRENT.

5.0 Introduction.

The experiments performed on the wave tank equipped with wave and current generating facilities. 3D displacement data (xyz) of points along the slender cylinder collected using **Pro Track III system (MCU 24 unit and Computer Software),** this system is used to calculate the 3D displacement of markers along the slender cylinder. In experiments two model test cylinders were used these are **Acryl model** and **Teflon model.**

The experimental studies focus on the following items:

(a) How the behavior of cylinder (Motion of points/markers) along the cylinder depend on:

(I) Mechanical properties of materials of the cylinder.

(II) Natural frequency and shedding frequency of the cylinder.

(III)Effect of wave heights (Hydrodynamic Forces) due to excitation source.

(b) Motion of points (markers) along the cylinder on XY and XZ plane.

The following experimental tests were carried out:

-Cylinder motion in still water (motion alone).

-Cylinder motion in Waves (Motion + Wave).

-Cylinder motion in current (Motion + Current).

Collection

-Fixed cylinder in wave (wave alone).

-Fixed cylinder in current (current alone).

-Fixed cylinder in wave and current (wave + current).

-Cylinder motion in both wave and current (Motion + Wave + Current)

5.1 EQUIPMENTS USED.

The following equipments used to perform experiments:

-Two dimensional wave tank, its dimensions are 25x1x1.3(LxBxD) all units are in meters, the main function of the tank is to generate waves and currents.

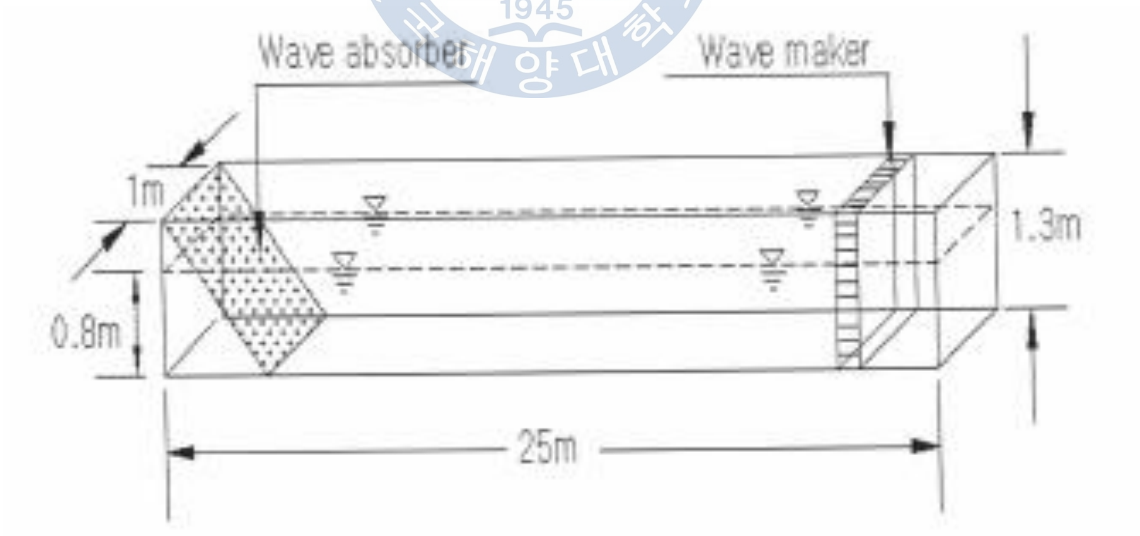

Figure 14: Two dimensional Wave tank.

Collection

-Towing carriage is one of the components of wave tank; the main function of towing carriage is to allow the motion of test cylinder.

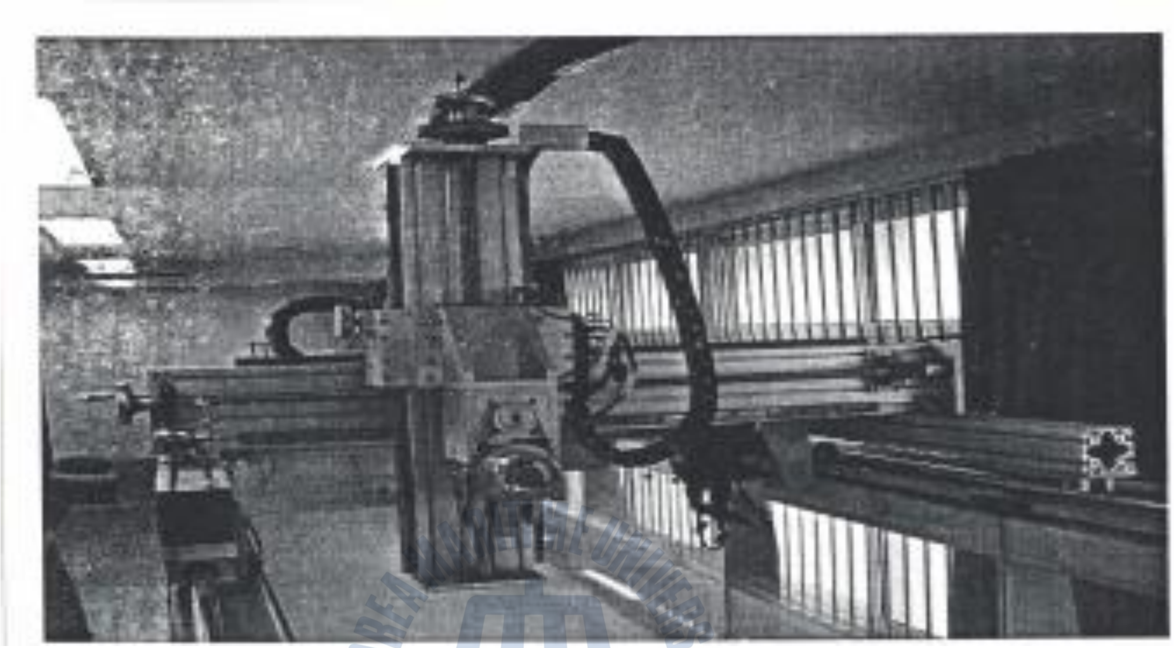

Photo 1: Towing Carriage system.

-Pro Tracker III system – This system is the motion capture system, it analyzes the 3D motion of points (markers) on a test cylinder i.e. x, y and z displacements. The system consist of imaging sensor (camera), multicamera unit (MCU 24) and personal computer with special software to calculate the 3D motion of points on the cylinder. In order to obtain accurate data recorded by Pro Track III system, Camera calibration process is very important before conducting any experiments; camera calibration is done by the method called DLT method. In this method the cameras set to have the same field of view as large as possible. To get 3D coordinates (xyz) the

Collection

marker must be seen by three cameras or more, as the number of cameras increases the accuracy of measurements also increases, in my case five cameras used to locate a marker.

Photo 2: Experimental arrangement of Pro Track III system.

Calibration Process-In order to do calibration, the calibration frame containing 10 markers is fixed on the working area, the cameras are allowed to take the images of 10 markers on the calibration frame, if all cameras detect all 10 markers on the frame then calibration is complete and we can perform experiment on the working area.

dCollection

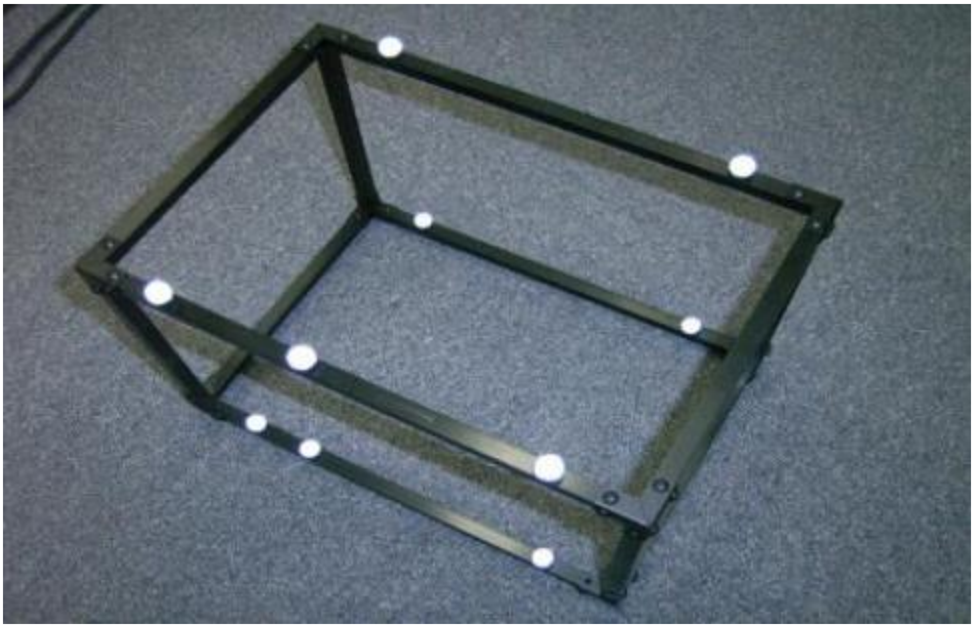

Figure 15: Calibration frame with markers.

-Flexible cylinder model used in experiment, two model are used these are Acryl and Teflon, each model is fitted with markers along its span at equal interval between the mark and another. When the model is set in motion either by towing carriage, wave, current or their combination, the markers also move , the 3D motion of a cylinder is recorded by MCU 24 unit which record the x, y and z displacement of these markers.

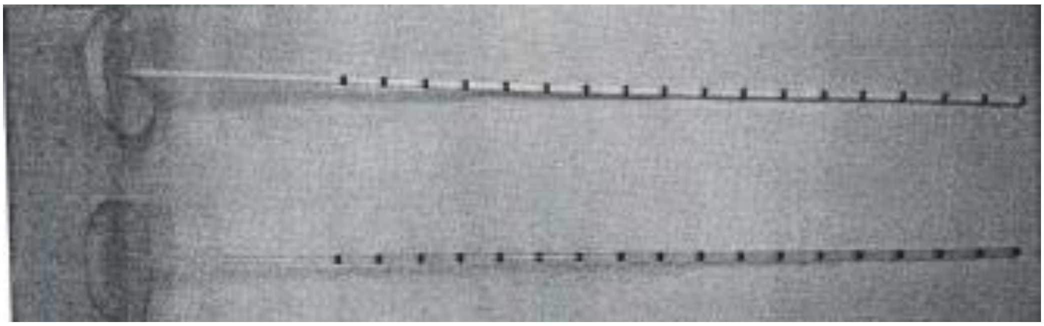

Photo3: Photo of slender cylinders used in experiments.

Collection

Table 6: Properties of Teflon model

Parameter	Symbol	Unit	Value
Diameter	D	mm	10.20
Length	L	m	0.88
Young's Modulus	E	N/m^2	$5x10^8$
Axial Stiffness	EA	N	40836
Bending Stiffness	EI	Nm^2	0.43
Aspect ratio	L/D		86.3
Density	ρ	Kg/m^3	2200
Mass	m	Kg	0.1581
Natural Frequency	fn	HZ	2.0

Table 7: Properties of Acryl Model.

Parameter	Symbol	Unit	Value
Diameter	D	mm	10.20
Length	L	m	0.88
Young's Modulus	E	N/m^2	$3.2x10^9$
Axial Stiffness	EA	N	261350
Bending Stiffness	EI	Nm^2	1.7
Aspect ratio	L/D		86.3
Density	ρ	Kg/m^3	1200
Mass	m	Kg	0.08624
Natural Frequency	fn	HZ	5.38

Collection

5.2 EFFECT OF MECHANICAL PROPERTIES OF MATERIALS ON BEHAVIOR OF SLENDER CYLINDER

Mechanical properties of material are one of the factors which influence the magnitude of cross flow displacements of a slender cylinder in ocean environments.

- Mass ratio: It is the ratio of model mass to mass of fluid that it displaces. As the mass ratio increases the potential of vibrations increases (Blevins1990). This means the larger the mass ratio the larger the amplitude of cross flow displacements. From Table 6 and Table 7 of properties of Teflon and Acryl model respectively, the mass of Teflon is 0.1581Kg and mass of Acryl is 0.08624Kg. The two model cylinders have same dimensions (diameters and lengths), so they displace same mass of fluid. From this fact the mass ratio of Teflon is larger than the mass ratio of Acryl. Under the same experimental conditions we expect Teflon to undergo large cross flow displacements.

5.2.1 EXPERIMENTAL RESULTS

The magnitude of cross flow displacement of Acryl and Teflon model under various experimental conditions were analyzed as shown below:

CASE STUDY 1

EXPERIMENT (WAVES+CURRENTS).

Experimental Conditions: WP=1s, WH=10cm, V_c=0.2m/s.

Collection

Table8: Magnitudes of cross flow displacements of Teflon and Acryl model, all displacements are in mm.

Time(Sec)	n0(Y)-Acryl	n1(Y)-Acryl	n2(Y)-Acryl	n0(Y)-Teflon	n1(Y)-Teflon	n2(Y)-Teflon
0.016667	34.136019	32.850753	32.226521	43.822788	43.418313	42.634929
0.033333	34.230978	32.732183	32.409052	44.200621	43.257017	42.873714
0.05	34.036134	33.138669	32.150322	43.892604	43.31637	42.930449
0.066667	34.150647	32.995173	31.903148	43.76257	43.278491	42.882556
0.083333	34.056513	32.745771	32.024048	43.887115	43.309198	42.857032
0.1	34.050605	33.138669	32.215981	43.88234	43.455727	42.918104
0.116667	34.114022	33.044078	32.212185	43.727614	43.473328	42.855145
0.133333	33.905867	32.751861	32.468061	43.938368	43.300939	42.845436
0.15	34.063419	32.780669	32.42468	43.678864	43.46868	42.931731

EXPERIMENT (MOTION+WAVES)

Experimental Conditions: WP=0.8s, WH=10cm, MP=1.5s, Displacement=30cm, Acc. =4m/s^2, $\boldsymbol{\theta}$=180°

Collection

Table 9: Magnitudes of cross flow displacements of Teflon and Acryl model, all displacements are in mm

Time(Sec)	n0(Y)-Acryl	n1(Y)-Acryl	n2(Y)-Acryl	n0(Y)-Teflon	n1(Y)-Teflon	n2(Y)-Teflon
0.016667	34.0885	33.642468	32.843634	44.303	43.5793	43.2398
0.033333	33.7499	33.532135	32.87682	44.4193	43.7406	43.4737
0.05	33.7423	33.267042	32.705067	44.4375	43.5624	43.1997
0.066667	33.8749	33.283649	32.814955	44.3001	43.6313	43.6601
0.083333	33.509	33.615214	32.666101	44.483	43.6969	43.6628
0.1	33.835	33.400624	32.862648	44.1393	43.7982	43.5028
0.116667	33.7913	33.324269	32.900511	44.4166	43.5552	43.6115
0.133333	33.8171	33.510014	33.134972	44.4375	43.5585	43.6918
0.15	33.9607	33.492548	32.797738	44.4648	43.712	43.4952

EXPERIMENT (WAVES+CURRENTS+MOTION).

Experimental Conditions: MP=1.5s, Displacement=30cm, Acc. =4m/s^2, WP=1s, WH=10cm, $\boldsymbol{\theta}$=180°, V_c=0.2m/s.

Collection

Table 10: Magnitude of cross flow displacements of Teflon and Acryl model, all displacements are in mm.

Time(Sec)	n0(Y)-Acryl	n1(Y)-Acryl	n2(Y)-Acryl	n0(Y)-Teflon	n1(Y)-Teflon	n2(Y)-Teflon
0.016667	34.247775	33.705039	31.764036	44.073033	43.385269	43.243381
0.033333	33.879786	33.645464	32.187611	43.516316	44.150819	43.350815
0.05	34.139476	33.203572	32.076216	44.04731	43.636348	43.217973
0.066667	34.234388	33.349166	32.214088	43.92961	43.607271	43.296526
0.083333	34.125888	33.329918	32.082682	44.013452	43.271687	43.490883
0.1	34.381343	33.660508	32.071355	44.141697	43.584235	43.330738
0.116667	34.045174	33.602146	31.694386	43.923	43.486962	43.404686
0.133333	33.872929	33.375227	32.0354	44.018169	43.49723	43.35457
0.15	33.826253	33.659128	32.491324	44.172541	43.547019	43.379851

The magnitudes of cross flow displacements of two models (Acryl and Teflon) investigated at different experimental conditions.

COMPARISON OF RESULTS

From Table 8, Table 9 and Table 10, the Tables give the magnitude of cross flow displacements of Acryl and Teflon model at n0, n1, n2. From the values in Table 8, Table 9 and Table 10 shows that the magnitude of cross flow displacement of Teflon model is greater than the magnitude of cross flow displacement of Acryl model, this is due to fact that the mass ratio of Teflon is greater than the mass ratio of Acryl model, hence greater potential of cross flow vibrations in Teflon model as the mass ratio increases.

5.3 LOCK IN EFFECT ON TRANSVERSE CYLINDER VIBRATIONS

Collection

Transverse cylinder vibrations with frequency at or near the excitation frequency have large effect on magnitude of Transverse vibrations of a cylinder. It is found that when the natural frequency of a cylinder matches with or near the excitation frequency the magnitude of Transverse Vibrations of cylinder increases. Lock in effect occurs in the range of frequencies over which the cylinder vibrations can shift the excitation frequency by as much as $\pm$40% from a stationary cylinder vibrations frequency.

CASE STUDY 2

Parameters:

Natural frequency of Teflon model f_n=2.0HZ.

Mass of Teflon m=0.1581Kg.

Natural frequency of Acryl model f_n=5.38HZ.

Mass of Acryl model m=0.08624Kg.

EXPERIMENT (MOTION+WAVES).

Experimental Conditions: WP=0.8s, WH=10cm, MP=1.5s,

Displacement=30cm, Acc. =4ms^2, $\boldsymbol{\theta}$=180°

Collection

Table 11: Magnitude of cross flow displacements of Teflon and Acryl model, all displacements are in mm.

Time(sec)	n0(Y)-Acryl	n1(Y)-Acryl	n2(Y)-Acryl	n0(Y)-Teflon	n1(Y)-Teflon	n2(Y)-Teflon
0.016667	34.088532	33.642468	32.843634	44.303042	43.5579281	43.23979
0.033333	33.749882	33.532135	32.87682	44.419261	43.740618	43.47369
0.05	33.742332	33.267042	32.705067	44.437471	43.562443	43.199657
0.066667	33.874874	33.283649	32.814955	44.300126	43.631274	43.660103
0.083333	33.509015	33.615214	32.666101	44.483009	43.696864	43.662835
0.1	33.835004	33.400624	32.862648	44.139298	43.798184	43.502808
0.116667	33.791289	33.324269	32.900511	44.416551	43.5552	43.611485
0.133333	33.817085	33.570014	33.134972	44.437471	43.558502	43.691761
0.15	33.960728	33.492548	32.797738	44.464758	43.711971	43.49517

EXPERIMENT (MOTION+CURRENTS+WAVES).

Experimental Conditions: MP=1.5s, Displacement=30cm, Acc. =4m/s^2, WP=1s, WH=10cm, V_c=0.2m/s

Motion excitation frequency f_m=0.67HZ.

Shedding frequency due to current f_s=3.92HZ.

Wave excitation frequency f_w=1HZ.

Collection

Table 12: Magnitude of cross flow displacements of Teflon and Acryl model, all displacements are in mm.

Time(sec)	n0(Y)-Acryl	n1(Y)-Acryl	n2(Y)-Acryl	n0(Y)-Teflon	n1(Y)-Teflon	n2(Y)-Teflon
0.016667	34.247775	33.705039	31.764036	44.231904	43.47084	43.197389
0.033333	33.879786	33.645464	32.187611	44.482736	43.677565	43.102583
0.05	34.139476	33.203572	32.076216	44.349516	43.546271	43.245303
0.066667	34.234388	33.349166	32.214088	44.221681	43.71103	43.050912
0.083333	34.125888	33.329918	32.082682	44.201463	43.639053	43.148911
0.1	34.381343	33.660508	32.071355	44.392771	43.590472	43.210682
0.116667	34.045174	33.602146	31.694386	44.279456	43.59849	43.447569
0.133333	33.872929	33.375227	32.0354	44.332253	43.657368	43.261907
0.15	33.826253	33.659128	32.491324	44.236023	43.607303	43.264963

COMPARISON OF RESULTS

From Table 11, it is found that the magnitude of cross flow displacement of Teflon model is greater than the magnitude of cross flow displacement of Acryl model, this is due to fact that the natural frequency of Teflon model is close to excitation frequency of the source and hence lock in condition is expected to occur in Teflon model and hence large cross flow displacements. Another reason is the mass ratio of Teflon model is also larger than the mass ratio of Acryl hence large cross flow displacements in Teflon model.

From Table 12, the cross flow displacement of Teflon model is larger than the cross flow displacements of Acryl model. In this case:

Teflon model is locked in with wave excitation and Acryl model is locked in by current excitation, both these effects increases the magnitude of cross

Collection

flow displacements on both models, but on top of that the mass ratio of Teflon model is larger than the mass ratio of Acryl model, that is why under the same experimental condition the magnitude of cross flow displacement of Teflon model is larger than Acryl model, because there are two reasons in Teflon model affecting the magnitude of cross flow which is mass ratio and excitation frequency of wave.

5.4: Experimental results of behavior of Acryl model under motion of Acryl model. Experimental condition (Motion Period T=1.5s and displacement=30cm).

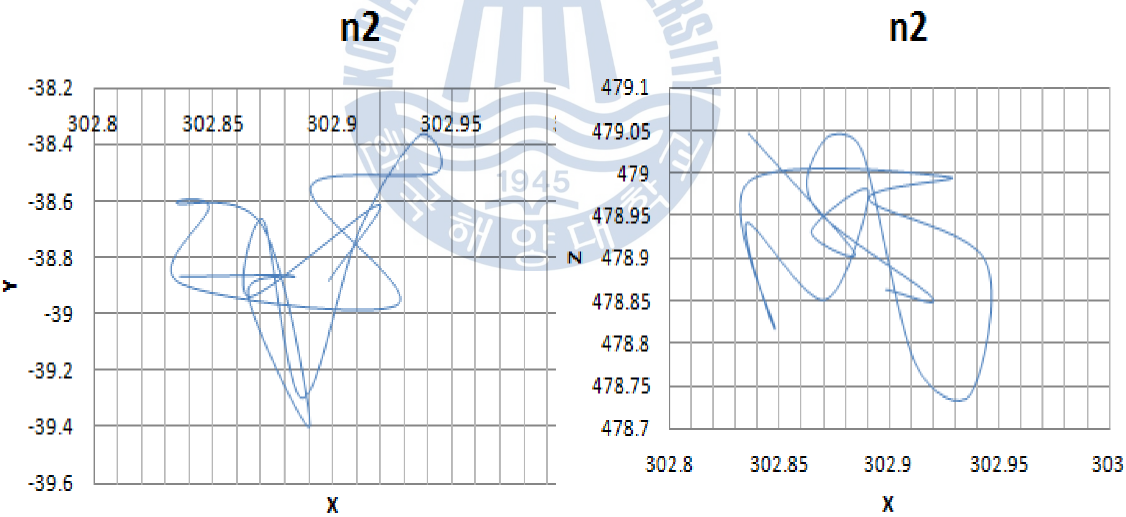

Figure 16: X-Y and X-Z trajectories of point n2.

Collection

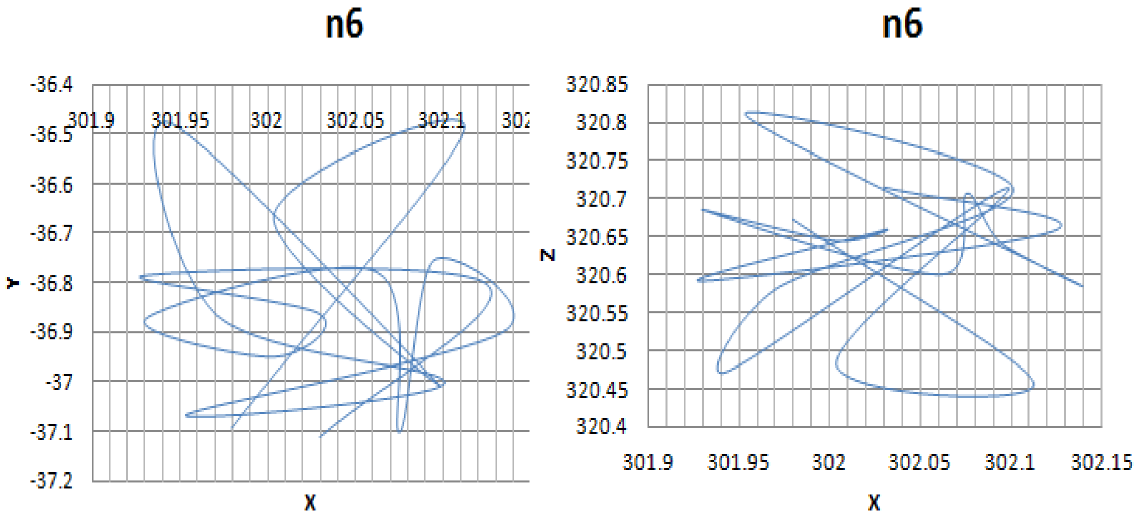

Figure 17: X-Y and X-Z trajectories of point n6.

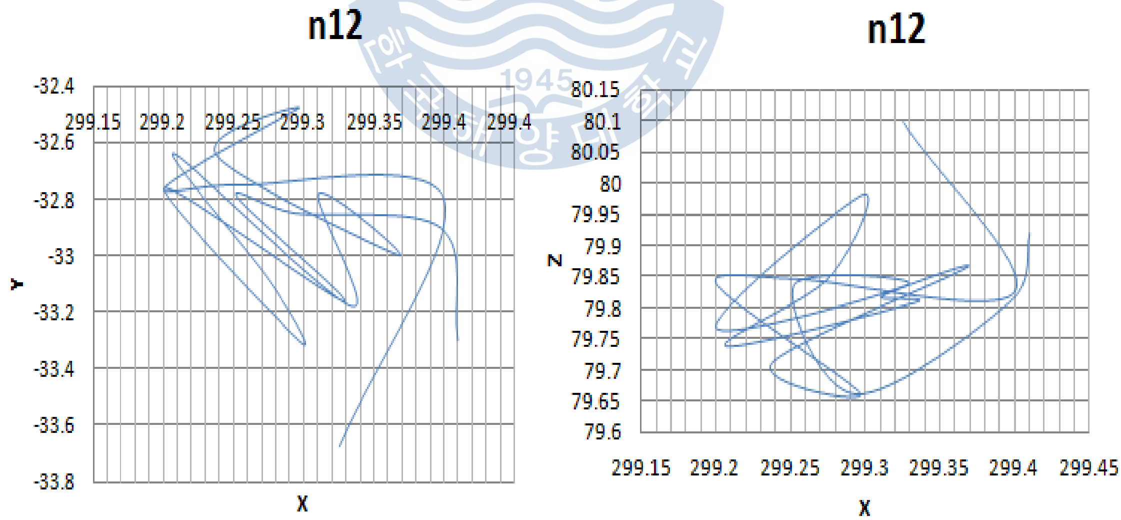

Figure 18: X-Y and X-Z trajectories of point n12.

5.5: Experimental results of behavior of Acryl model under effect of motion of a cylinder alone. Experimental Conditions (Motion Period T=3s, Displacement 30cm).

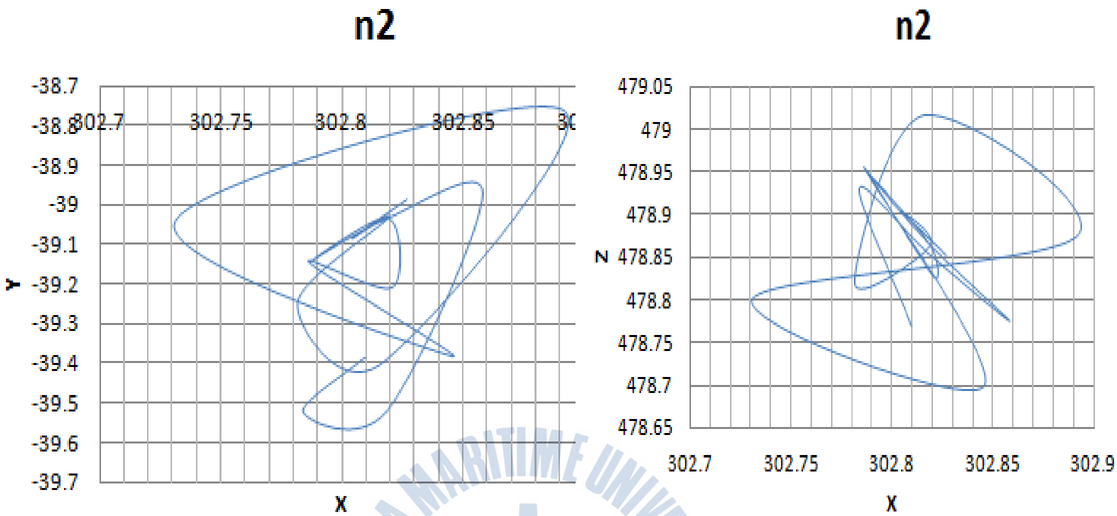

Figure 19: X-Y and X-Z trajectories of point n2.

KOREA MARITIME UNIVERSITY
1945
한국해양대학교

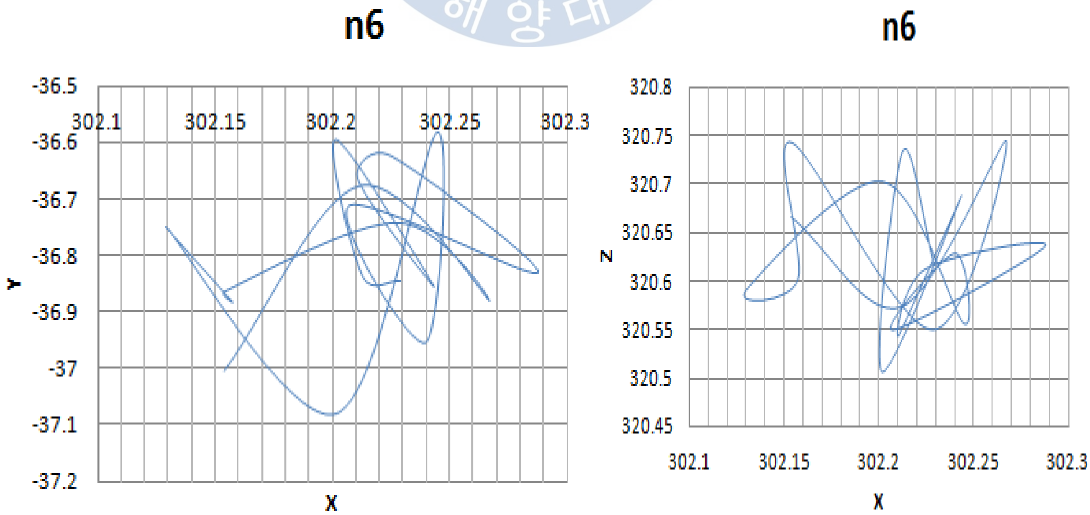

Figure 20: X-Y and X-Z trajectories of point n6

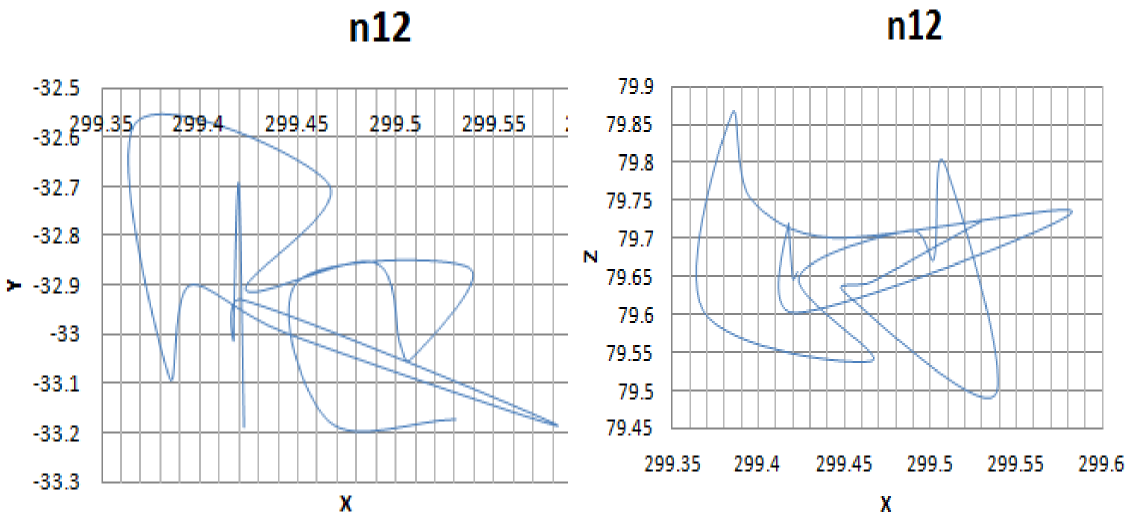

Figure 21: X-Y and X-Z trajectories of point n12.

5.6: Experimental results of behavior of Teflon model under effect of Motion.

Experimental Conditions (Motion period T=1.5s and Displacement 30cm).

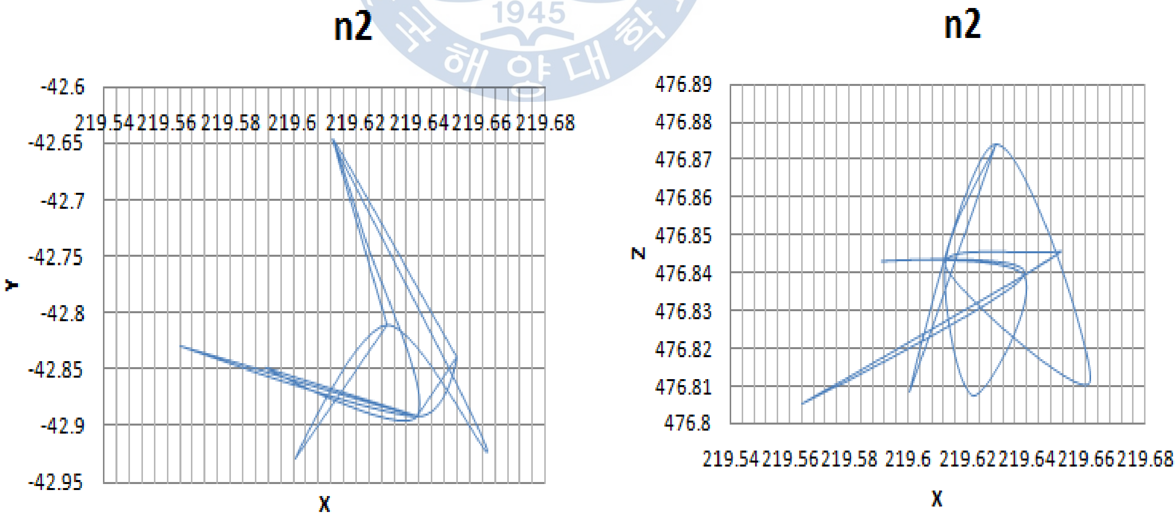

Figure 22: X-Y and X-Z trajectories of point n2

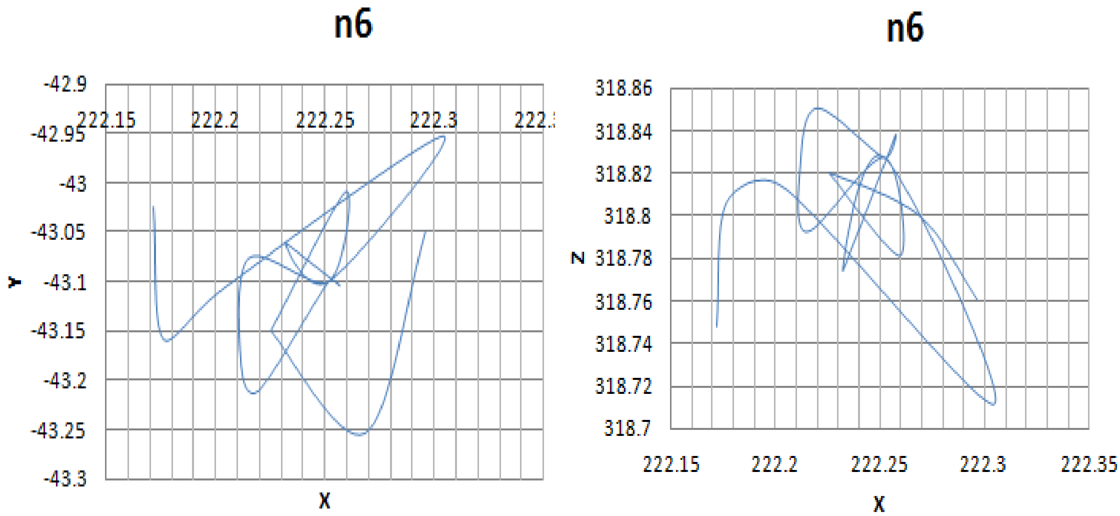

Figure 23: X-Y and X-Z trajectories of point n6.

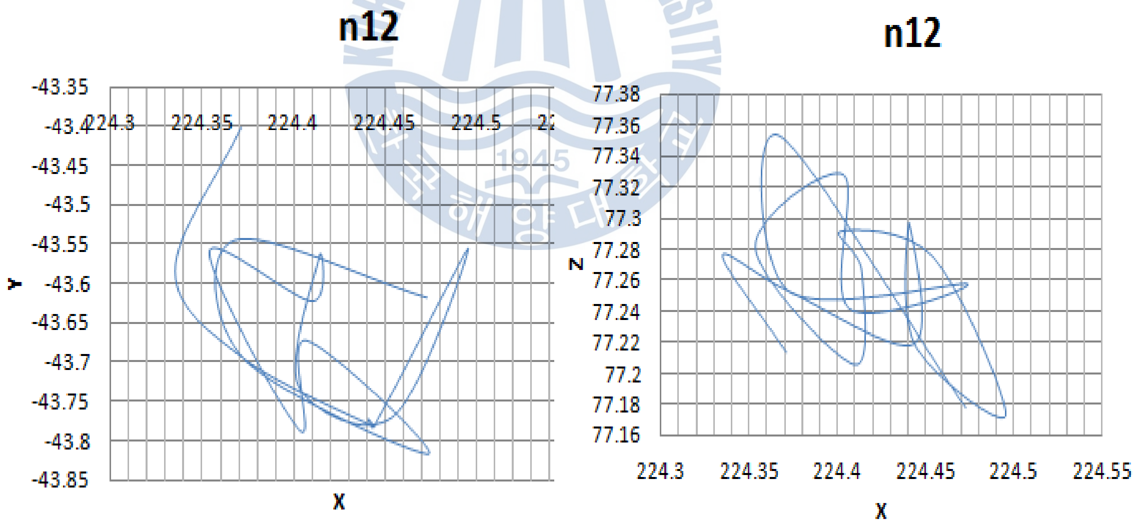

Figure 24: X-Y and X-Z trajectories of point n12.

5.7: Experimental results of behavior of Teflon Model under effect of Motion. Experimental Conditions (Motion Period T=3s and Displacement 30cm).

dCollection

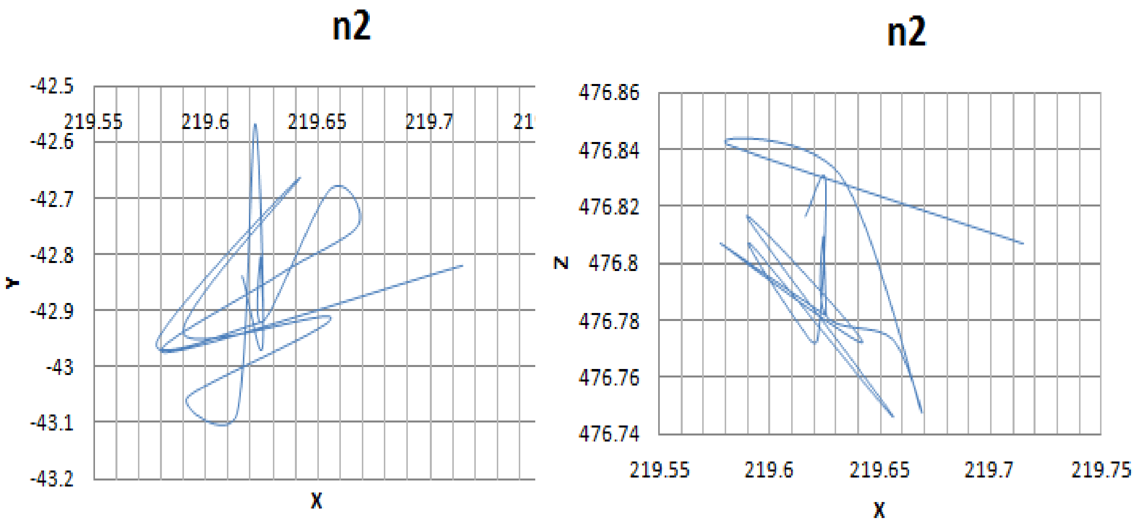

Figure 25: X-Y and X-Z trajectories of point n2.

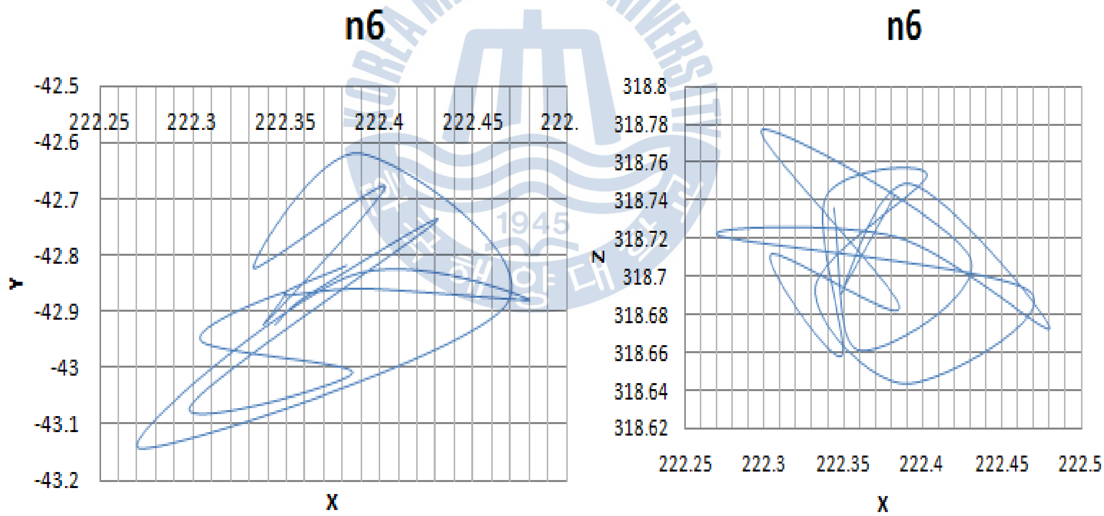

Figure 26: X-Y and X-Z trajectories of point n6.

dCollection

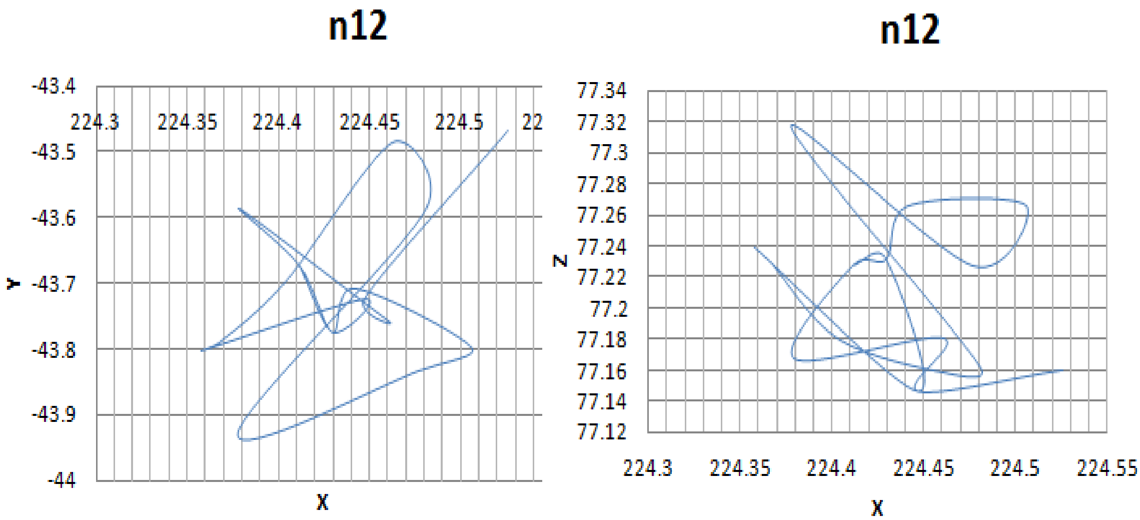

Figure 27: X-Y and X-Z trajectories of point n12.

5.8: Experimental results of behavior of Acryl Model under Wave.

Experimental Conditions (Wave period T=0.8s and Wave Height H=5cm).

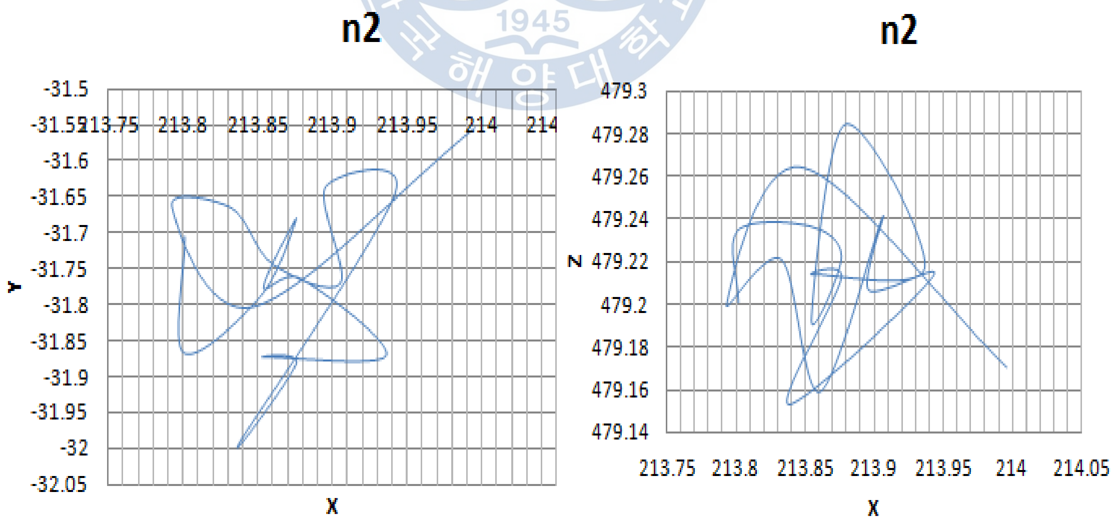

Figure 28: X-Y and X-Z trajectories of point n2.

Collection

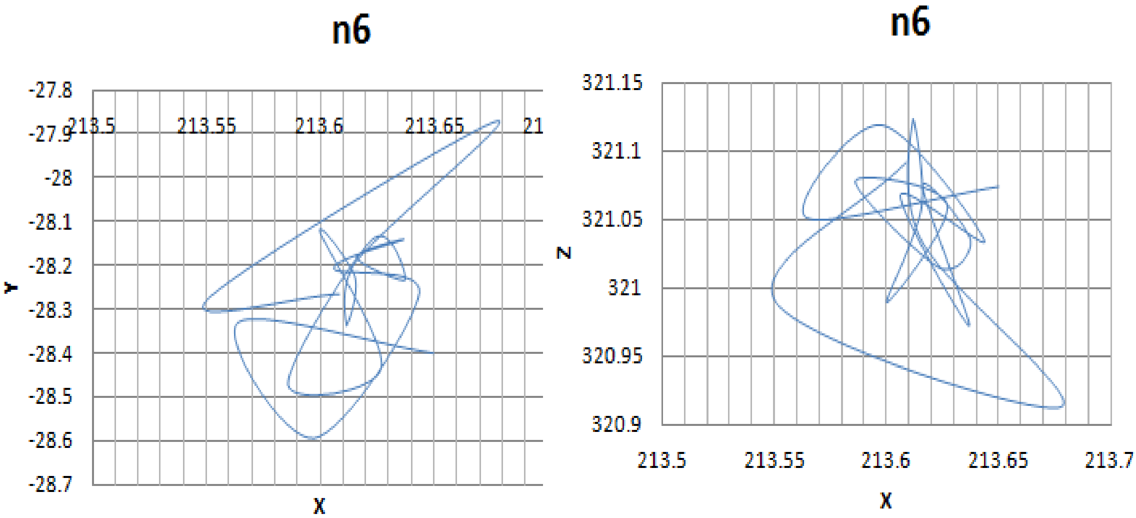

Figure 29: X-Y and X-Z trajectories of point n6.

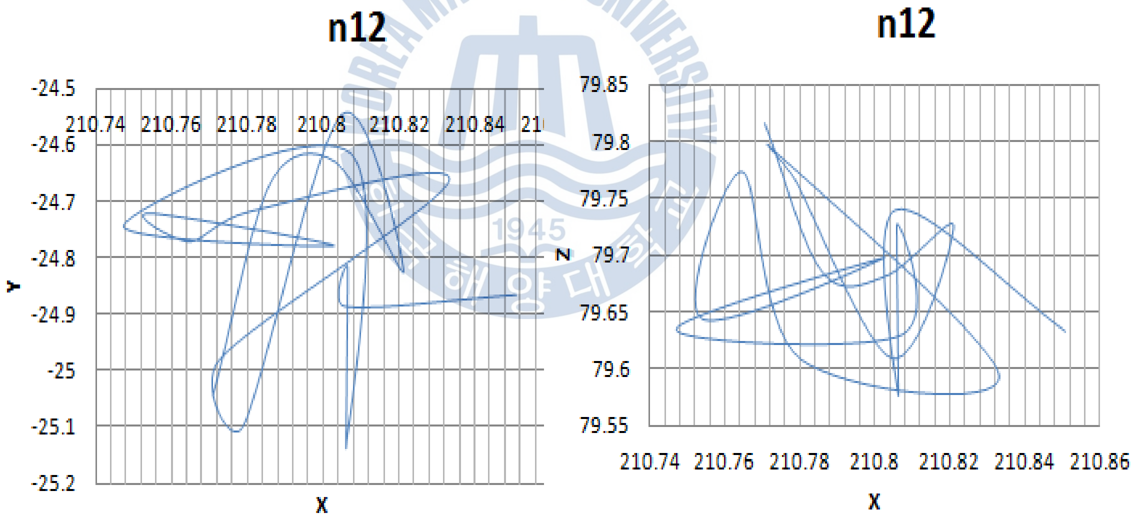

Figure 30: X-Y and X-Z trajectories of point n12.

Collection

5.9: Experimental results of behavior of Acryl Model under Wave.

Experimental Conditions (Wave period T=0.8s and Wave Height H=10cm).

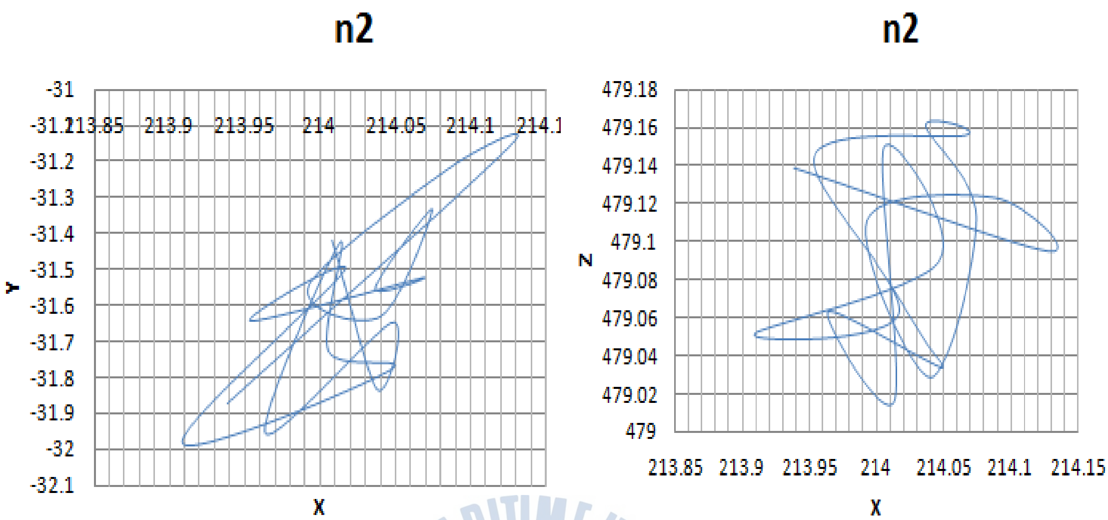

Figure 31: X-Y and X-Z trajectories of point n2.

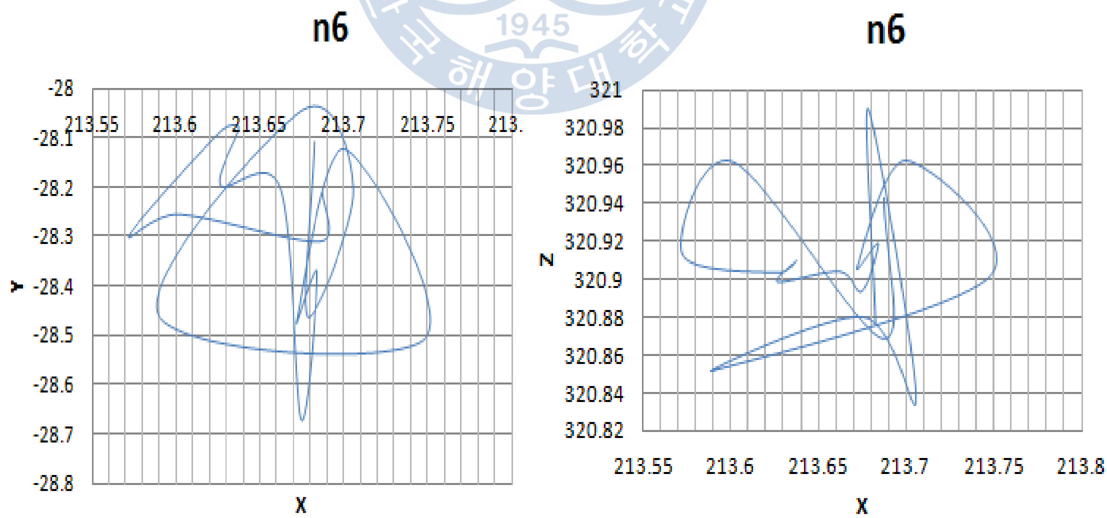

Figure 32: X-Y and X-Z trajectories of point n6.

Collection

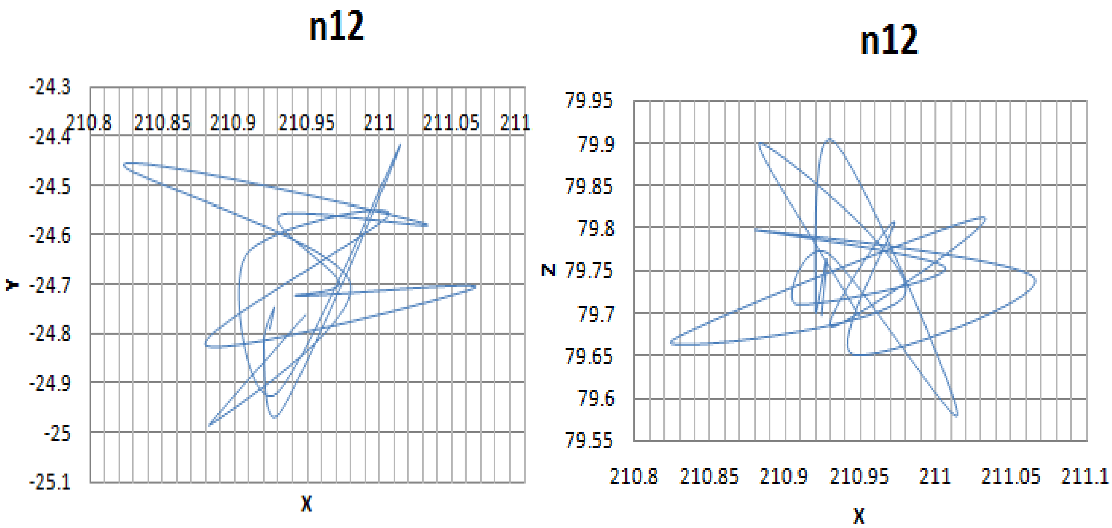

Figure33: X-Y and X-Z trajectories of point n12.

5.10: Experimental results of behavior of Teflon Model under effect of Wave.

Experimental Conditions (Wave period T=0.8s and Wave Height H=10cm).

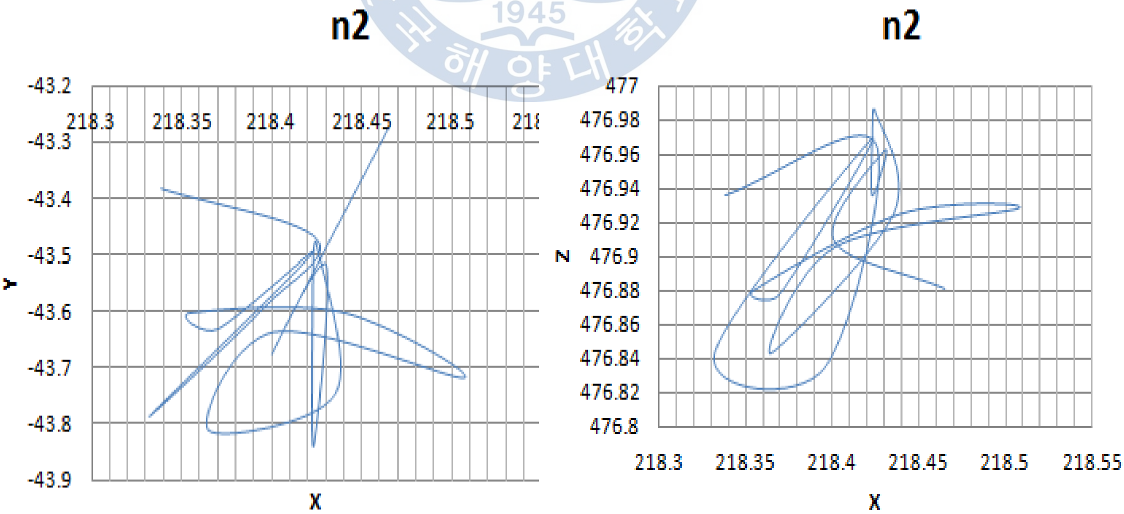

Figure 34: X-Y and X-Z trajectories of point n2.

Collection

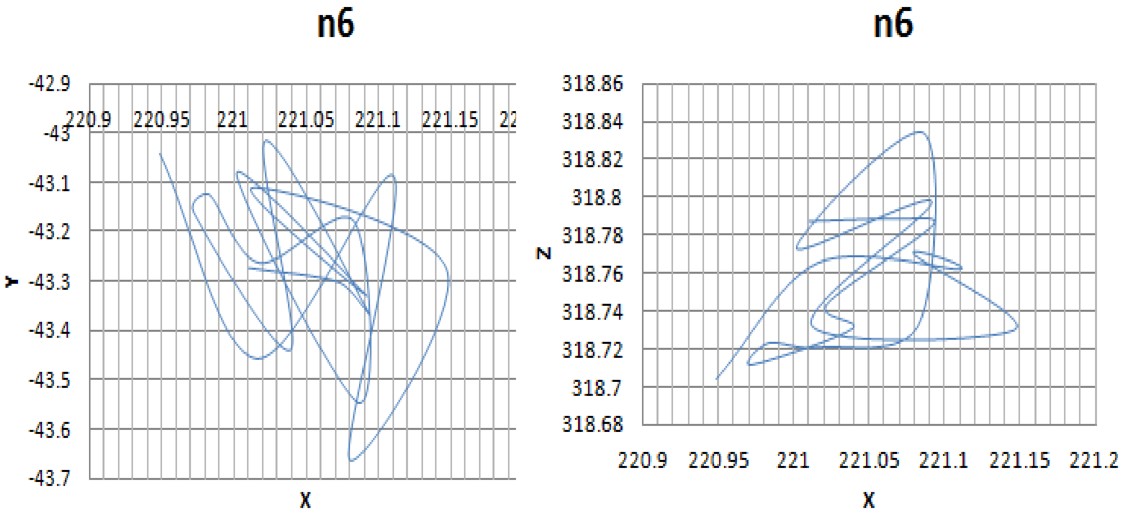

Figure 35: X-Y and X-Z trajectories of point n6.

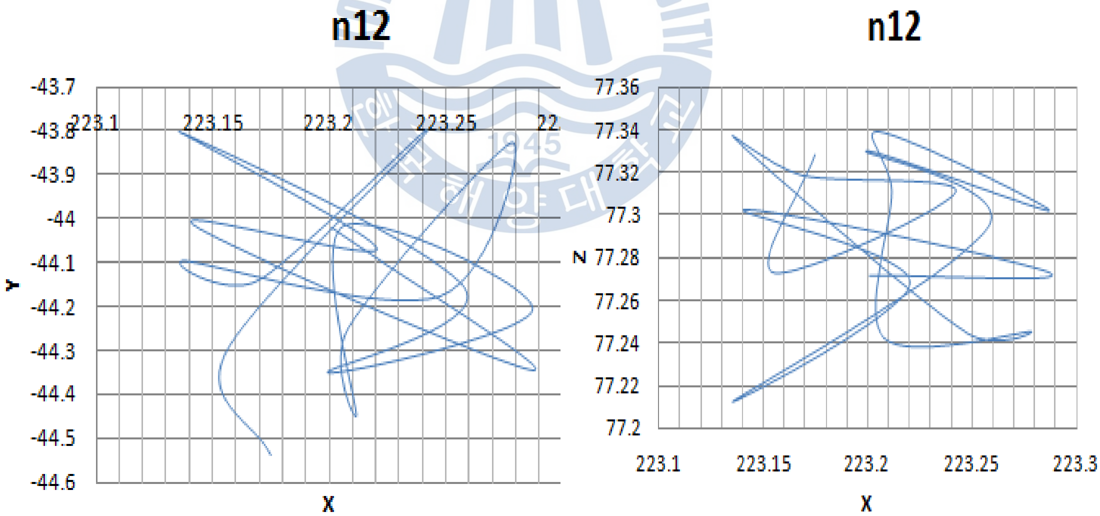

Figure 36: X-Y and X-Z trajectories of point n12.

Collection

5.11: Experimental results of behavior of Acryl Model under effect of Wave.

Experimental Conditions (Wave Period T=1s and Wave height H=5cm).

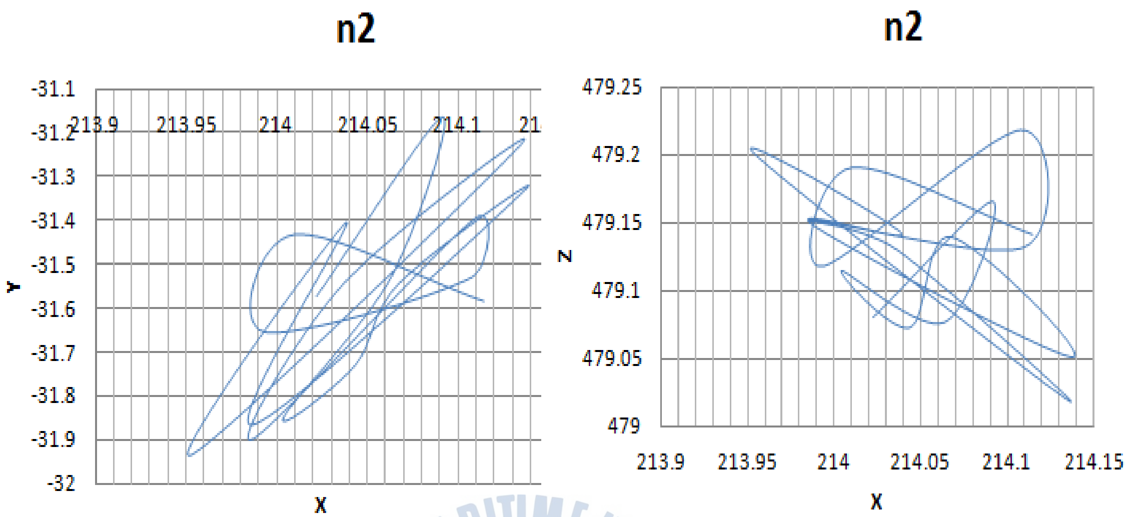

Figure 37: X-Y and X-Z trajectories of point n2.

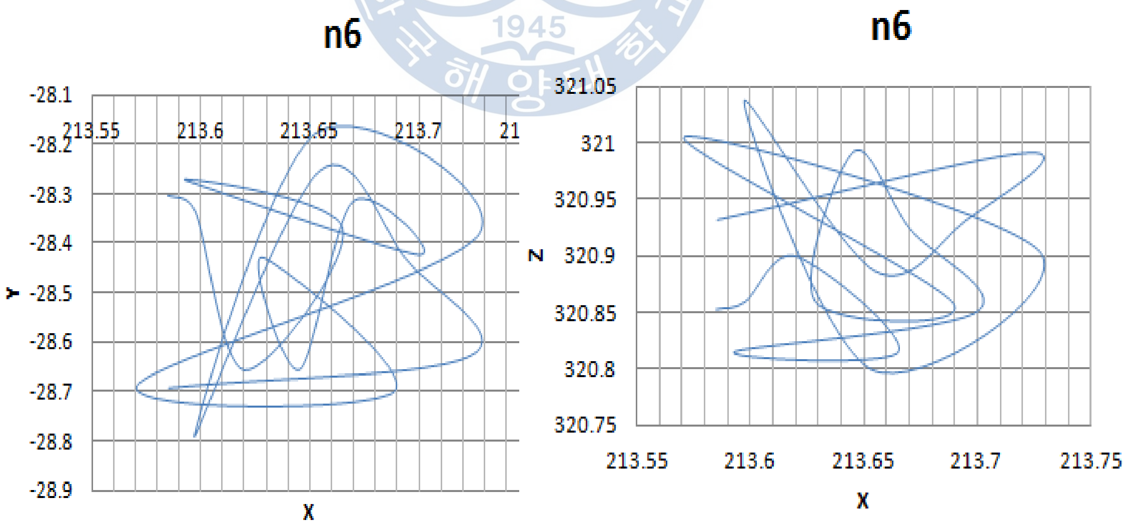

Figure 38: X-Y and X-Z trajectories of point n6.

KOREA MARITIME UNIVERSITY 1945 한국해양대학교

dCollection

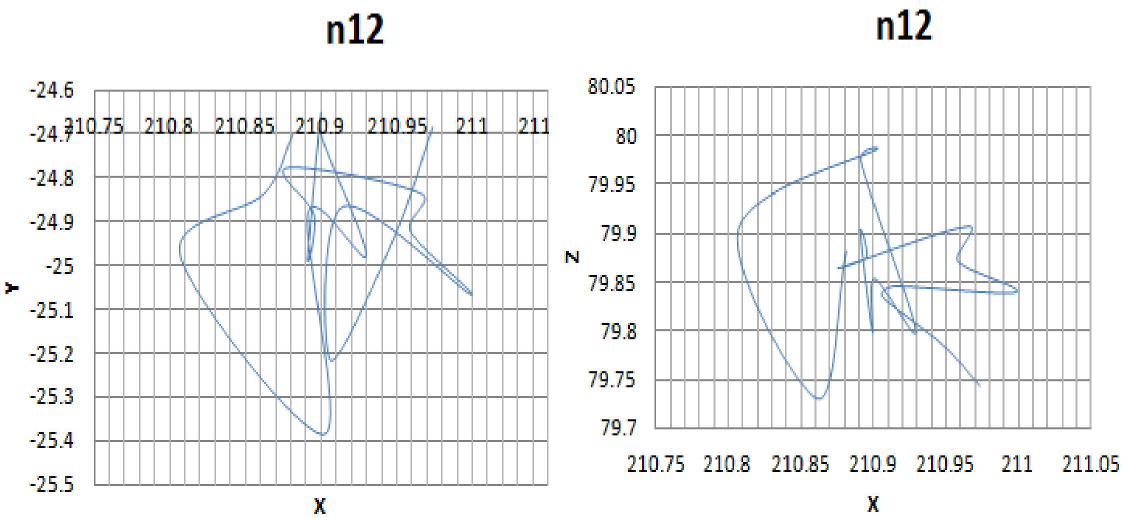

Figure 39: X-Y and X-Z trajectories of point n12.

KOREA MARITIME UNIVERSITY
1945
한국해양대학교

5.12: Experimental results of behavior of Teflon Model under effect of Wave.

Experimental Conditions (Wave Period T=1s and Wave Height H=5cm).

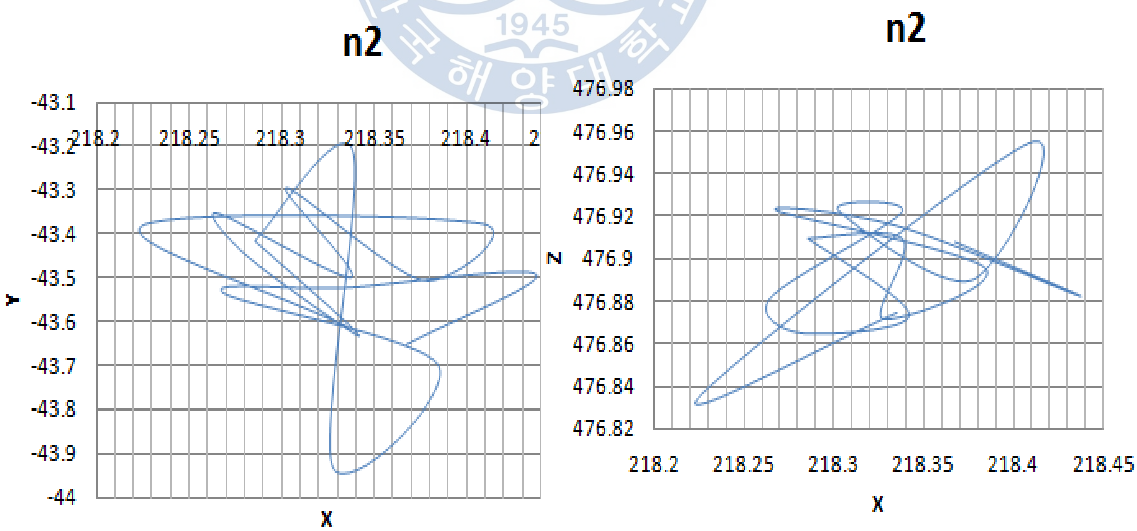

Figure 40: X-Y and X-Z trajectories of point n2.

dCollection

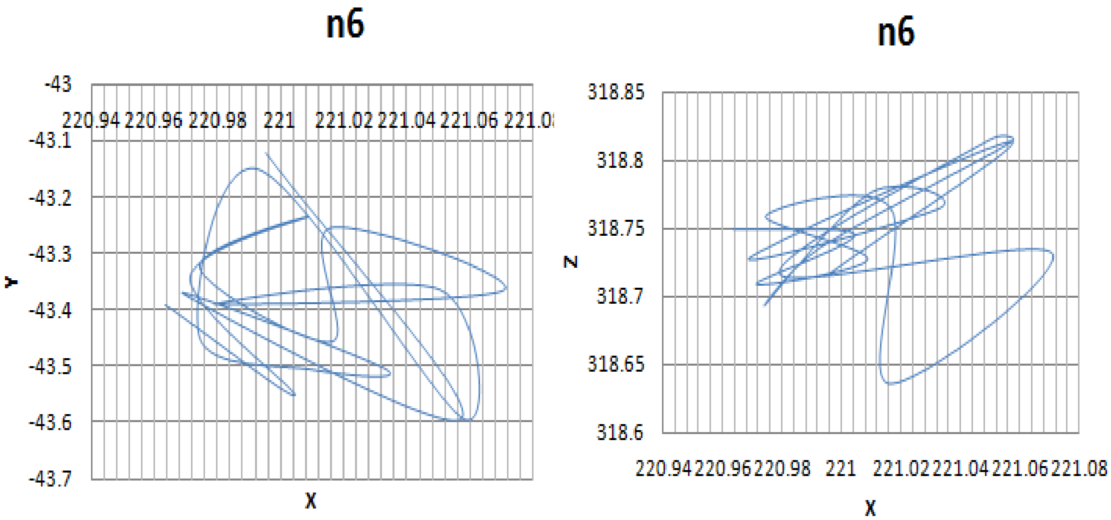

Figure 41: X-Y and X-Z trajectories of point n6.

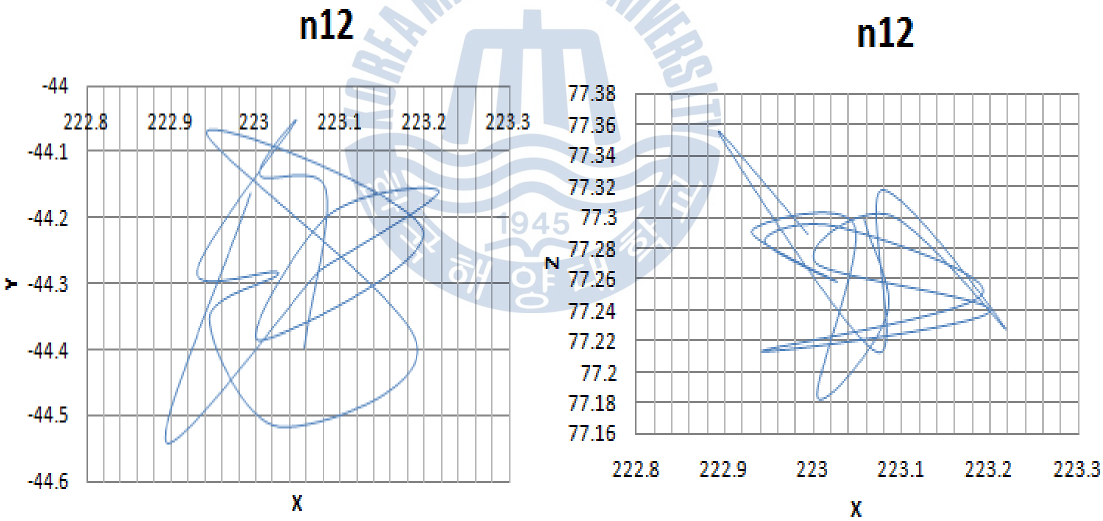

Figure 42: X-Y and X-Z trajectories of point n12.

KOREA MARITIME UNIVERSITY 1945

dCollection

5.13: Experimental results of behavior of Acryl Model under effects of Wave.

Experimental Conditions (Wave Period T=1s and Wave Height H=10cm) .

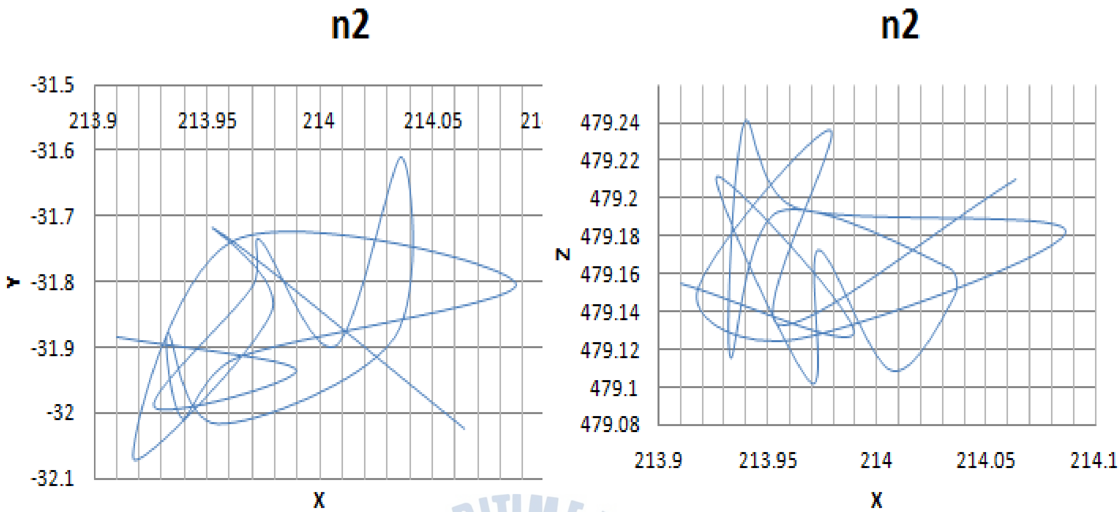

Figure 43: X-Y and X-Z trajectories of point n2.

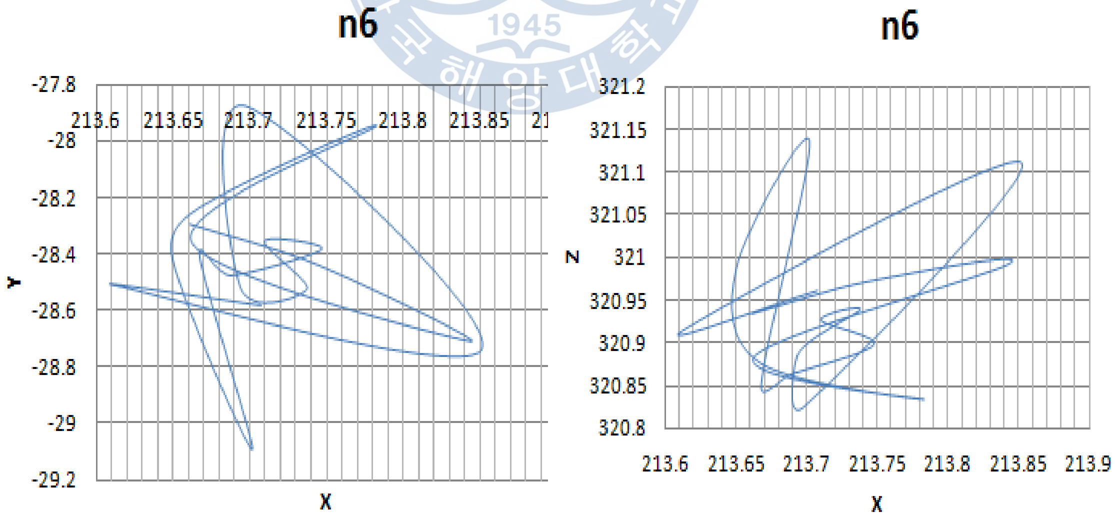

Figure 44: X-Y and X-Z trajectories of point n6.

KOREA MARITIME UNIVERSITY
1945
dCollection

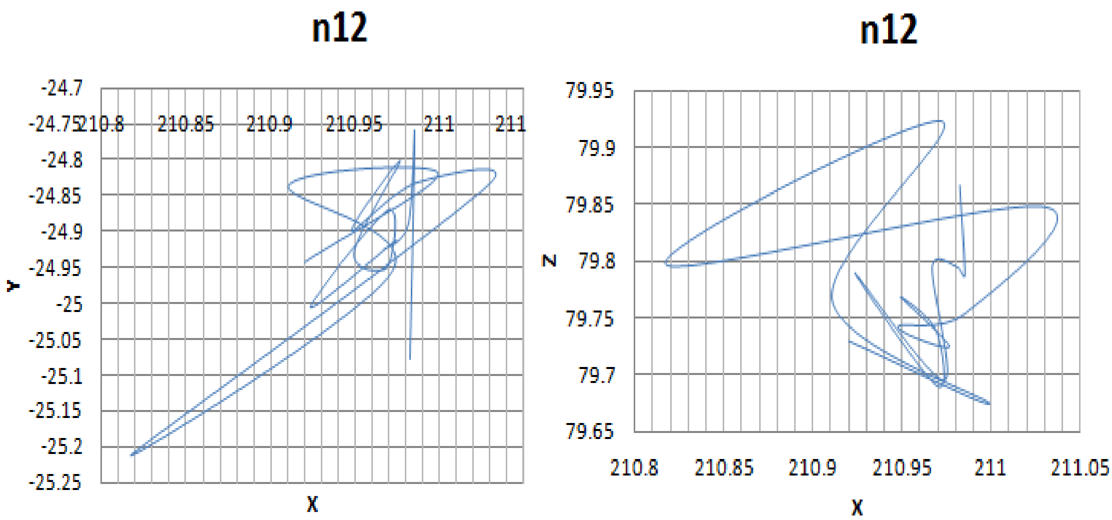

Figure 45: X-Y and X-Z trajectories of point n12.

5.14: Experimental results of behavior of Teflon Model under effect of Wave. Experimental Conditions (Wave Period T=1s and Wave Height H=10cm).

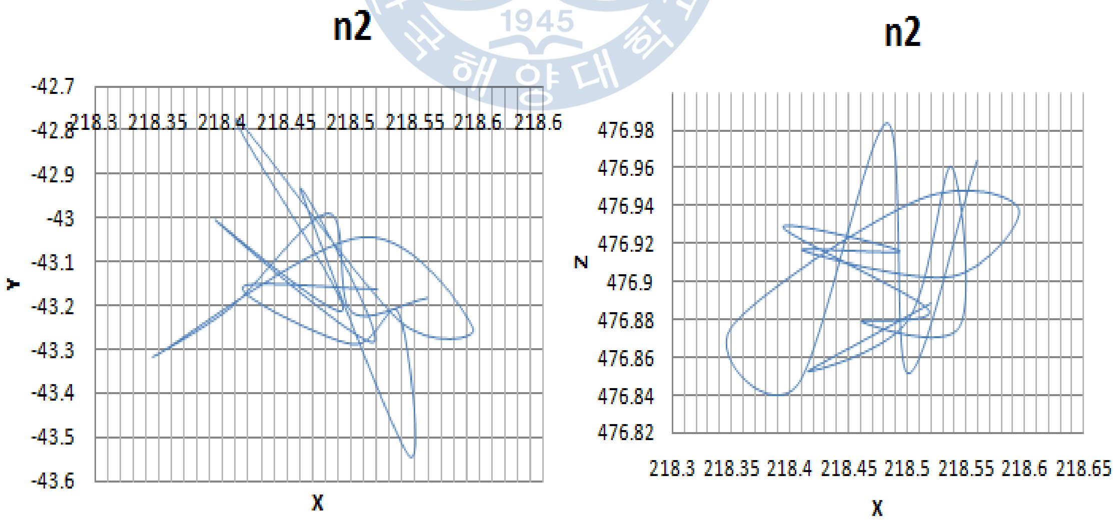

Figure 46: X-Y and X-Z trajectories of point n2.

dCollection

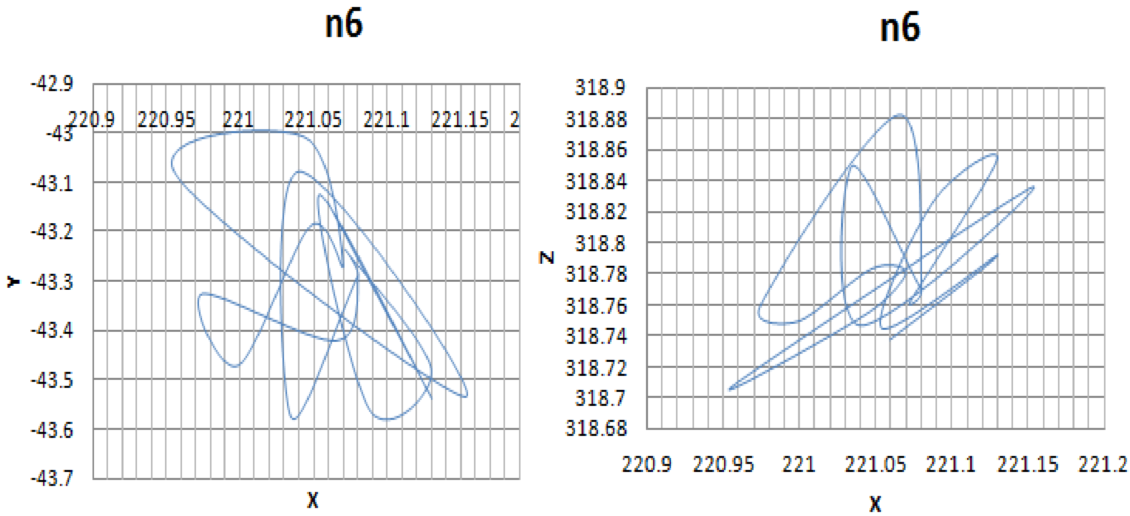

Figure 47: X-Y and X-Z trajectories of point n6.

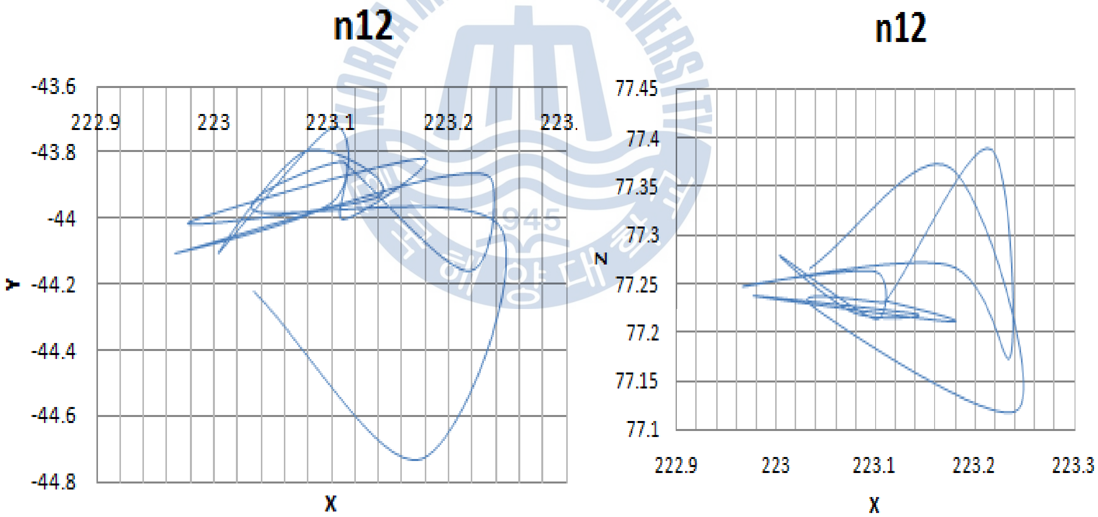

Figure 48: X-Y and X-Z trajectories of point n12.

Collection

5.15: Experimental results of Acryl Model under effect of Motion and Wave. Experimental Conditions (Motion Period T=1.5s, Displacement 30cm, Wave Height H=10cm, Wave period T=0.8s and angle$\boldsymbol{\theta}$=180°)

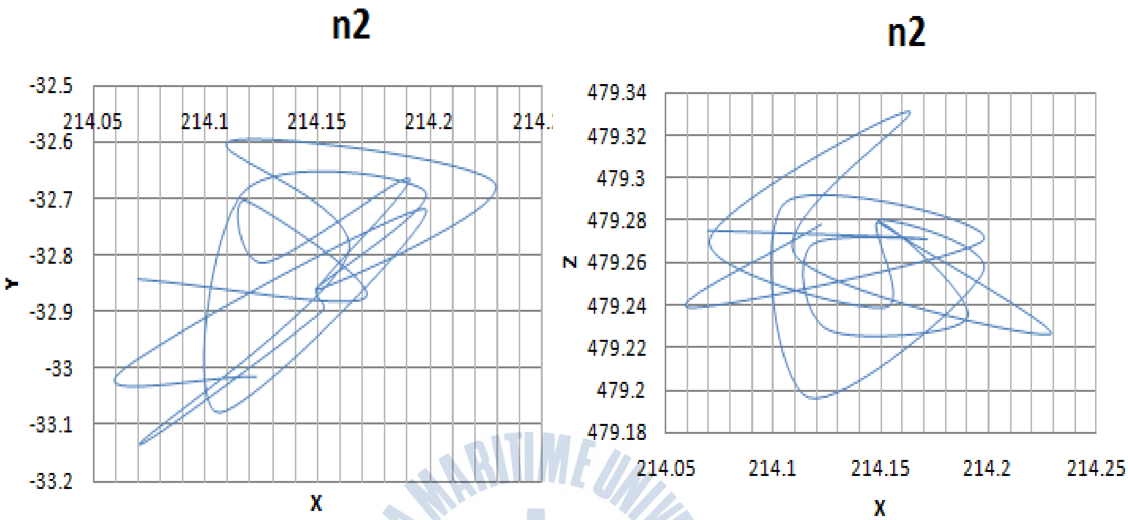

Figure 49: X-Y and X-Z trajectories of point n2.

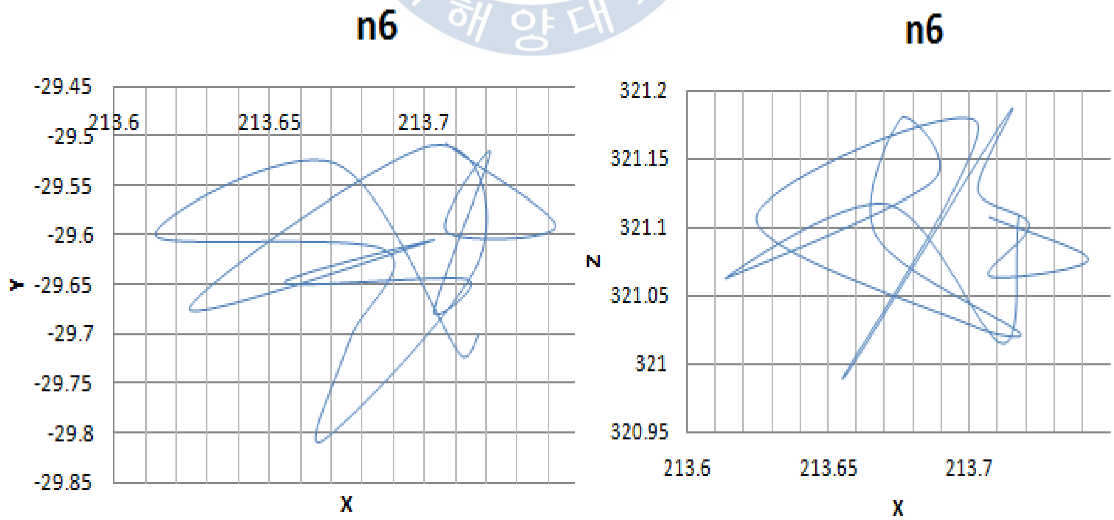

Figure 50: X-Y and X-Z trajectories of point n6.

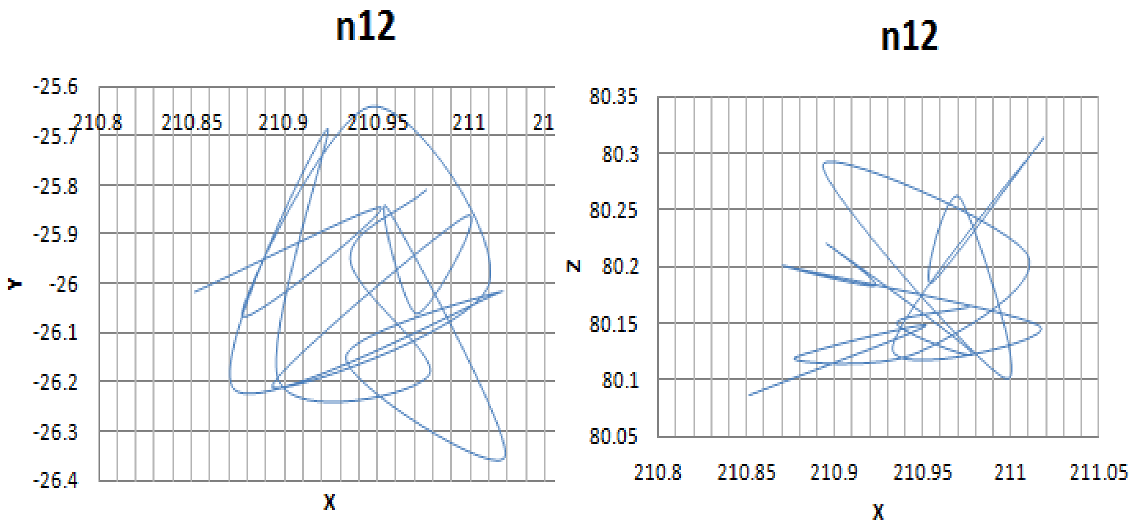

Figure 51: X-Y and X-Z trajectories of point n12.

5.16: Experimental results of behavior of Teflon Model under effect of Wave and Motion. Experimental Conditions (Motion Period T=1.5s, Displacement 30cm, Wave Period T=0.8s, Wave Height H=10cm and angle θ=180°).

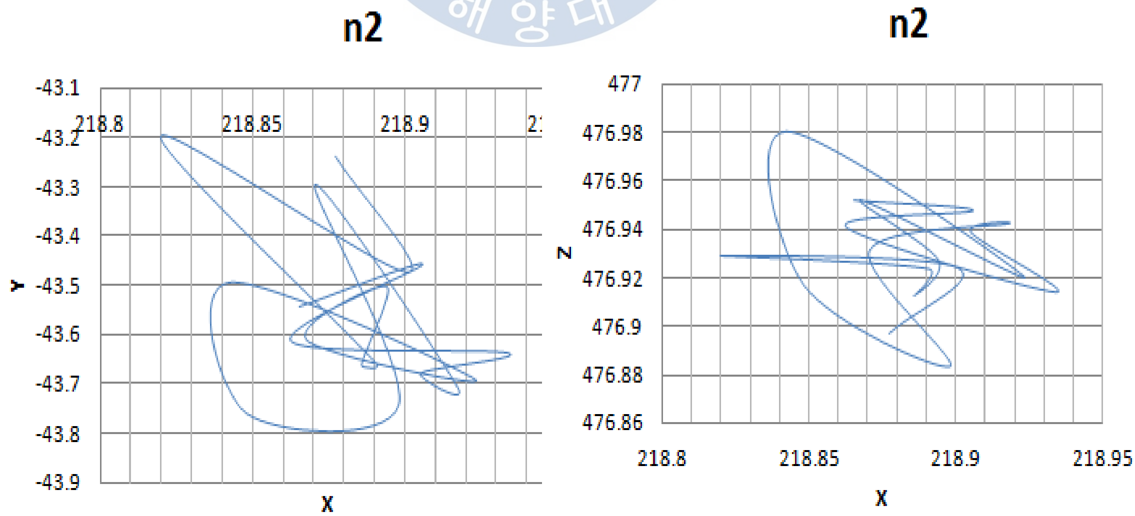

Figure 52: X-Y and X-Z trajectories of point n2.

dCollection

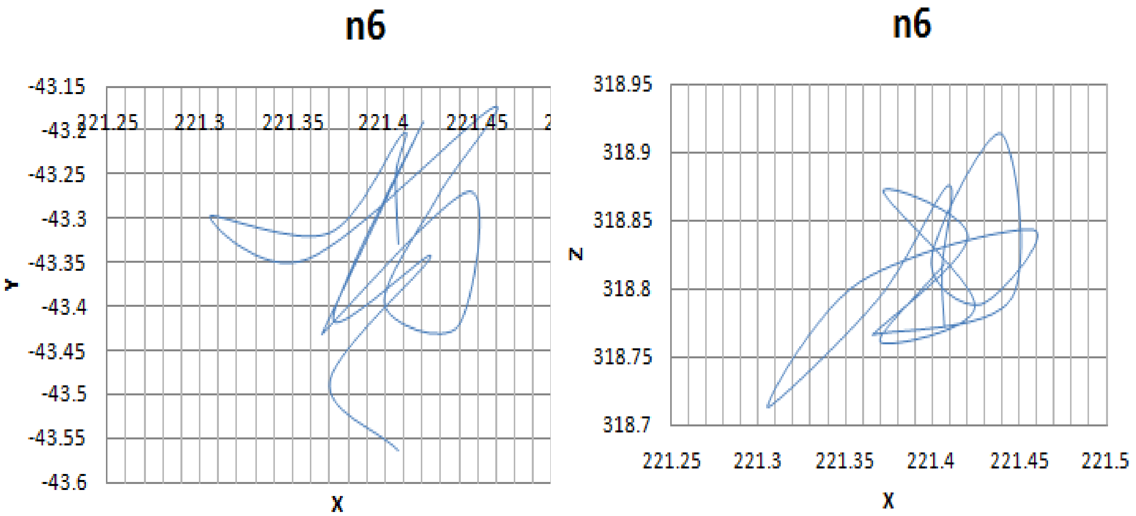

Figure 53: X-Y and X-Z trajectories of point n6.

KOREA MARITIME UNIVERSITY
1945

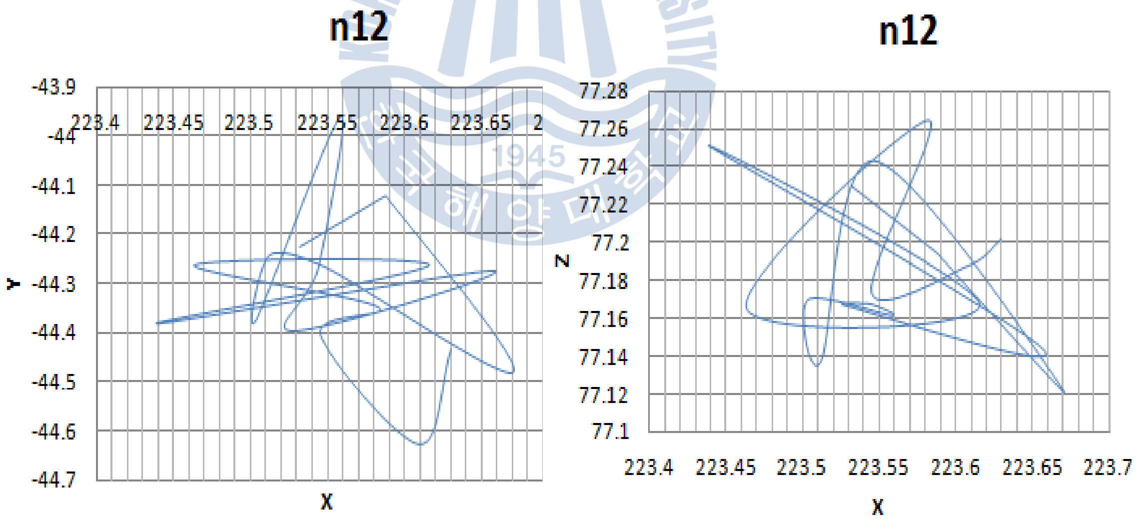

Figure 54: X-Y and X-Z trajectories of point n 12.

dCollection

5.17: Experimental results of Acryl model under effect of Motion and Wave. Experimental Conditions (Motion Period T=1.5s, Displacement 30cm, Wave period T=0.8s, Wave Height H=10cm and angle θ=360°).

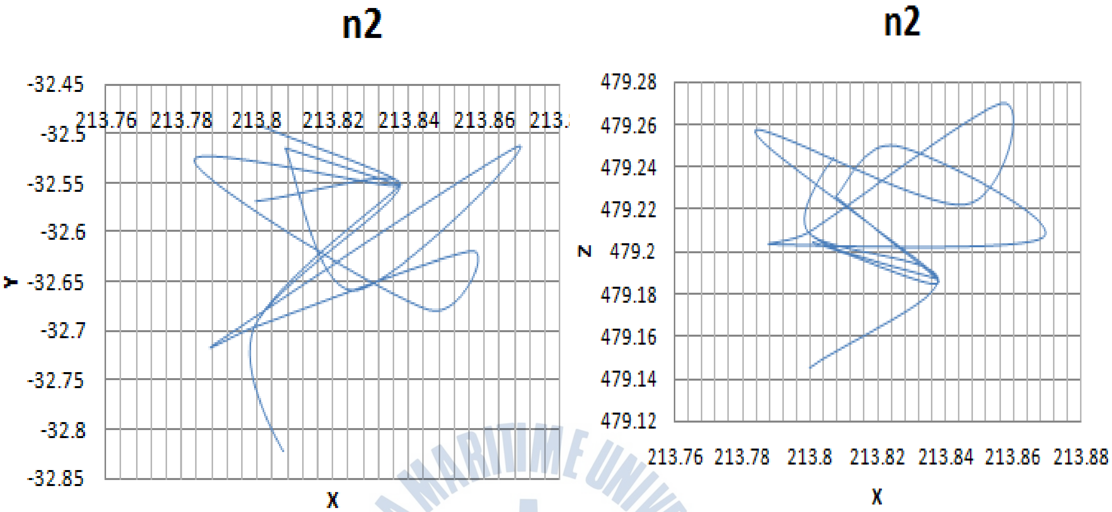

Figure 55: X-Y and X-Z trajectories of point n2.

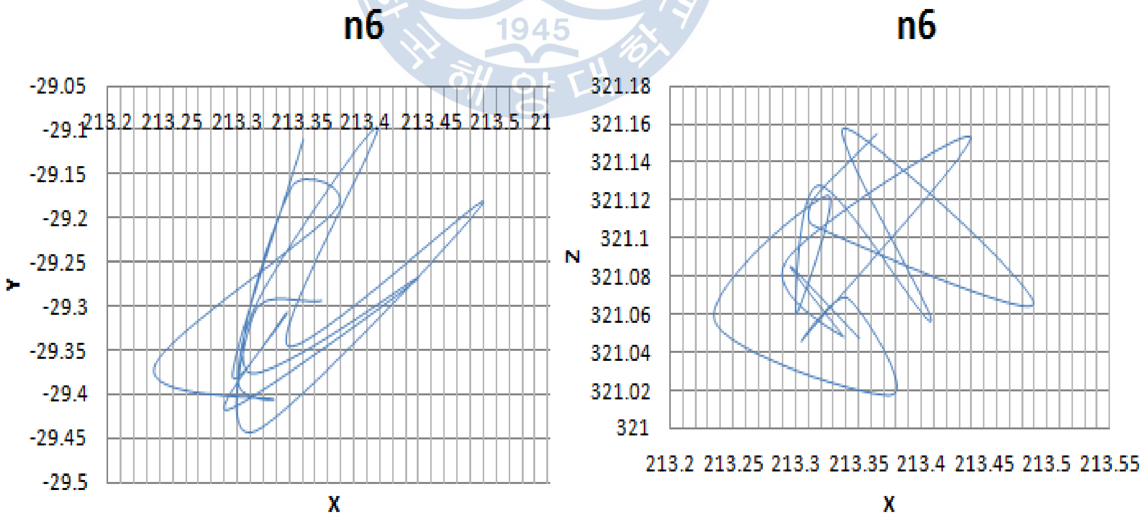

Figure 56: X-Y and X-Z trajectories of point n6.

dCollection

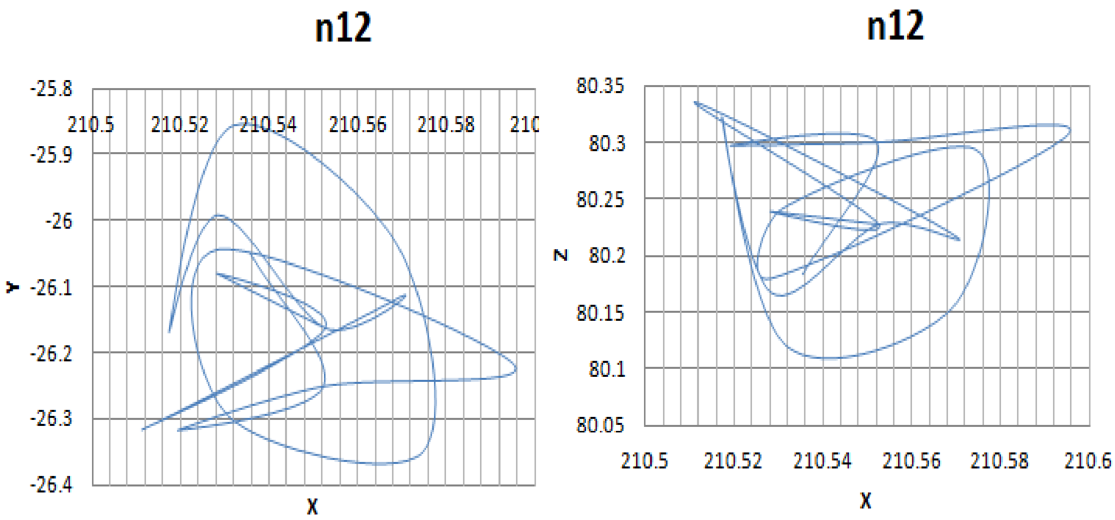

Figure 57: X-Y and X-Z trajectories of point n12.

5.18: Experimental results of behavior of Teflon Model under effect of Wave and Motion. Experimental Conditions (Motion Period T=1.5s, Displacement 30cm, Wave Period T=0.8s, Wave Height H=10cm and angle θ=360°).

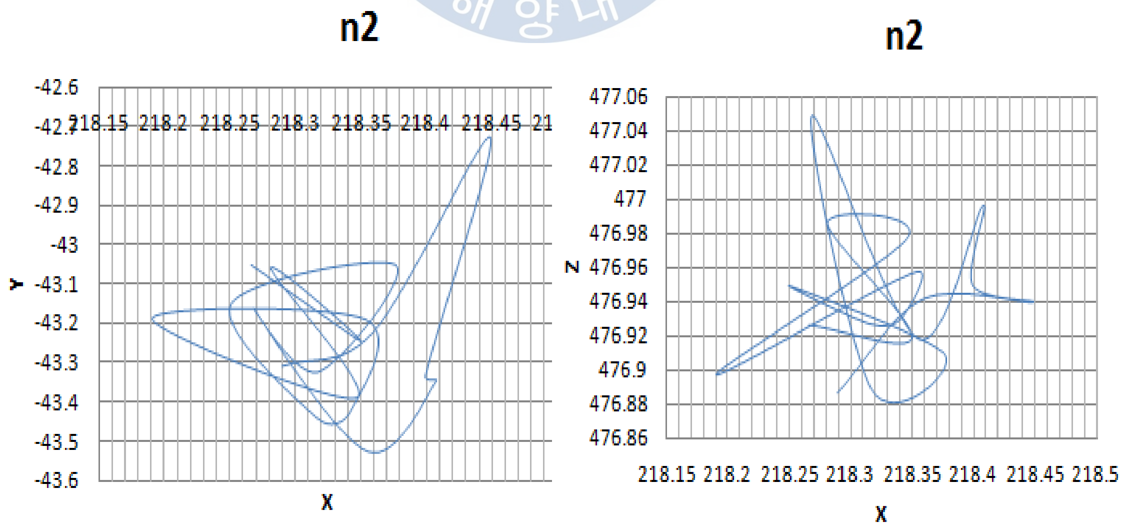

Figure 58: X-Y and X-Z trajectories of point n2.

Collection

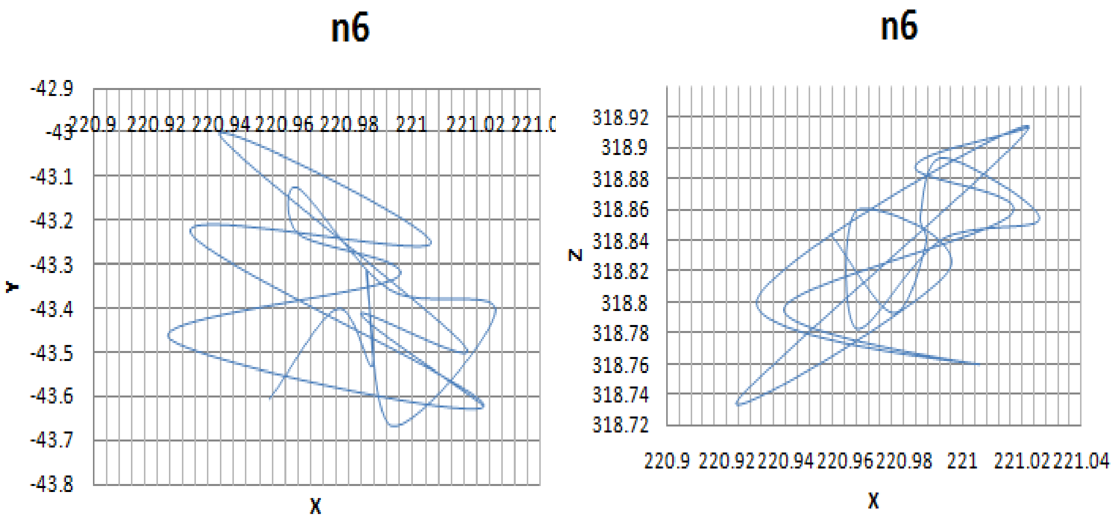

Figure 59: X-Y and X-Z trajectories of point n6.

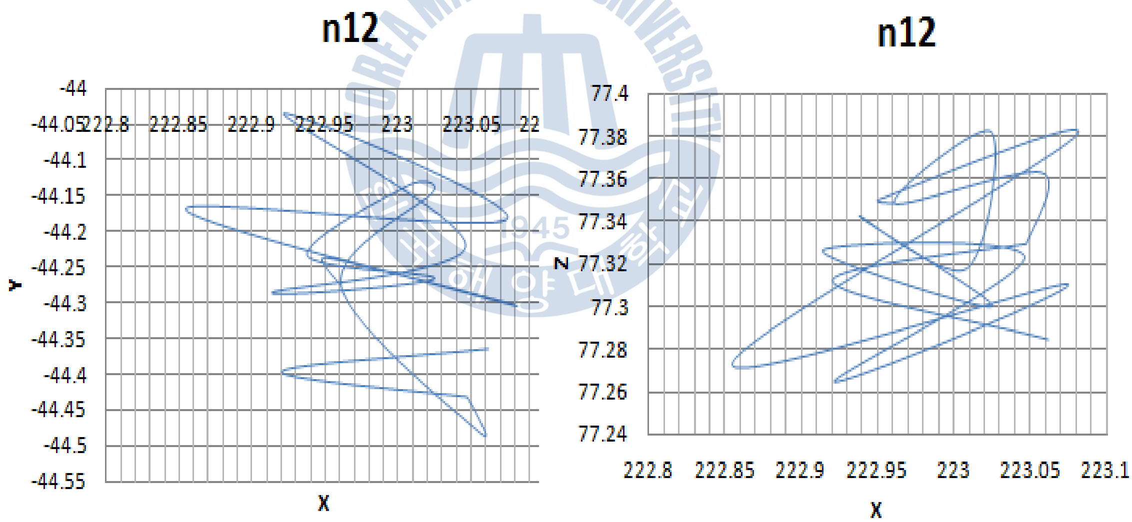

Figure 60: X-Y and X-Z trajectories of point n12.

5.19: Experimental results of behavior of Acryl model under effect of Wave and Motion. Experimental Conditions (Motion Period T=1.5s, Displacement 30cm, Wave Period T=1s, Wave Height H=10cm and angleθ=180°).

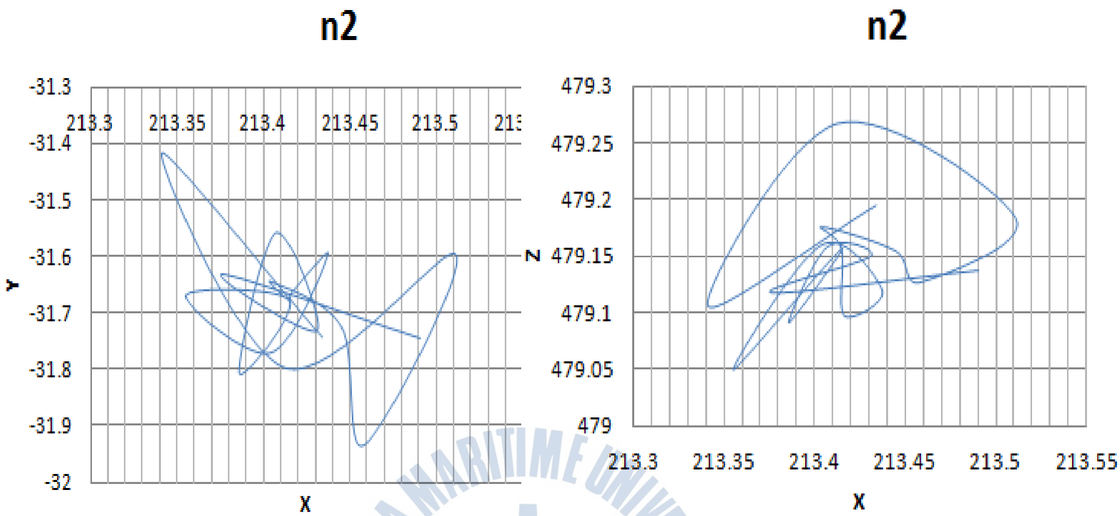

Figure 61: X-Y and X-Z trajectories of point n2.

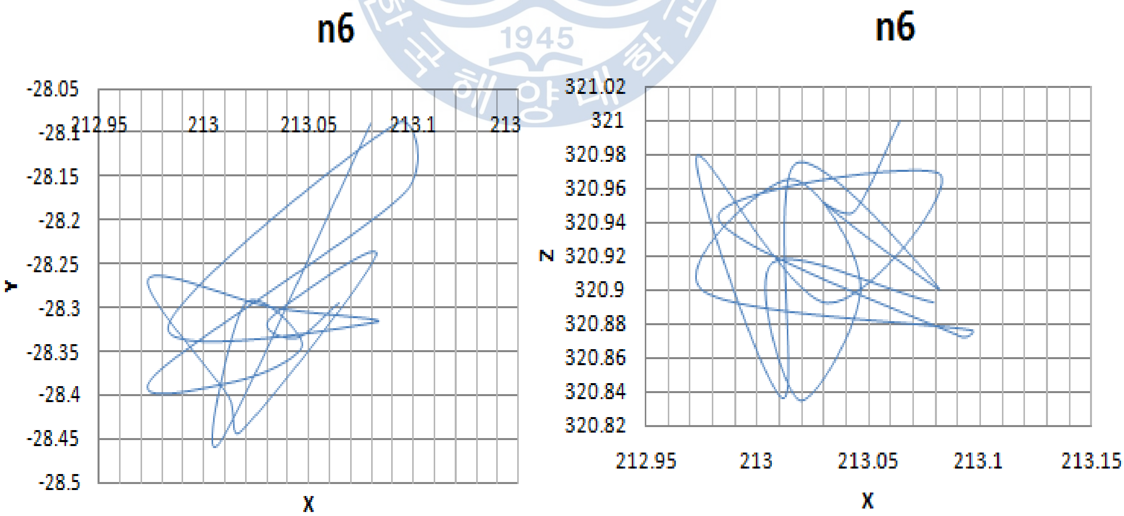

Figure 62: X-Y and X-Z trajectories of point n6.

Collection

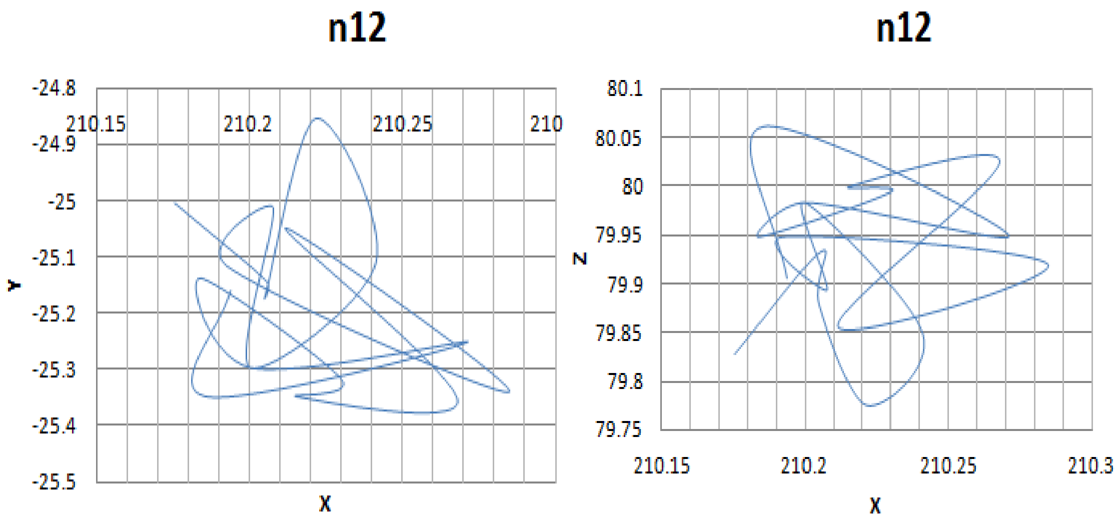

Figure 63: X-Y and X-Z trajectories of point n12.

5.20: Experimental results of behavior of Teflon Model under effect of Wave and Motion. Experimental Conditions (Motion Period T=1.5s, Displacement 30cm, Wave Period T=1s, Wave Height H=10cm and angle *θ*=180°).

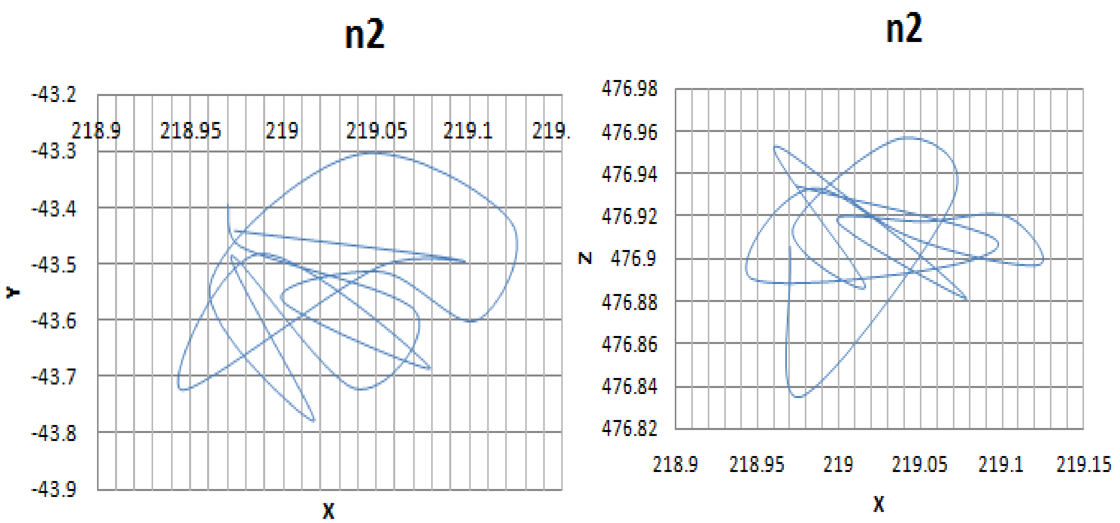

Figure 64: X-Y and X-Z trajectories of point n2.

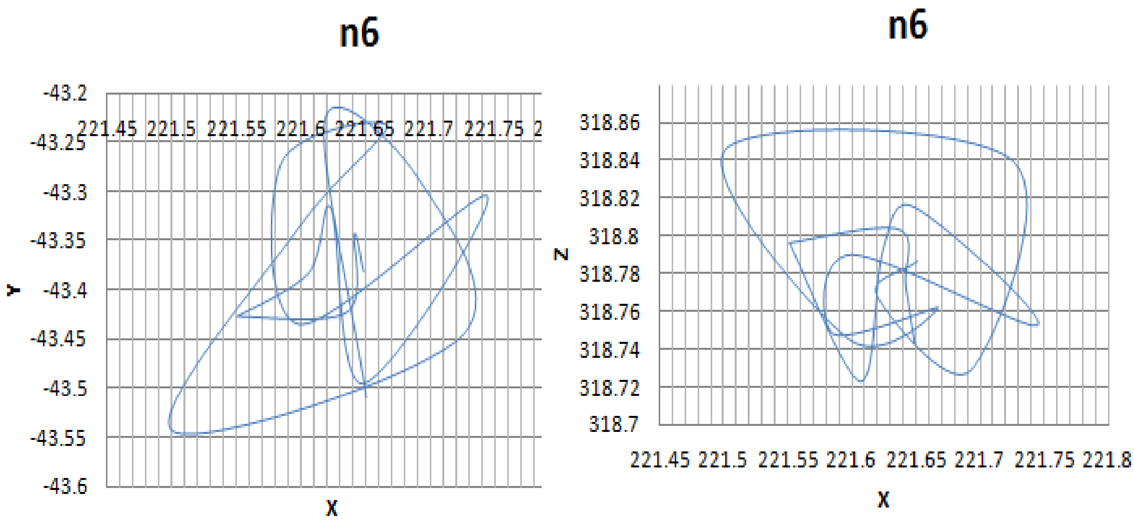

Figure 65: X-Y and X-Z trajectories of point n6.

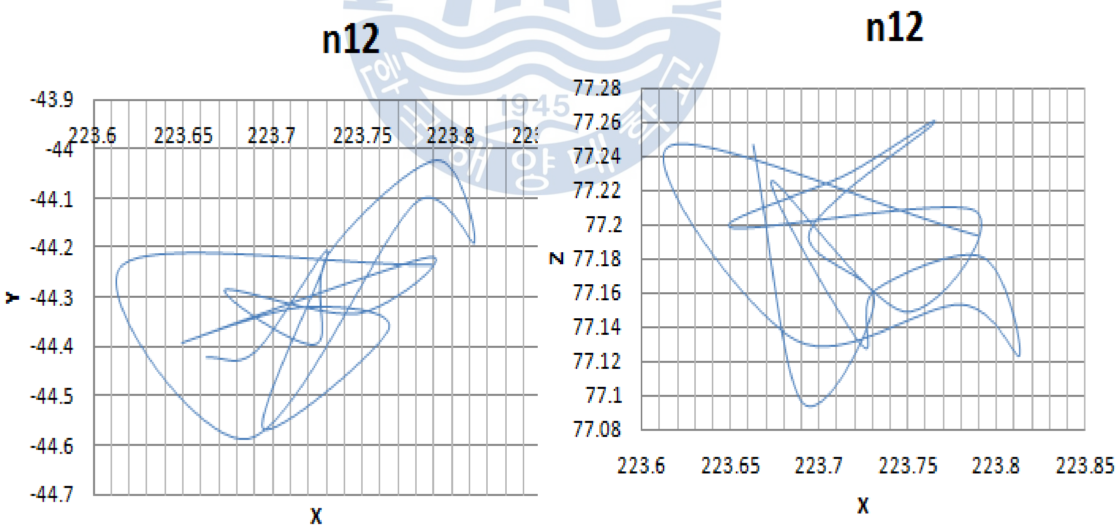

Figure 66: X-Y and X-Z trajectories of point n12.

5.21: Experimental results of behavior of Acryl Model under effect of Wave and Motion. Experimental Conditions (Motion Period T=1.5s, Displacement 30cm, Wave Height H=10cm, Wave Period T=1s and angle $\boldsymbol{\theta}$=360°).

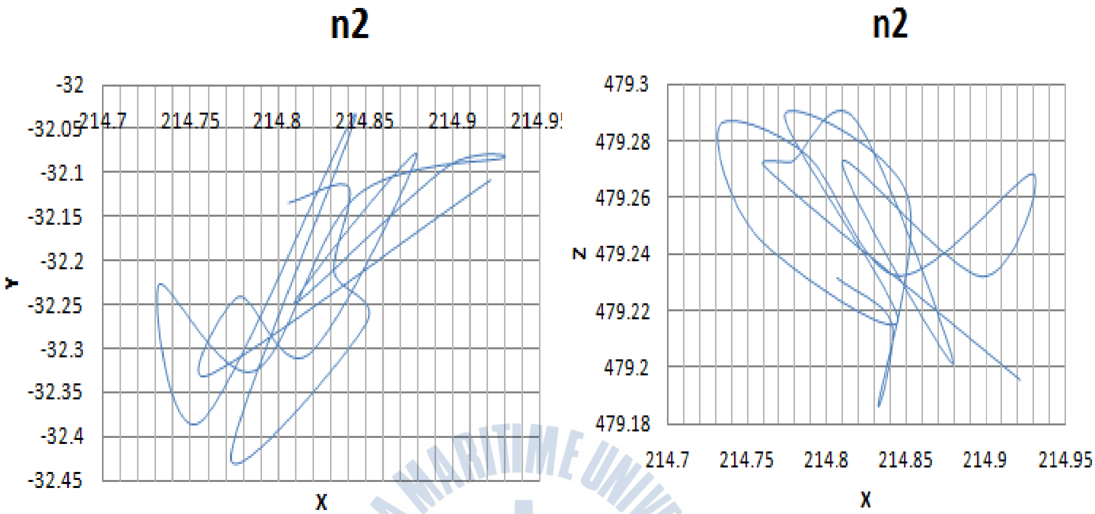

Figure 67: X-Y and X-Z are trajectories of point n2.

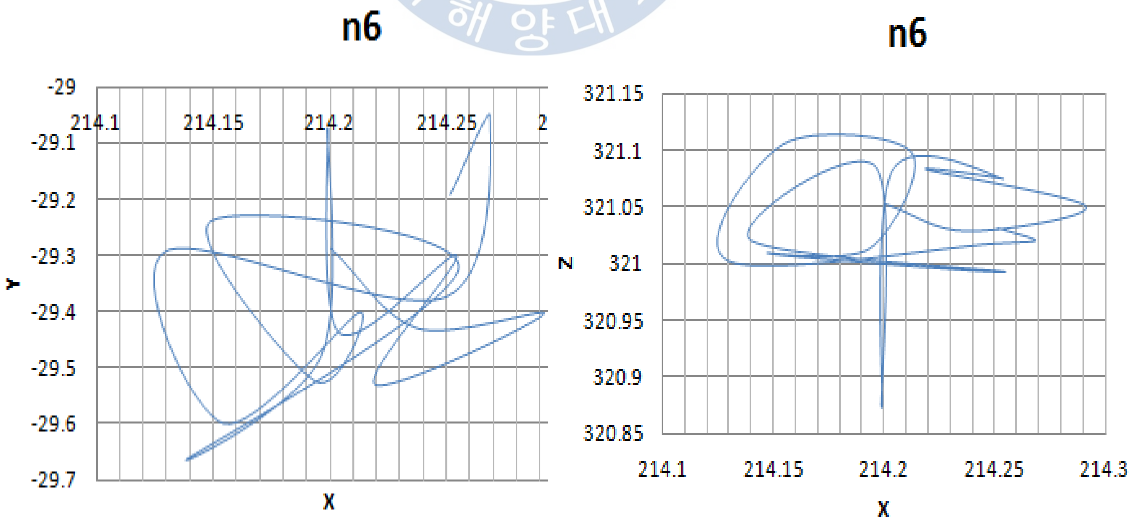

Figure 68: X-Y and X-Z trajectories of point n6.

KOREA MARITIME UNIVERSITY
1945
한국해양대학교

dCollection

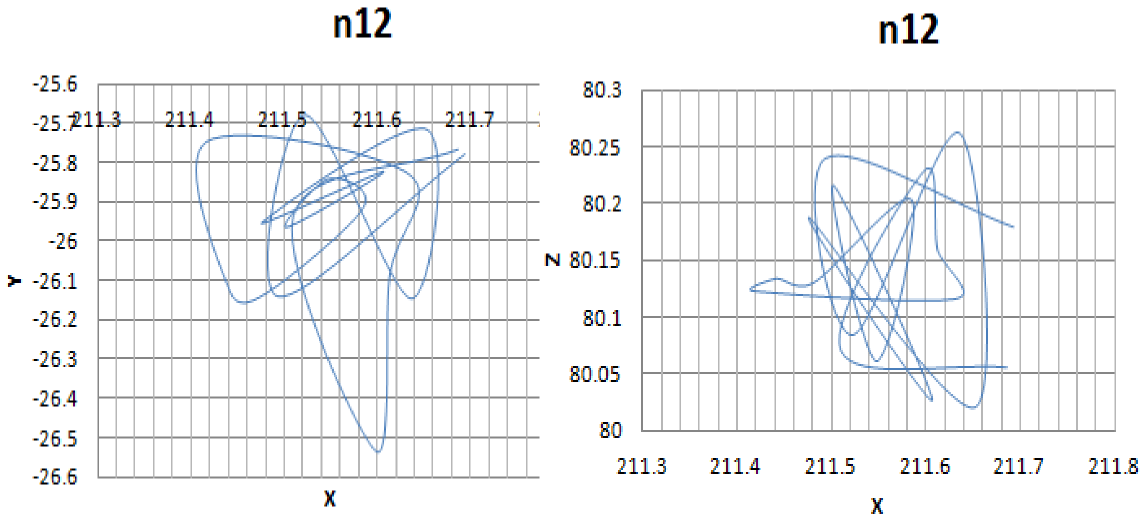

Figure 69: X-Y and X-Z trajectories of point n12.

5.22: Experimental results of behavior of Teflon Model under effect of Wave and Motion. Experimental Conditions (Motion Period T=1.5s, Displacement 30cm, Wave period T=1s, Wave Height H=10cm and angle $\boldsymbol{\theta}$=360°).

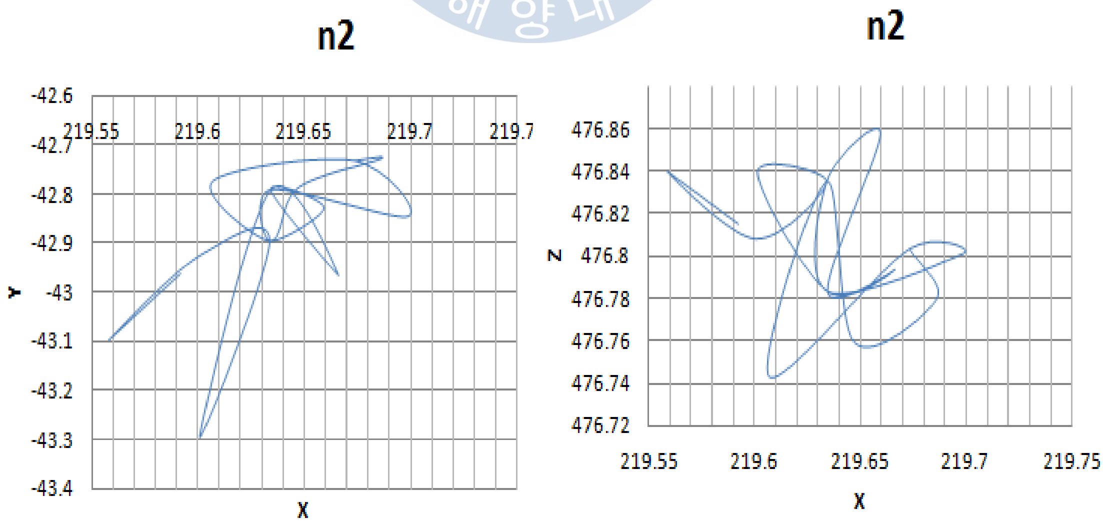

Figure 70: X-Y and X-Z trajectories of point n2.

Collection

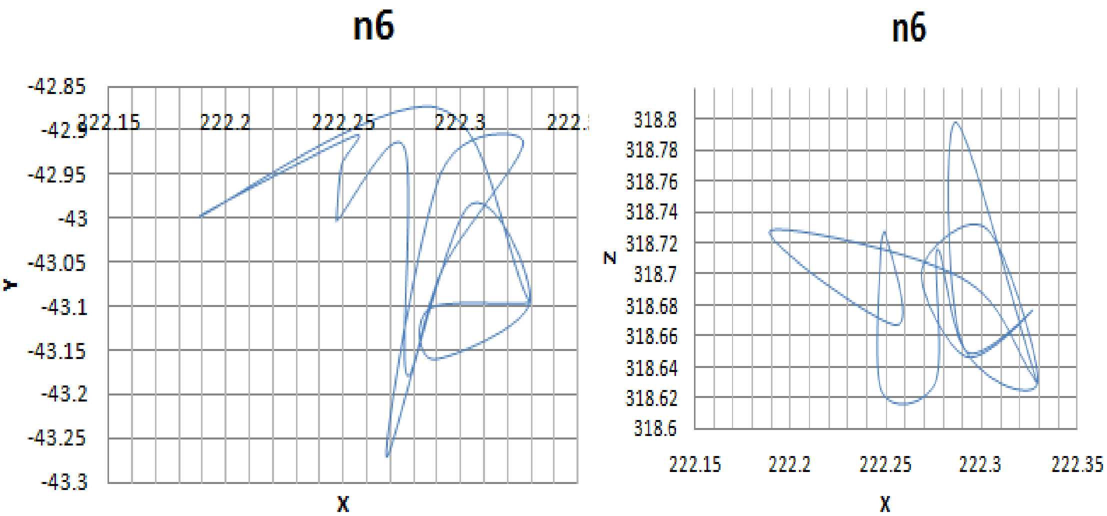

Figure 71: X-Y and X-Z trajectories of point n6.

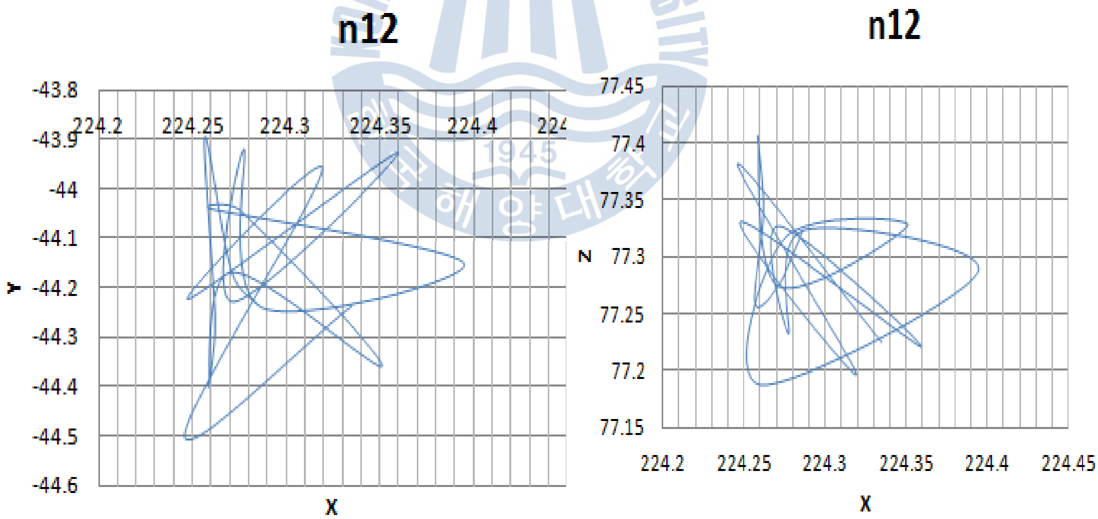

Figure 72: X-Y and X-Z trajectories of point n12.

5.23: Experimental results of behavior of Teflon Model effect of Wave and Current. Experimental Conditions (Wave period T=1s, Wave Height H=10cm and Current Velocity V=0.2m/s).

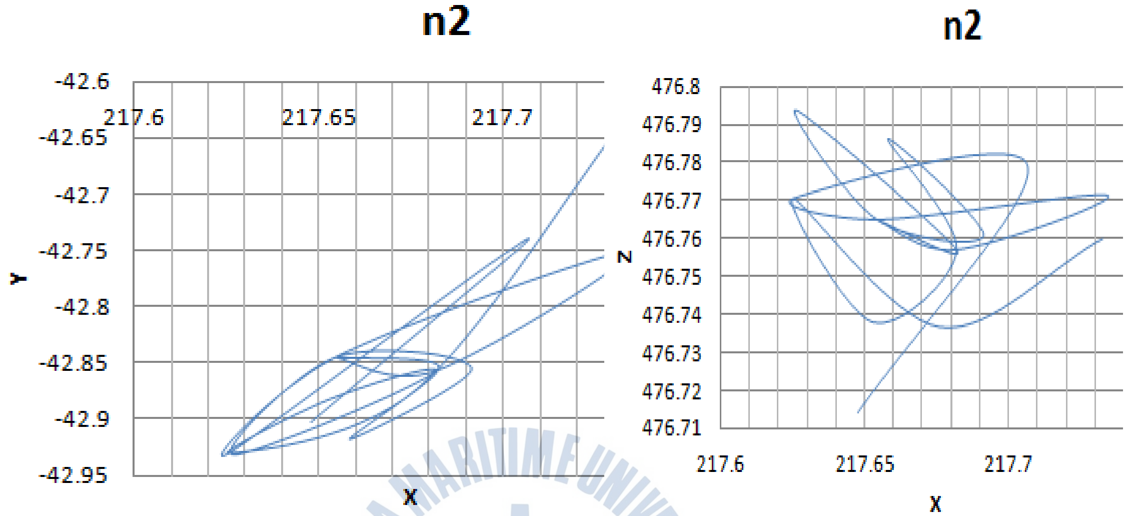

Figure 73: X-Y and X-Z trajectories of point n2.

KOREA MARITIME UNIVERSITY
1945
한국해양대학교

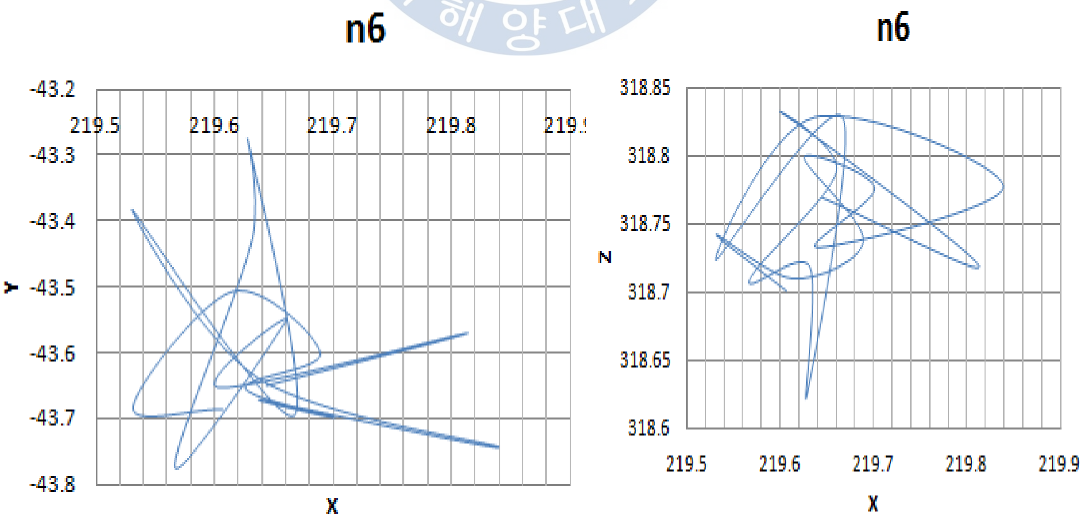

Figure 74: X-Y and X-Z trajectories of point n6.

dCollection

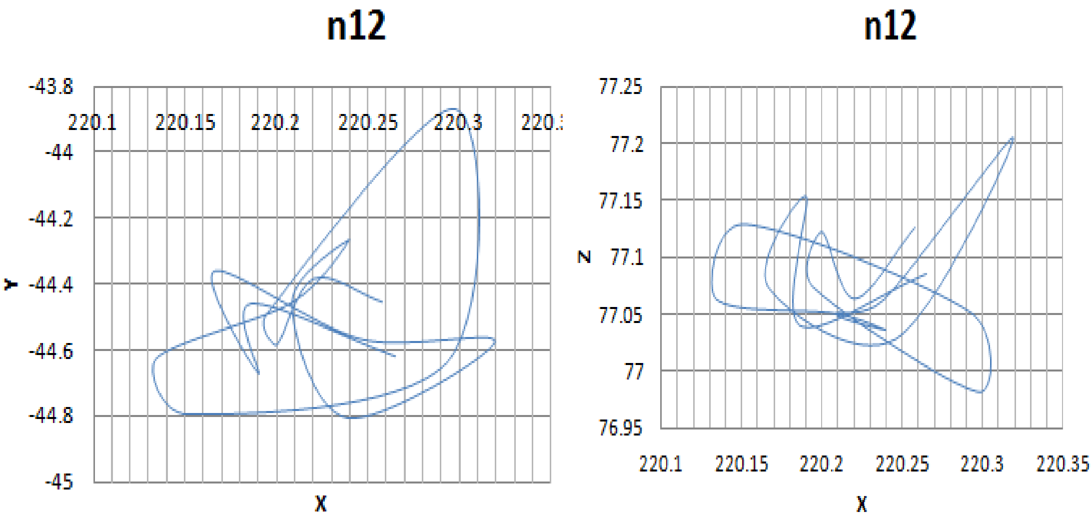

Figure 75: X-Y and X-Z trajectories of point n12.

5.24: Experimental results of behavior of Acryl model under effect of Wave and Current. Experimental Conditions (Wave Period T=1s, Wave Height H=10cm and Current Velocity V=0.2m/s).

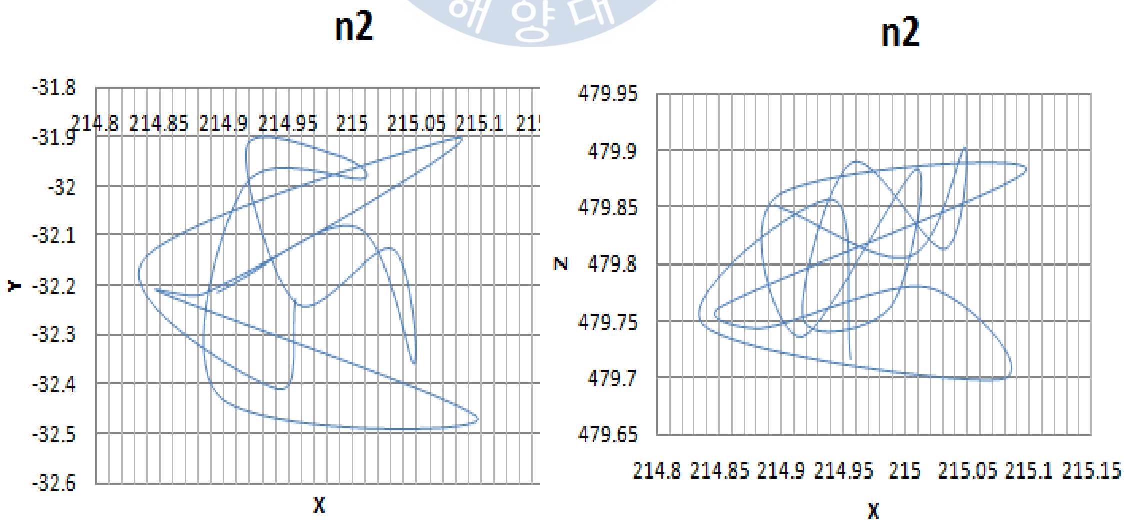

Figure 76: X-Y and X-Z trajectories of point n2.

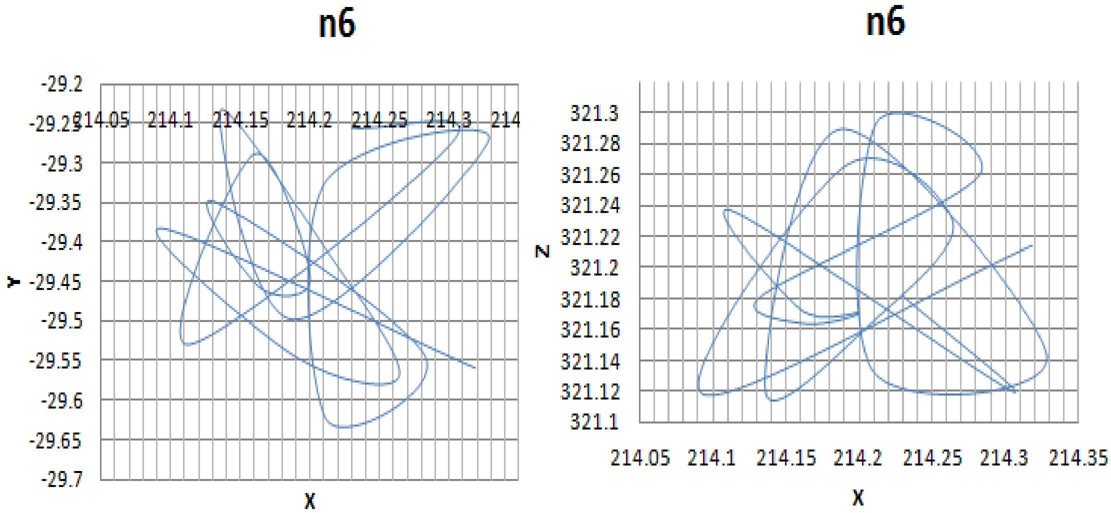

Figure 77: X-Y and X-Z trajectories of point n6.

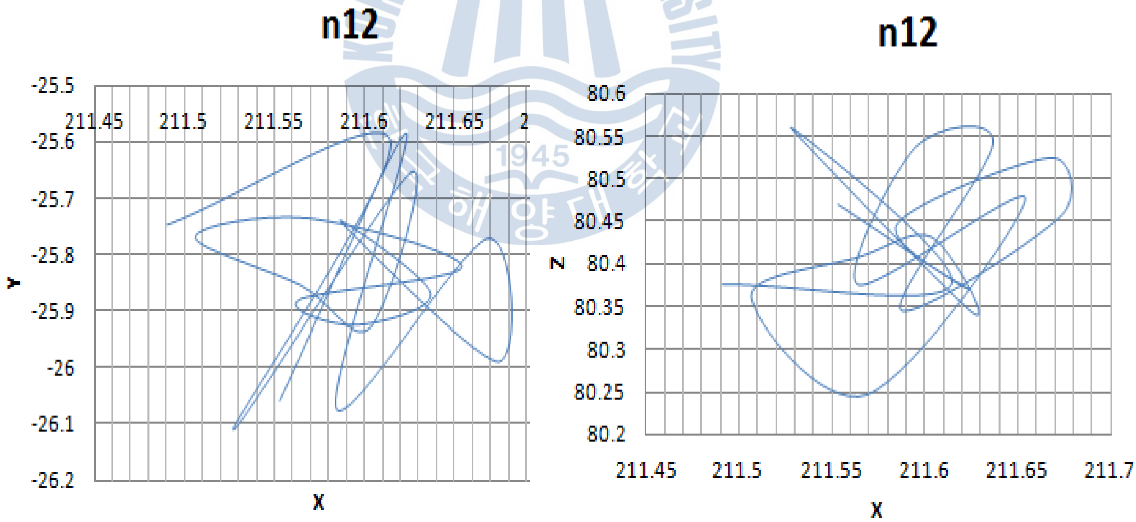

Figure 78: X-Y and X-Z trajectories of point n12.

dCollection

5.25: Experimental results of behavior of Acryl Model under effect of Wave and Current. Experimental Conditions (Wave Period T=1.5s, Wave Height H=10cm and Current velocity V=0.2m/s).

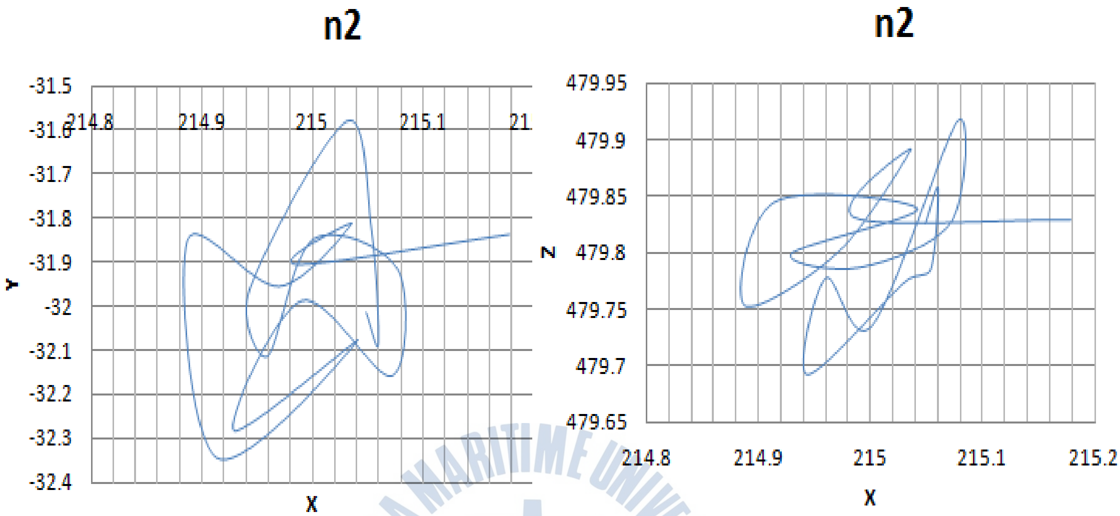

Figure 79: X-Y and X-Z trajectories of point n2.

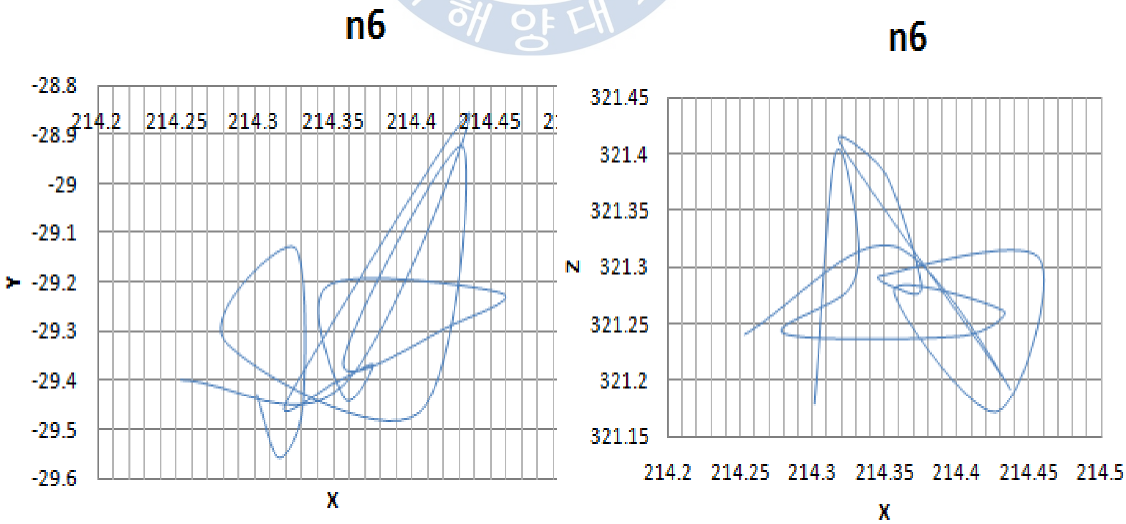

Figure 80: X-Y and X-Z trajectories of point n6.

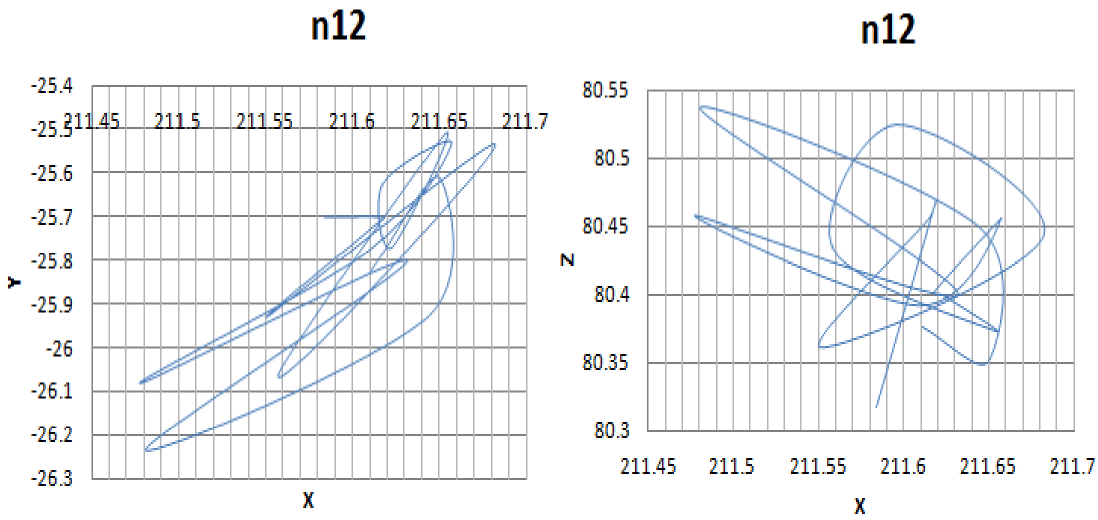

Figure 81: X-Y and X-Z trajectories of point n12.

5.26: Experimental results of behavior of Teflon Model under effect of Wave and Current. Experimental Conditions (Wave Period T=1.5s, Wave Height H=10cm and Current Velocity V=0.2m/s).

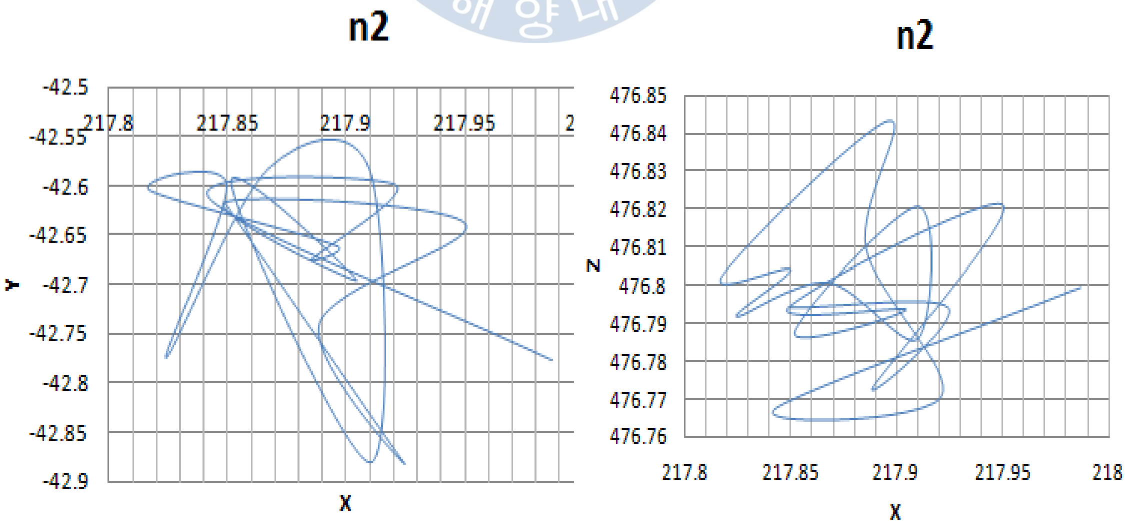

Figure 82: X-Y and X-Z trajectories of point n2.

Collection

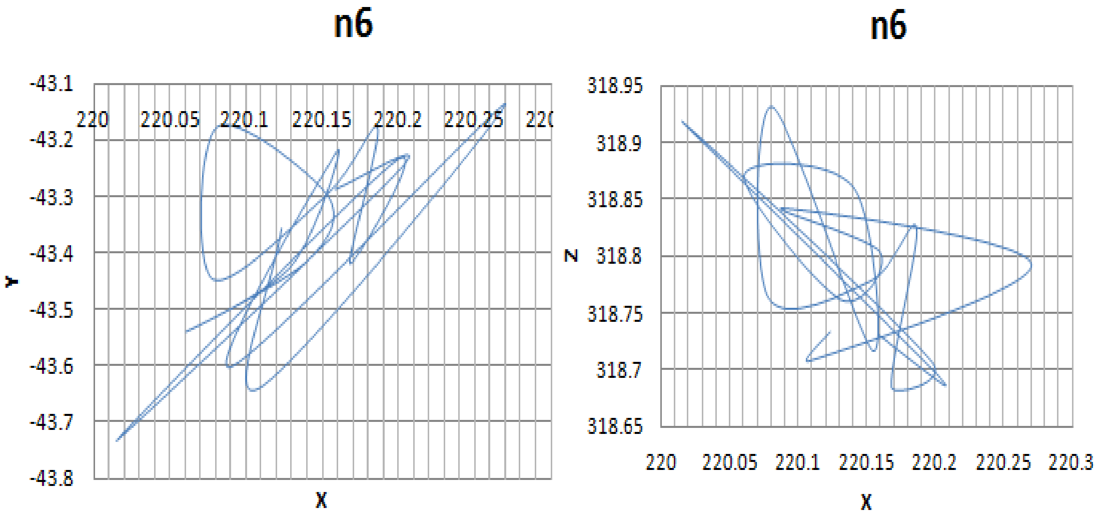

Figure 83: X-Y and X-Z trajectories of point n6.

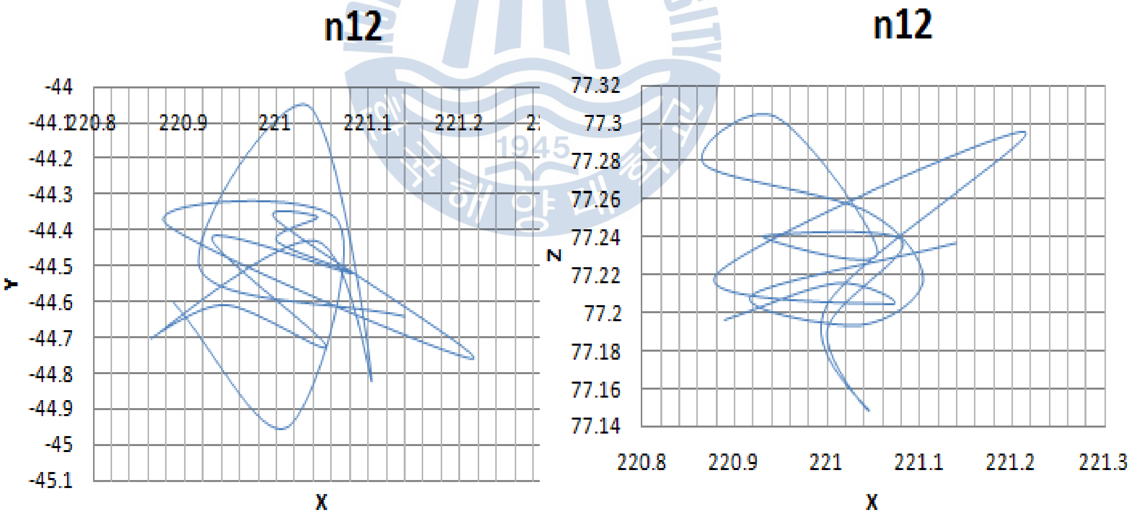

Figure 84: X-Y and X-Z trajectories of point n12.

Collection

5.27: Experimental results of behavior of Acryl Model under effect of Current and Motion. Experimental Conditions (Motion Period T=1.5s, Displacement 30cm and Current Velocity V=0.2m/s).

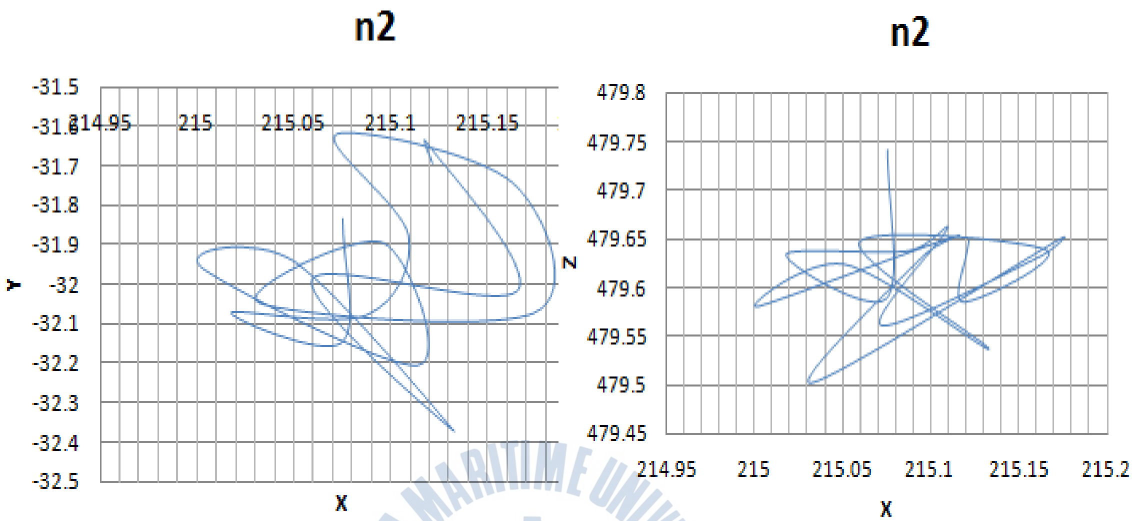

Figure 85: X-Y and X-Z trajectories of point n2.

KOREA MARITIME UNIVERSITY
1945
한국해양대학교

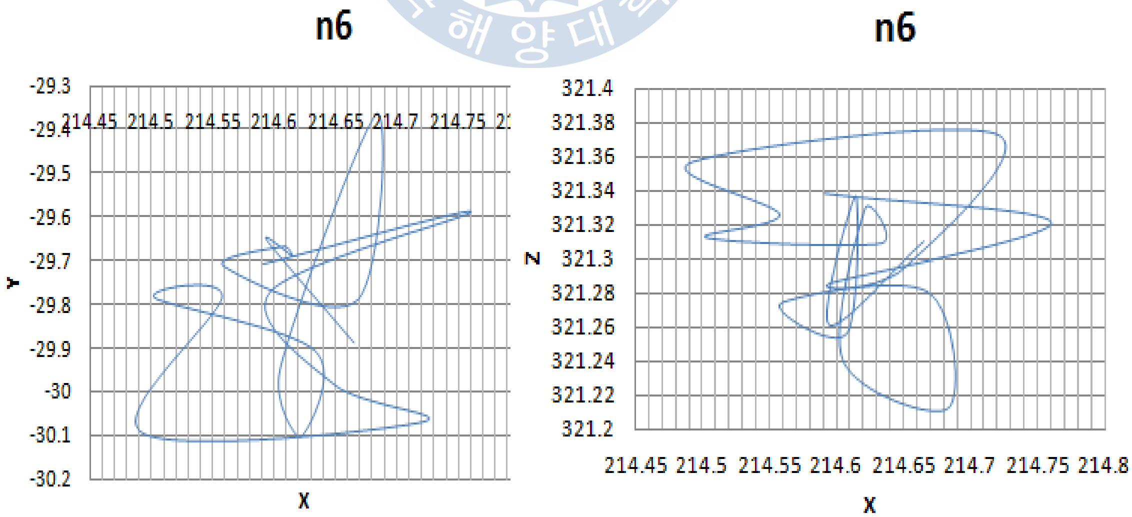

Figure 86: X-Y and X-Z trajectories of point n6.

Collection

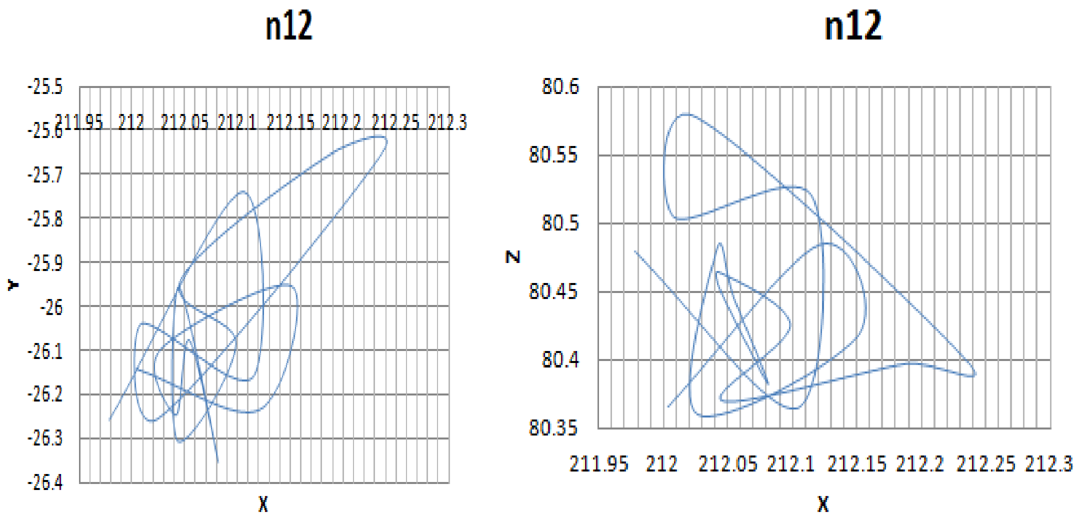

Figure 87: X-Y and X-Z trajectories of point n12.

KOREA MARITIME UNIVERSITY
한국해양대학교

5.28: Experimental results of behavior of Teflon Model under effect of Motion and Current. Experimental Conditions (Motion Period T=1.5s, Displacement 30cm and Current Velocity V=0.2m/s).

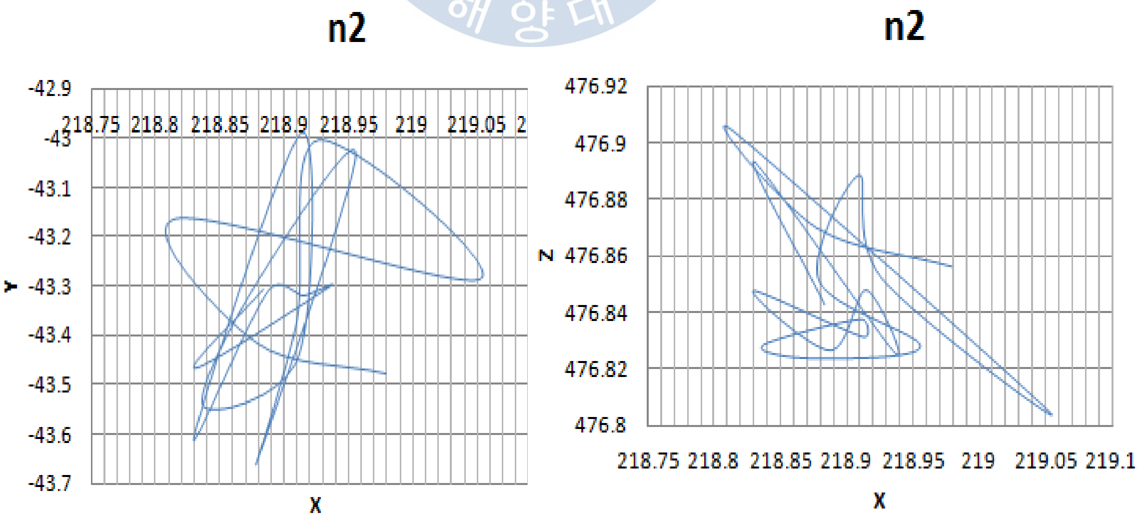

Figure 88: X-Y and X-Z trajectories of point n2.

dCollection

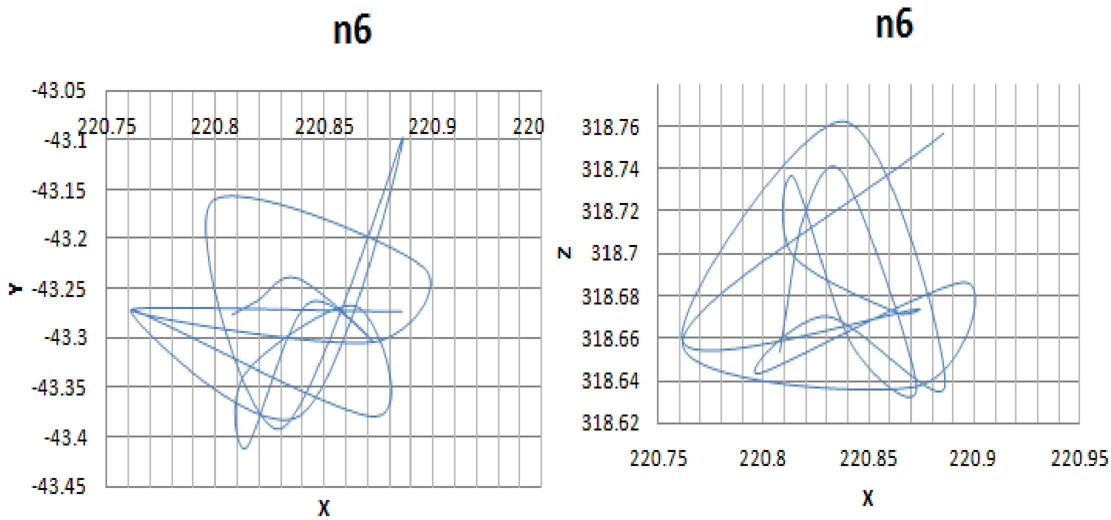

Figure 89: X-Y and X-Z trajectories of point n6.

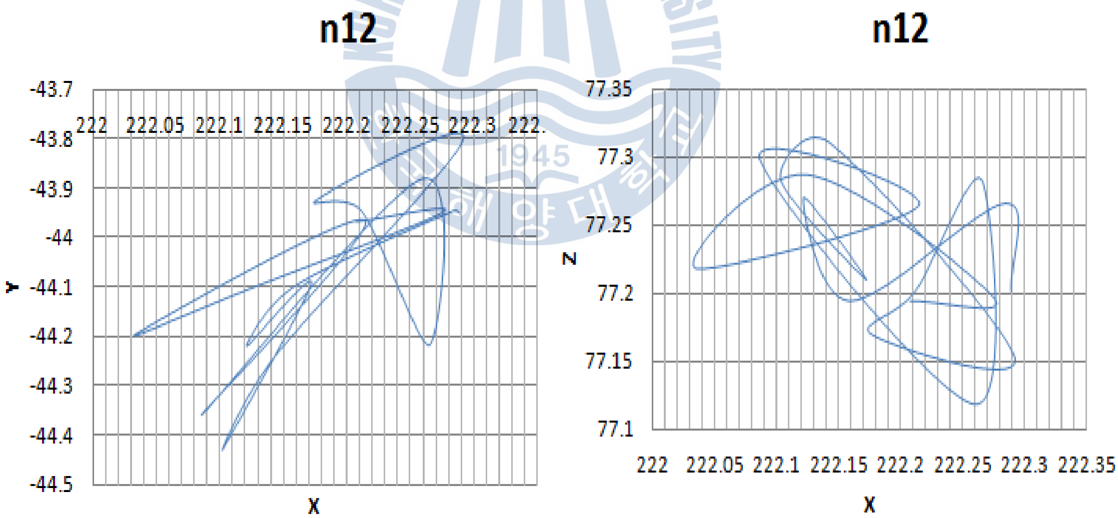

Figure 90: X-Y and X-Z trajectories of point n12.

5.29: Experimental results of behavior of Acryl Model under effect of Current and Motion. Experimental Conditions (Motion Period T=3s, Displacement 30cm and Current Velocity V=0.2m/s).

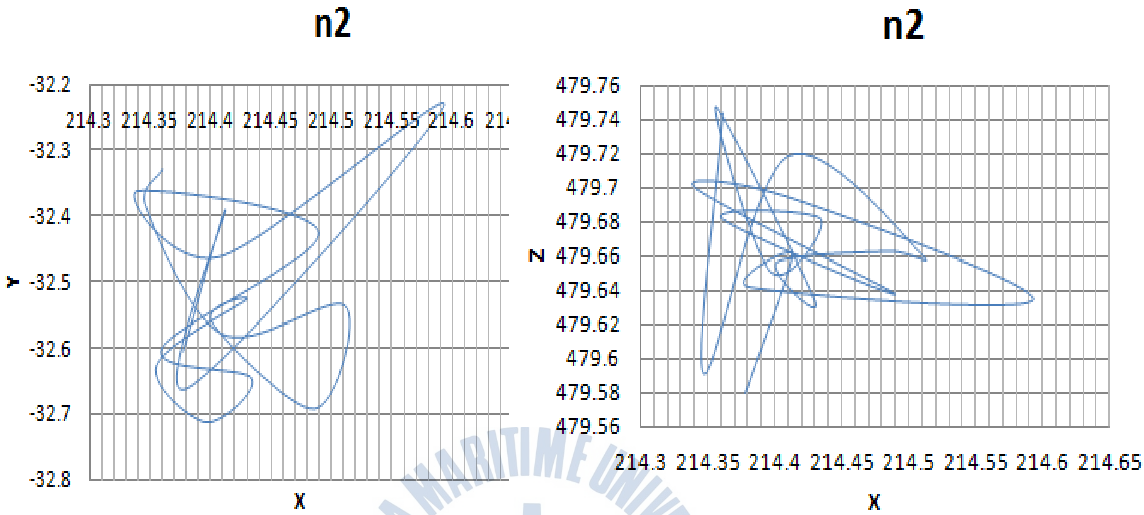

Figure 91: X-Y and X-Z trajectories of point n2.

KOREA MARITIME UNIVERSITY
1945
한국해양대학교

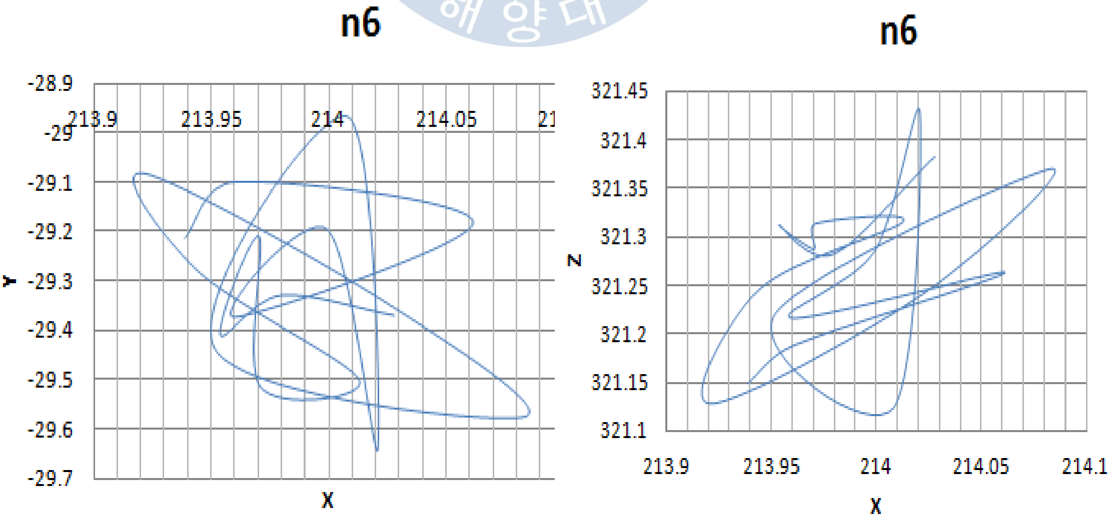

Figure 92: X-Y and X-Z trajectories of point n6.

Collection

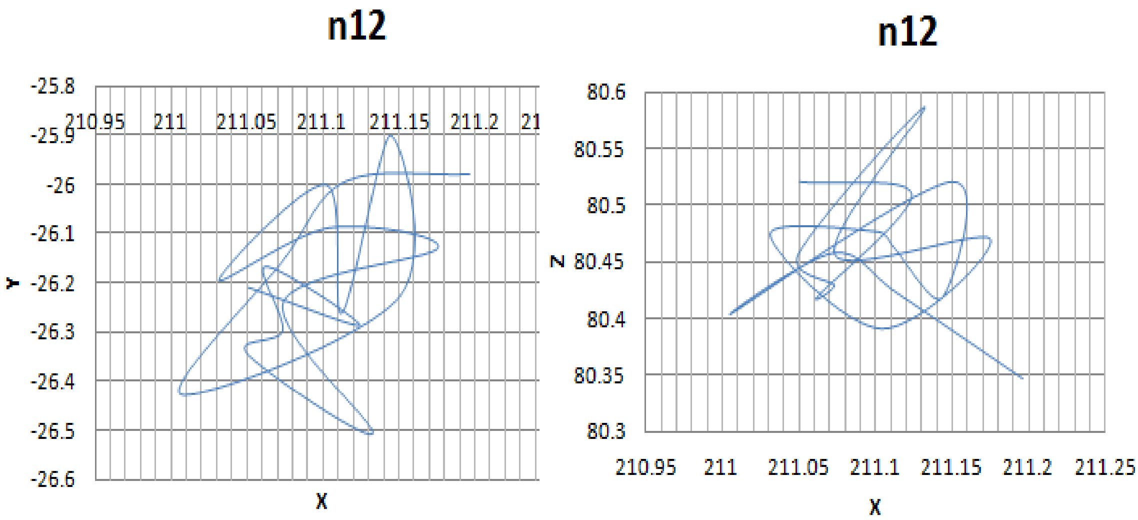

Figure 93: X-Y and X-Z trajectories of point n12.

5.30: Experimental results of behavior of Teflon Model under the effect of Motion and Current. Experimental Conditions (Motion Period T=3s, Displacement 30cm and Current Velocity V=0.2m/s).

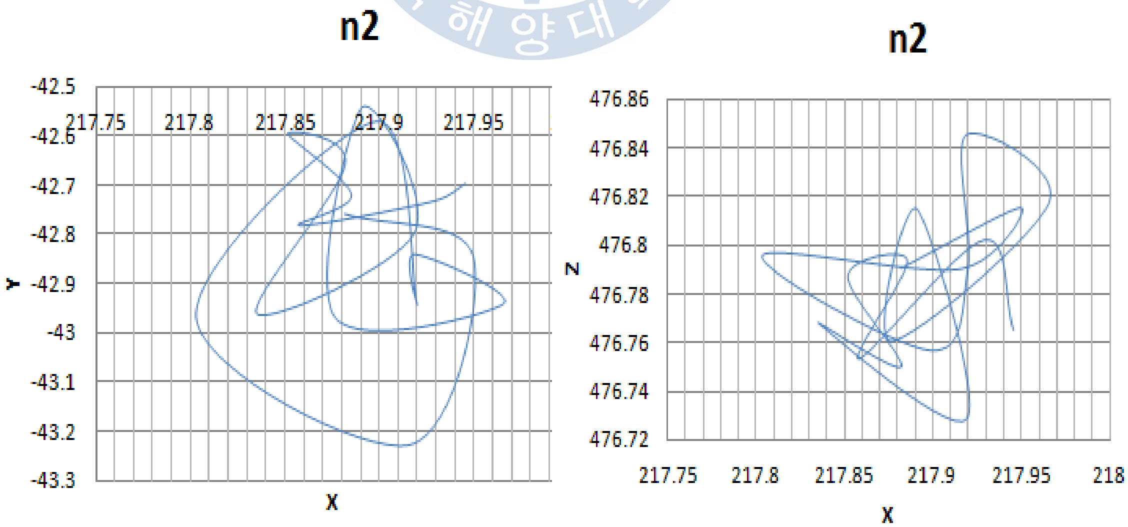

Figure 94: X-Y and X-Z trajectories of point n2.

dCollection

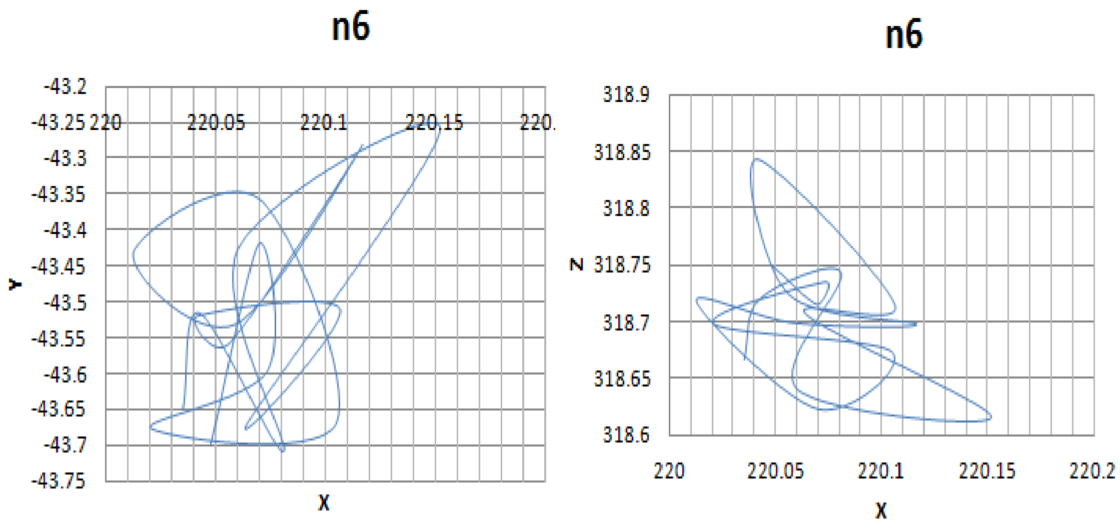

Figure 95: X-Y and X-Z trajectories of point n6.

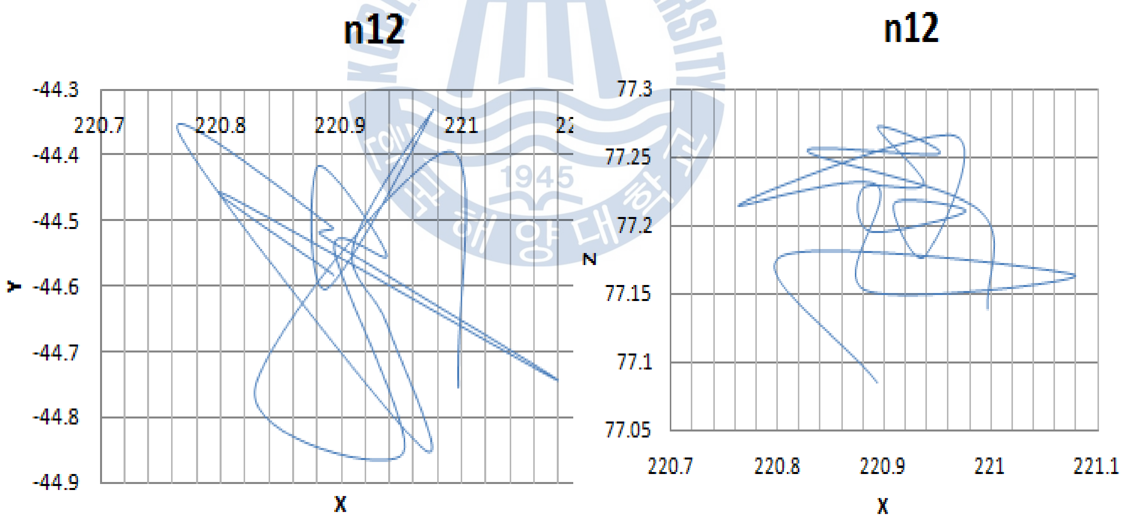

Figure 96: X-Y and X-Z trajectories of point n12.

5.31: Experimental results of behavior of Acryl model under effect of Current. Experimental Conditions (Current Velocity V=0.2m/s).

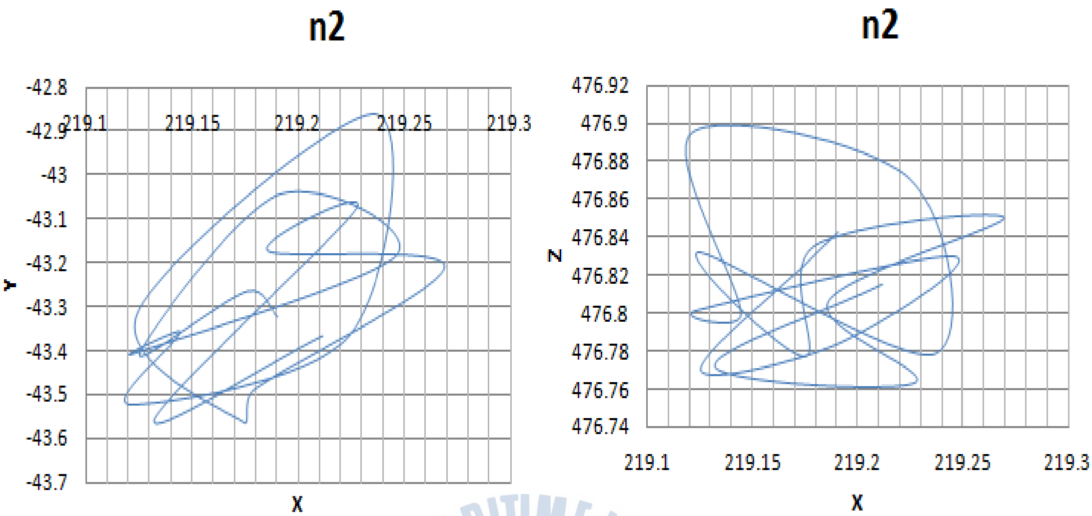

Figure 97: X-Y and X-Z trajectories of point n2.

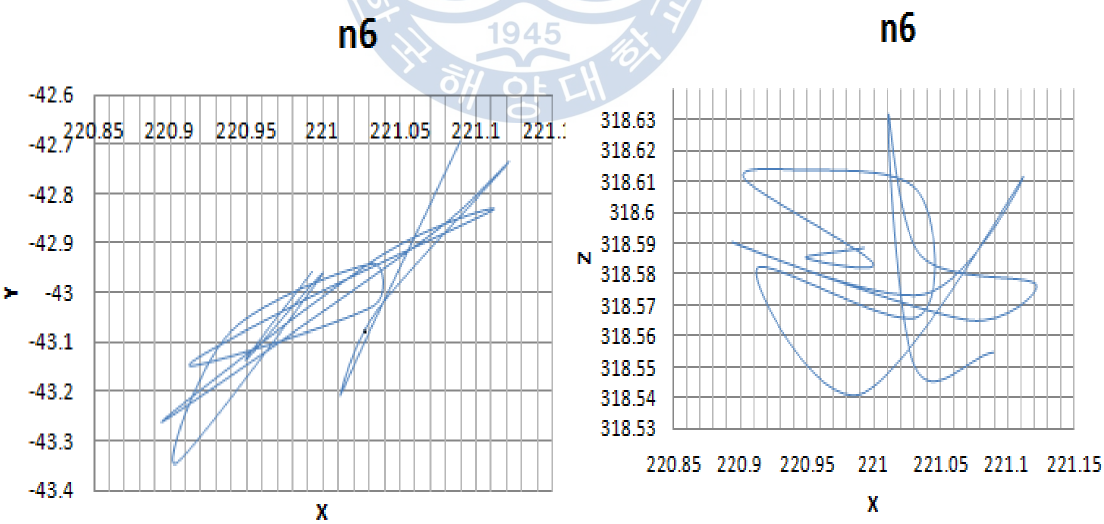

Figure 98: X-Y and X-Z trajectories of point n6.

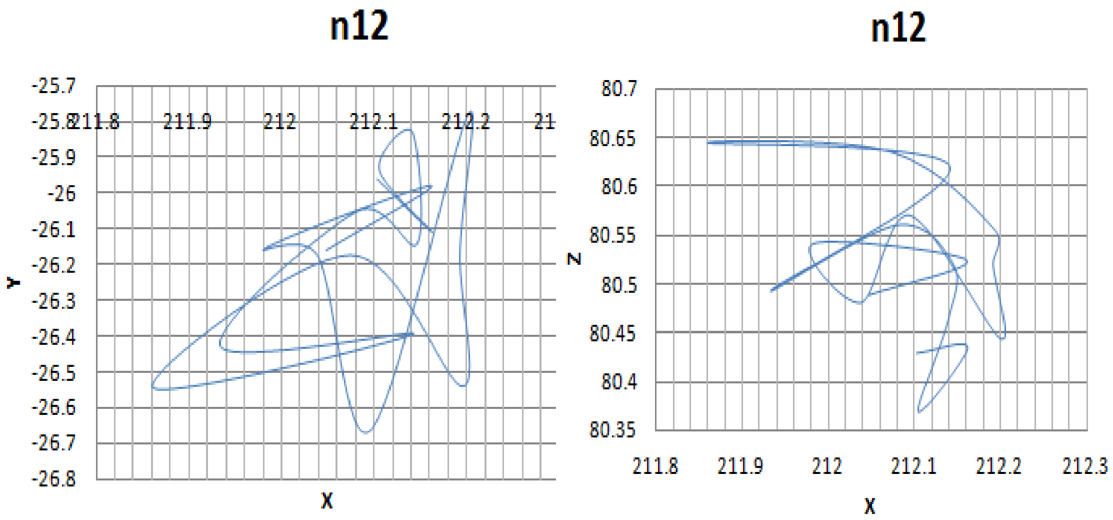

Figure 99: X-Y and X-Z trajectories of point n12.

5.32: Experimental results of behavior of Teflon Model under effect of Current. Experimental Conditions (Current Velocity V=0.2m/s).

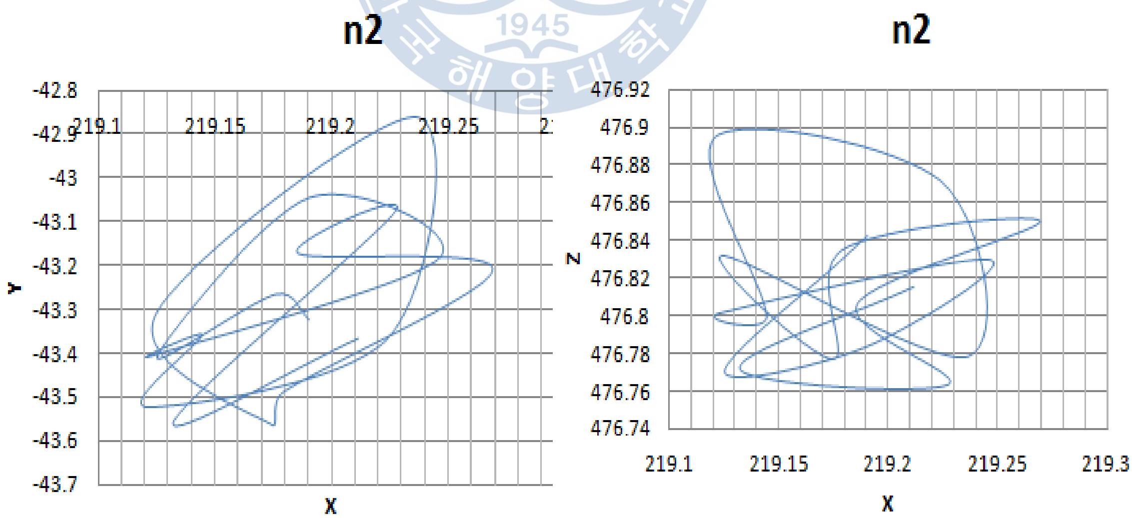

Figure 100: X-Y and X-Z trajectories of point n2.

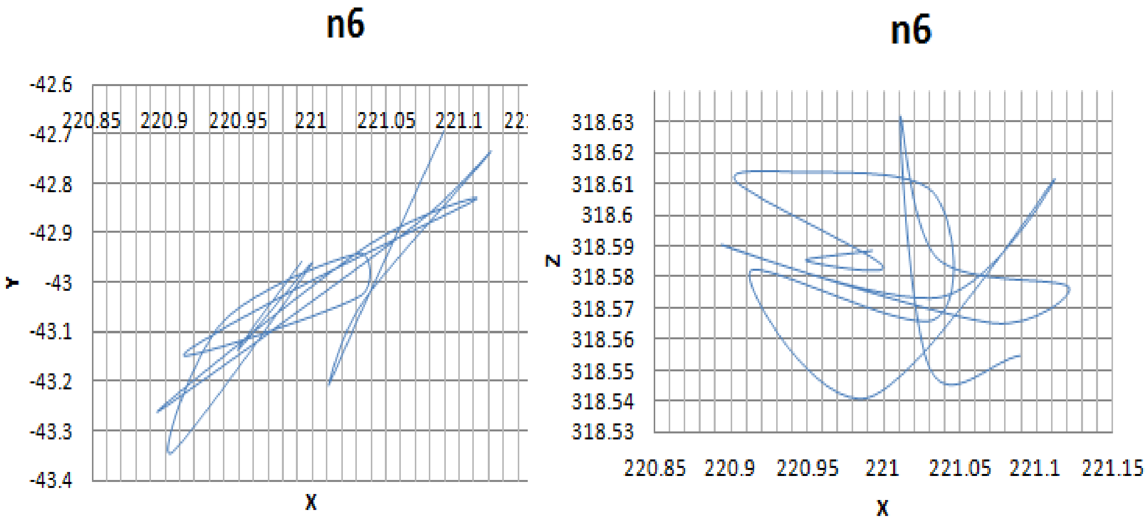

Figure 101: X-Y and X-Z trajectories of point n6.

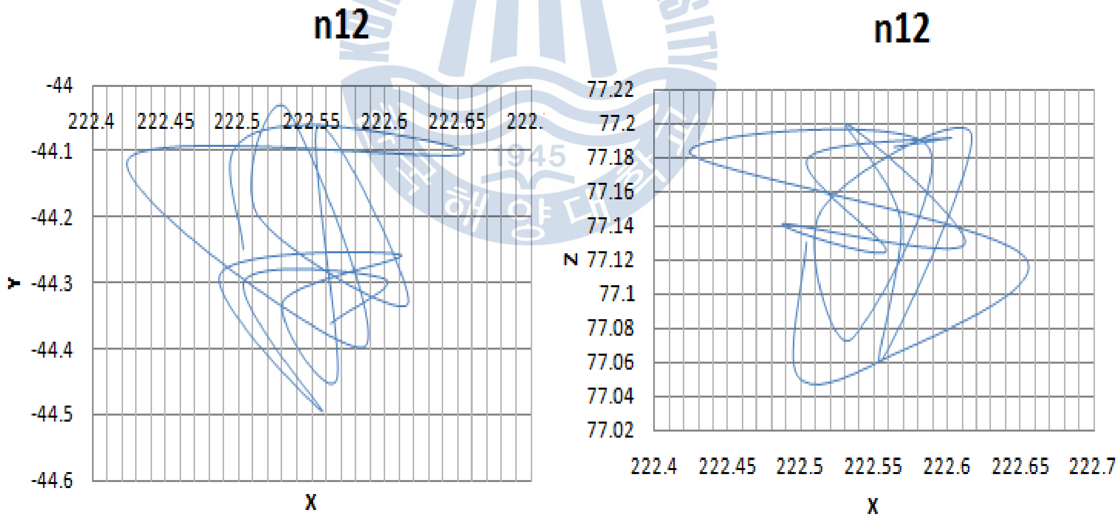

Figure 102: X-Y and X-Z trajectories of point n12.

Collection

5.33: Experimental results of behavior of Acryl Model under effect of Current, Motion and Wave. Experimental Conditions (Motion Period T=1.5s, Displacement 30cm, Wave Period T=1s, Wave Height H=10cm and Current Velocity V=0.2m/s, θ=180°).

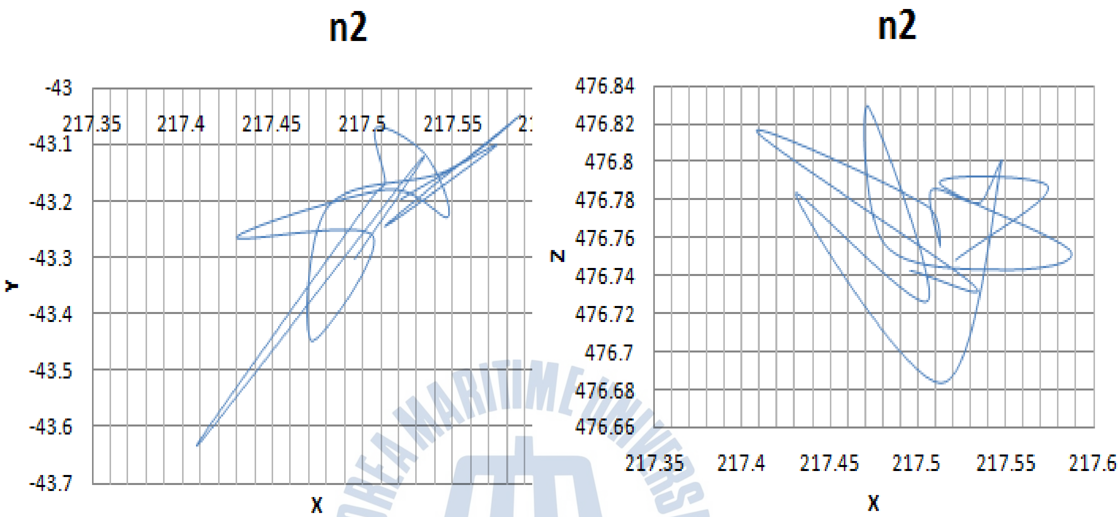

Figure 103: X-Y and X-Z trajectories of point n2.

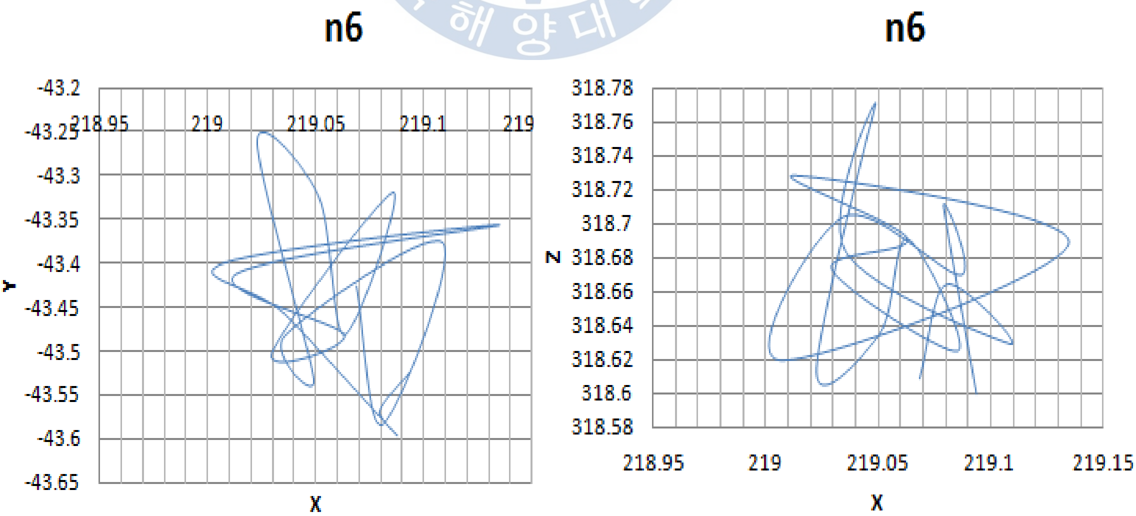

Figure 104: X-Y and X-Z trajectories of point n6.

Collection

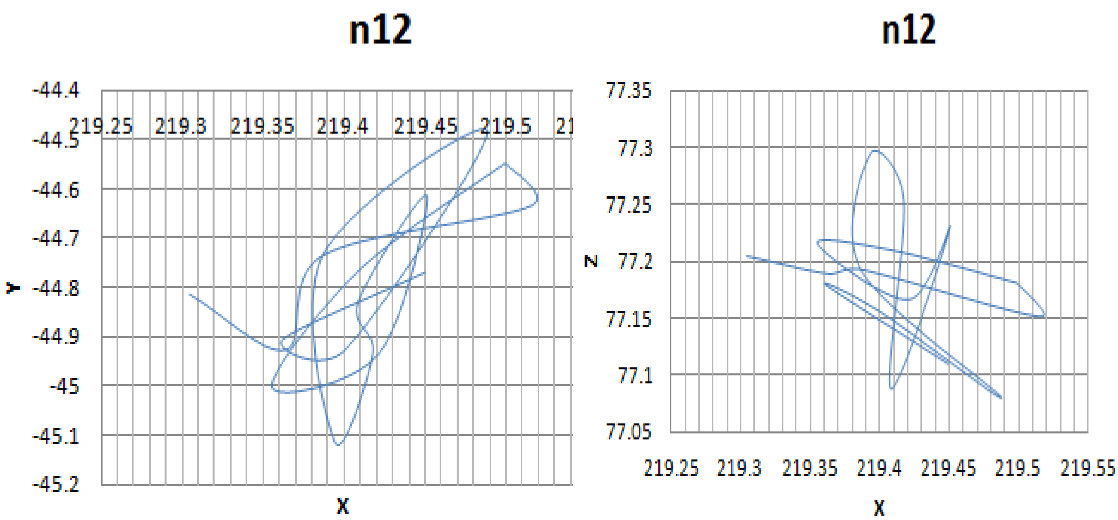

Figure 105: X-Y and X-Z trajectories of point n12.

5.34: Experimental results of behavior of Teflon Model under effect of Motion, Wave and Current. Experimental Conditions (Motion Period T=1.5s, Displacement 30cm, Wave Period T=1s, Wave Height H=10cm, Current Velocity V=0.2m/s and θ=180°).

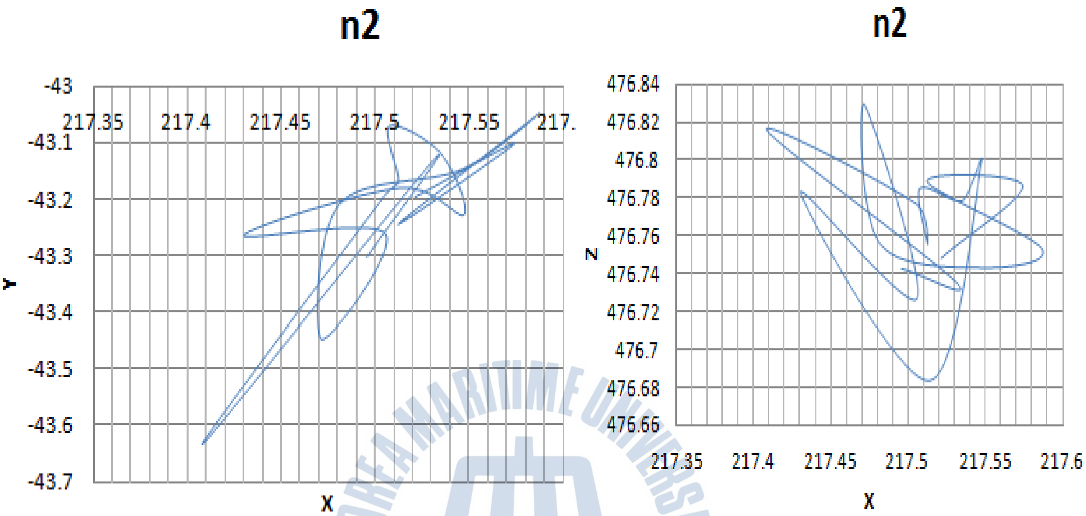

Figure 106: X-Y and X-Z trajectories of point n2.

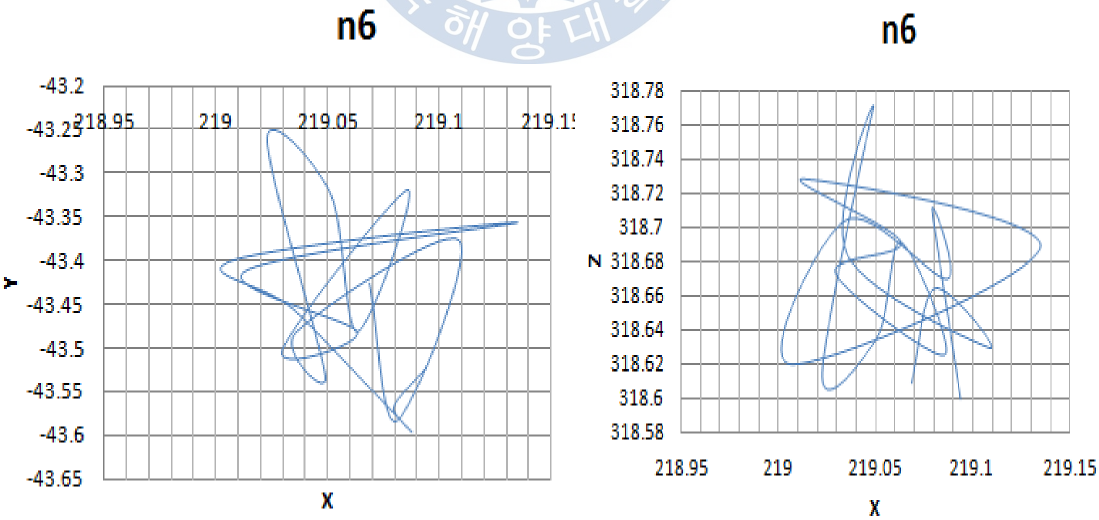

Figure 107: X-Y and X-Z trajectories of point n6.

dCollection

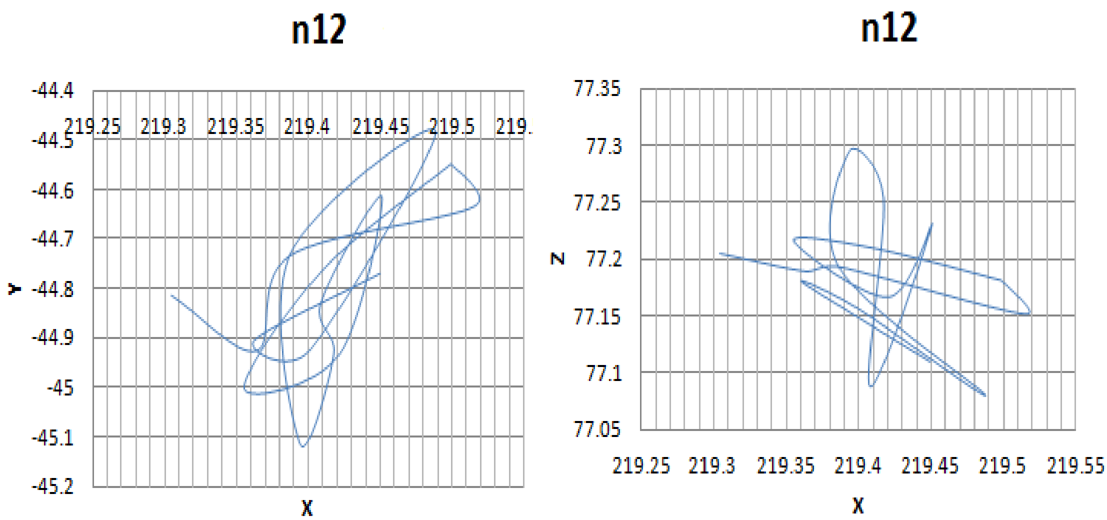

Figure 108: X-Y and X-Z trajectories of point n12.

5.35: Experimental results of behavior of Acryl Model under effect of Motion, Current and Wave. Experimental Conditions (Motion Period T=1.5s, Displacement 30cm, Wave Period T=1s, Wave Height H=10cm, Current Velocity V=0.2m/s and θ=360°).

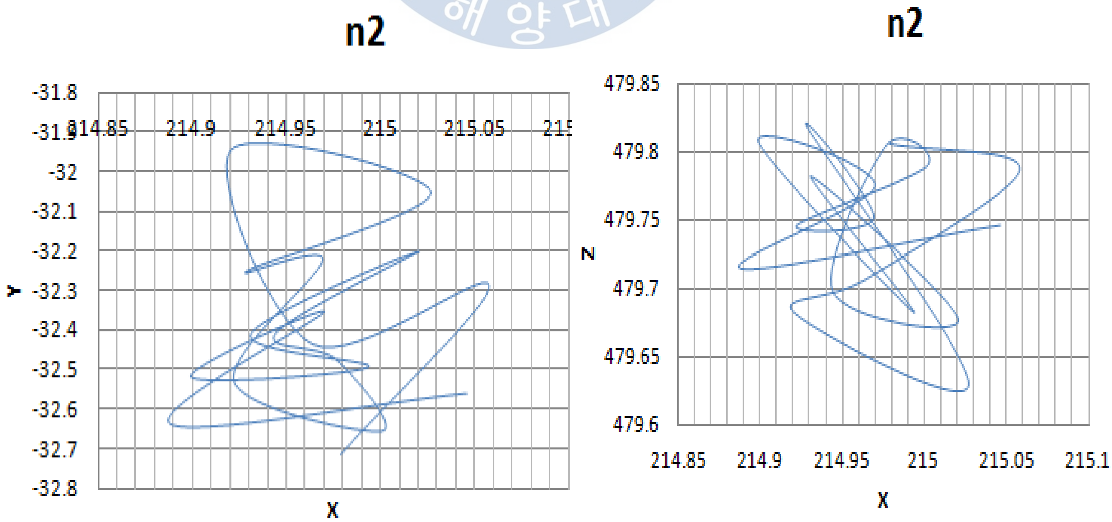

Figure 109: X-Y and X-Z trajectories of point n2.

Collection

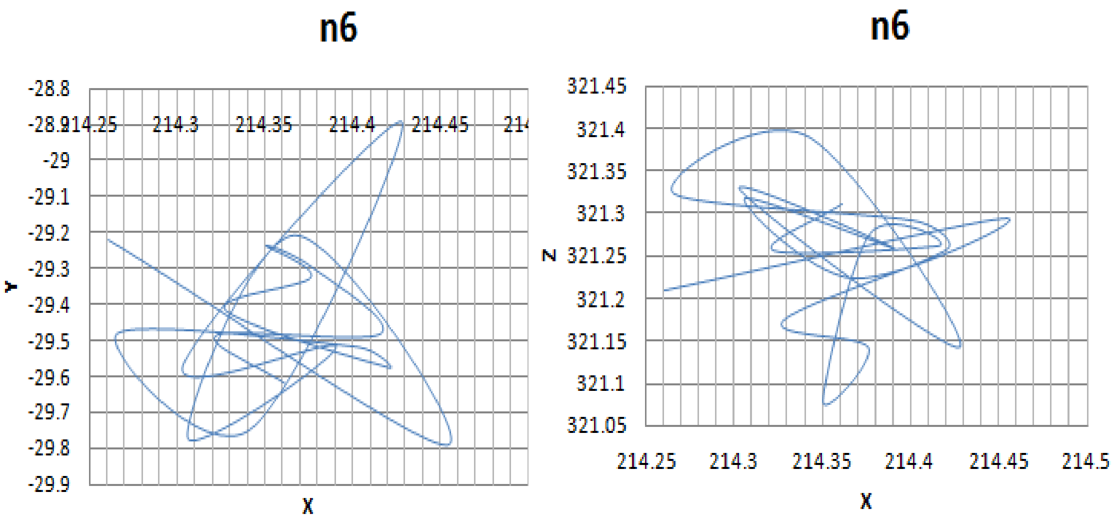

Figure 110: X-Y and X-Z trajectories of point n6.

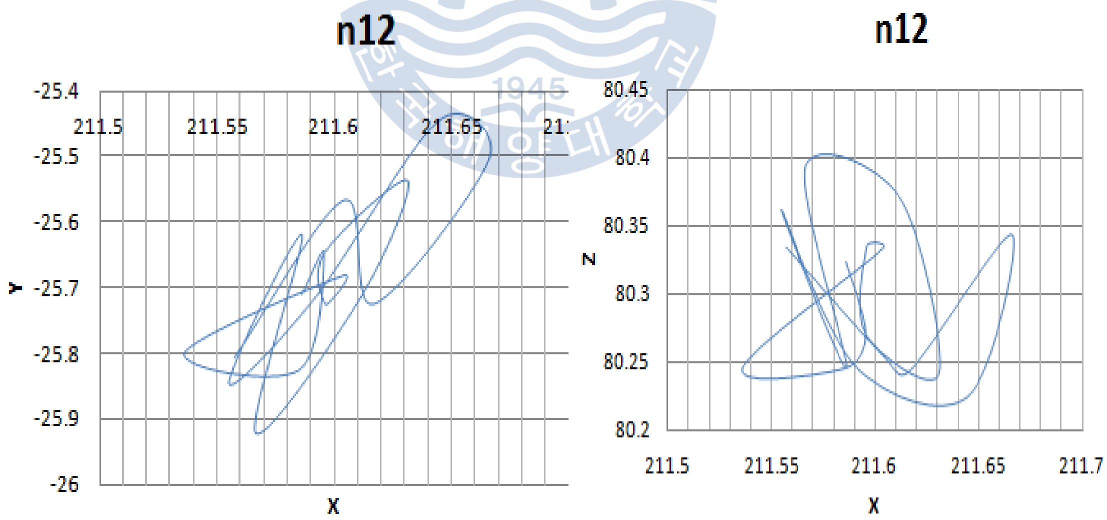

Figure 111: X-Y and X-Z trajectories of point n12.

Collection

5.36: Experimental results of Teflon Model under effect of Motion, Wave and Current. Experimental Conditions (Motion Period T=1.5s, Displacement 30cm, Wave Period T=1s, Wave Height H=10cm, Current Velocity V=0.2m/s and θ=360°).

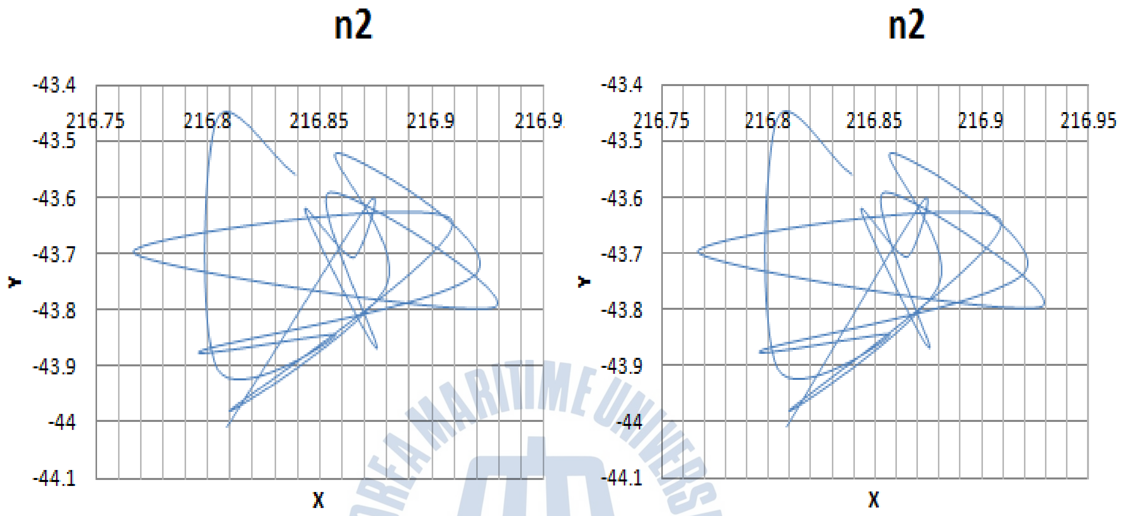

Figure 112: X-Y and X-Z trajectories of point n2.

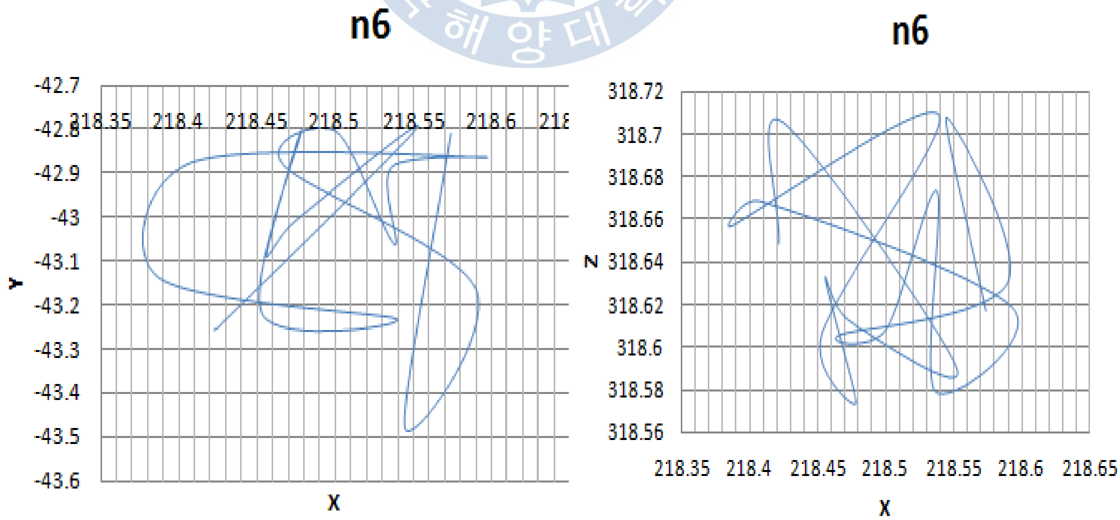

Figure 113: X-Y and X-Z trajectories of point n6.

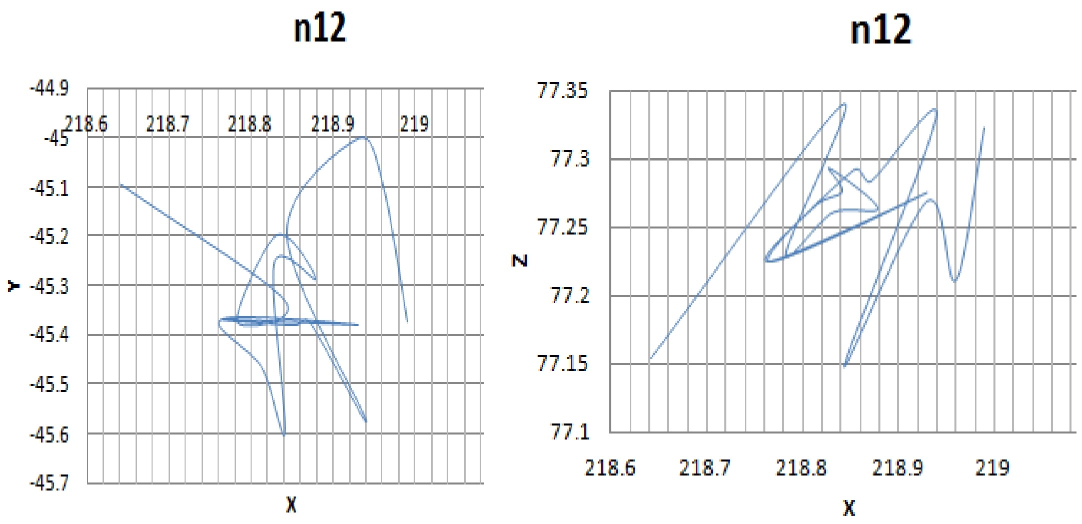

Figure 114: X-Y and X-Z trajectories of point n12.

5.37: Experimental results of behavior of Acryl Model under effect of Motion, Wave and Current. Experimental Conditions (Motion Period T=1.5s, Displacement 30cm, Wave Period T=1.5s, Wave height H =10cm, Current Velocity V=0.2m/s and *θ*=180°).

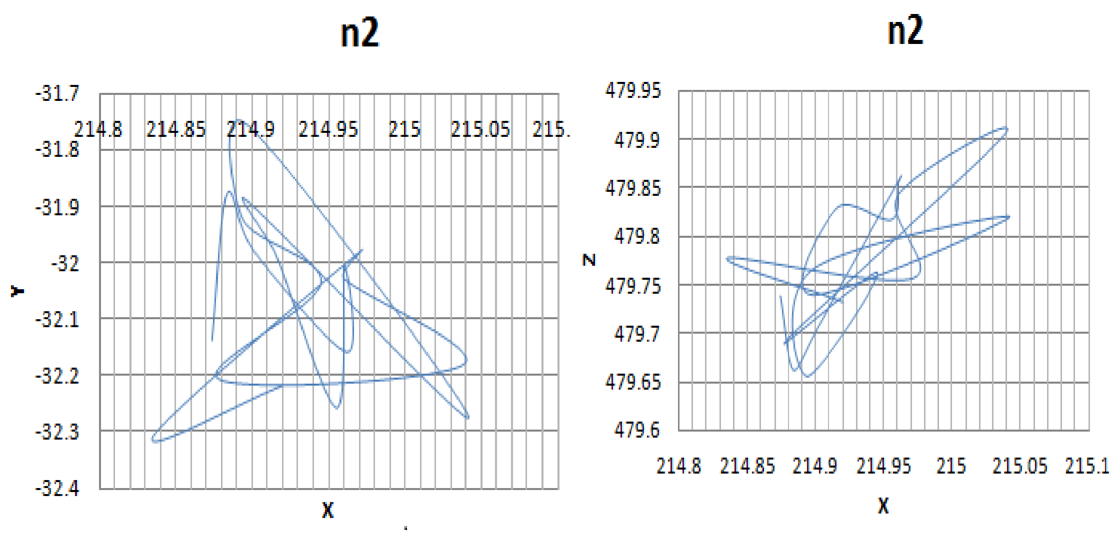

Figure 115: X-Y and X-Z trajectories of point n2.

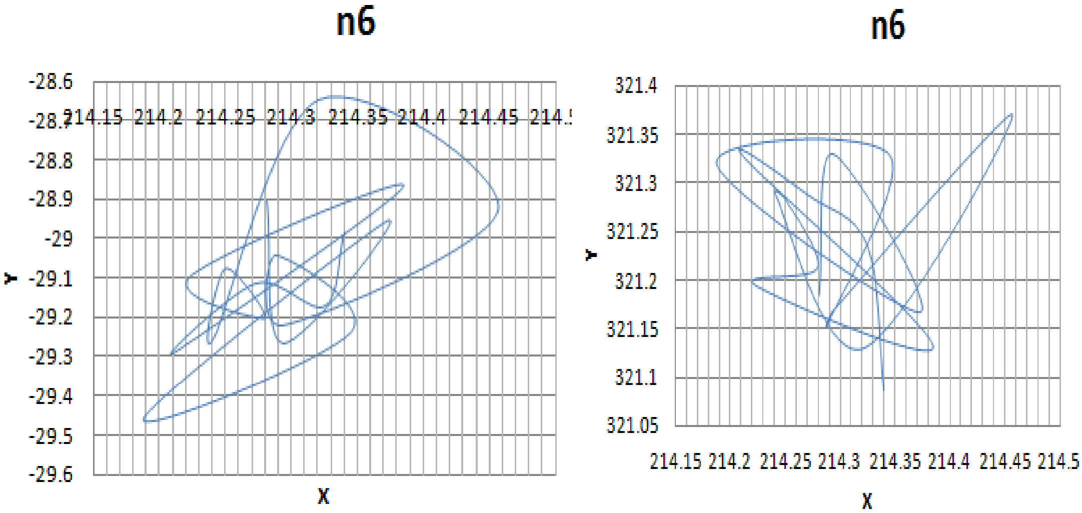

Figure 116: X-Y and X-Z trajectories of point n6.

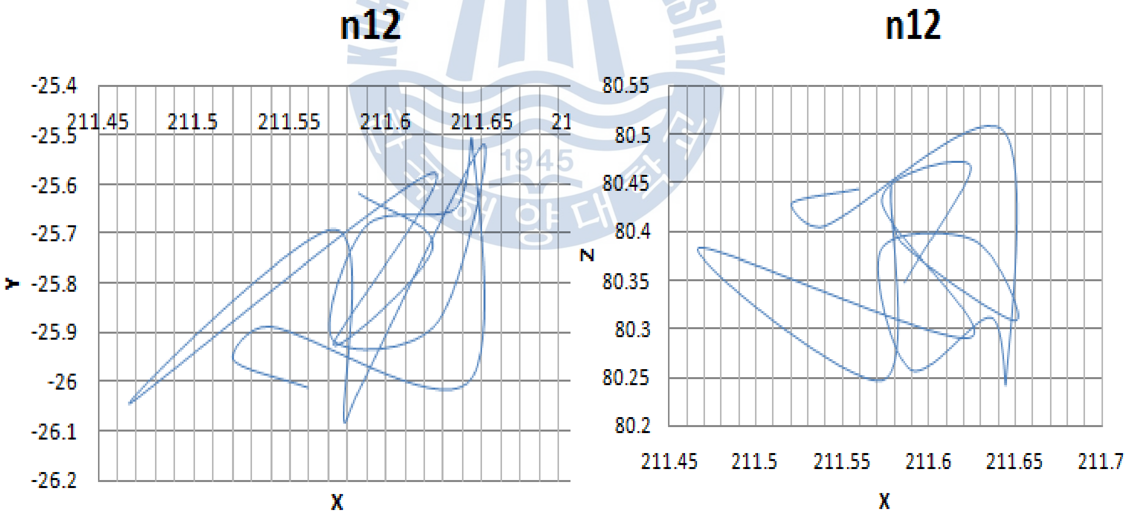

Figure 117: X-Y and X-Z trajectories of point n12.

Collection

5.38: Experimental results of behavior of Teflon Model under effect of Wave, Motion and Current. Experimental Conditions (Motion Period T=1.5s, Displacement 30cm, Wave Period T=1.5s, Wave Height H=10cm, Current Velocity V=0.2m/s and $\boldsymbol{\theta}$=180°).

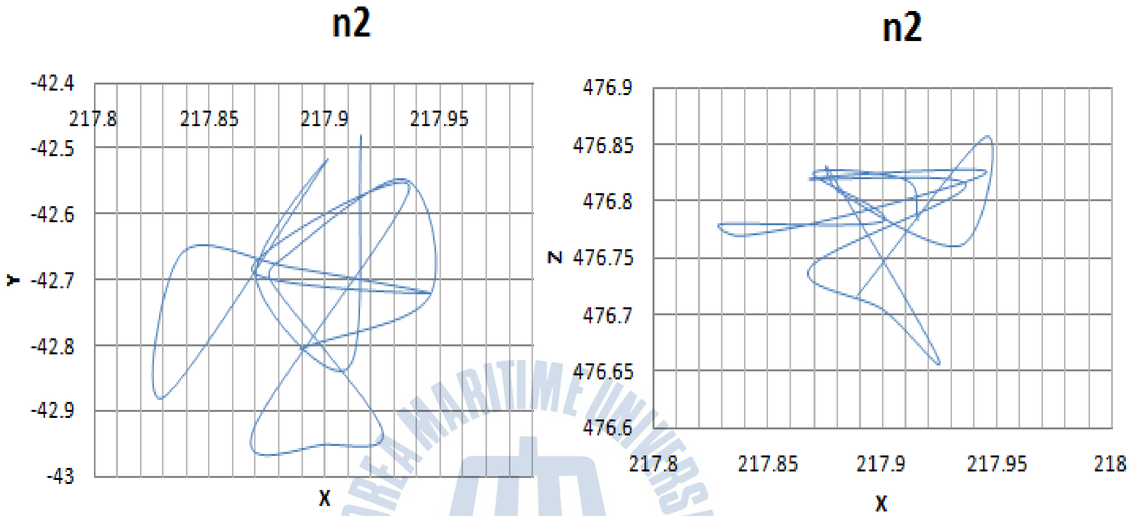

Figure 118: X-Y and X-Z trajectories of point n2.

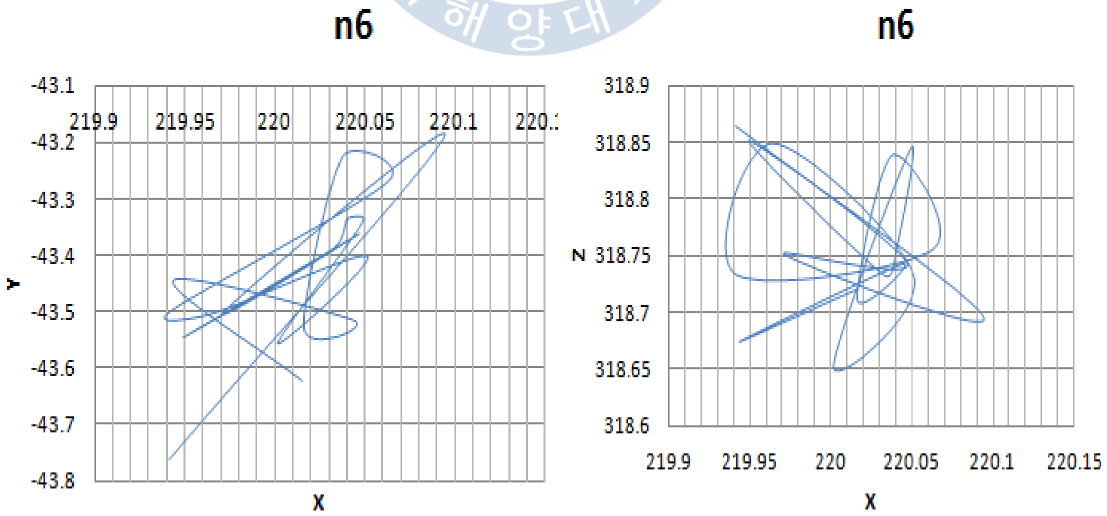

Figure 119: X-Y and X-Z trajectories of point n6.

Collection

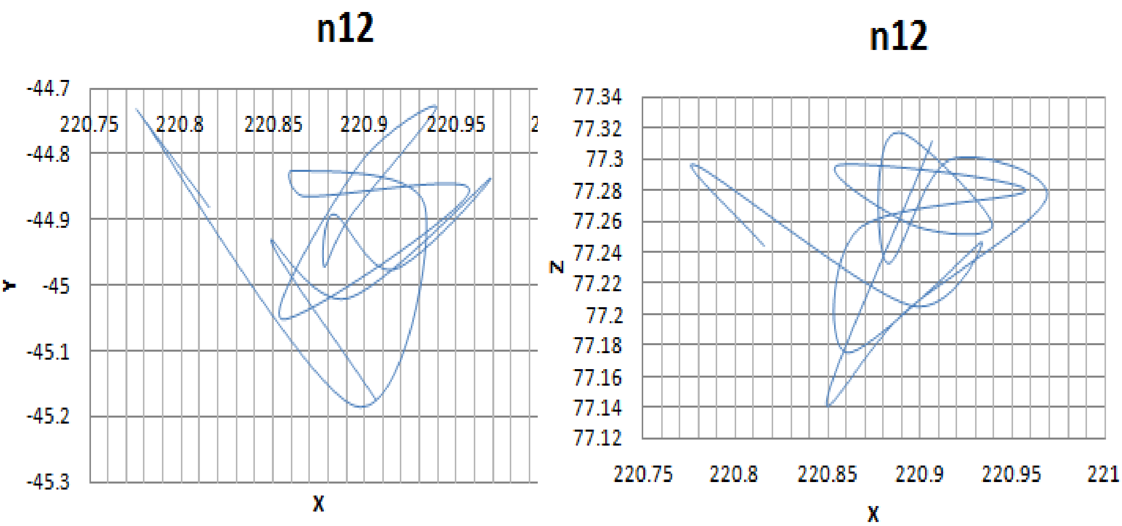

Figure 120: X-Y and X-Z trajectories of point n12.

5.39: Experimental results of behavior of Acryl Model under effect of Motion, Current and Wave. Experimental Conditions (Motion Period T=1.5s, Displacement 30cm, Wave Period T=1.5s, Wave Height H=10cm, Current Velocity V=0.2m/s and θ=360°).

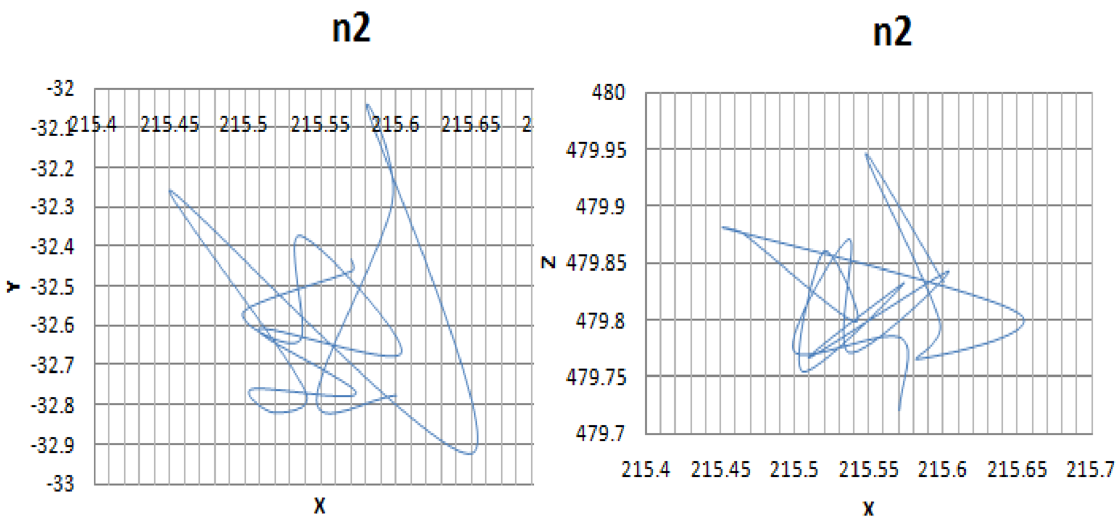

Figure 121: X-Y and X-Z trajectories of point n2.

Collection

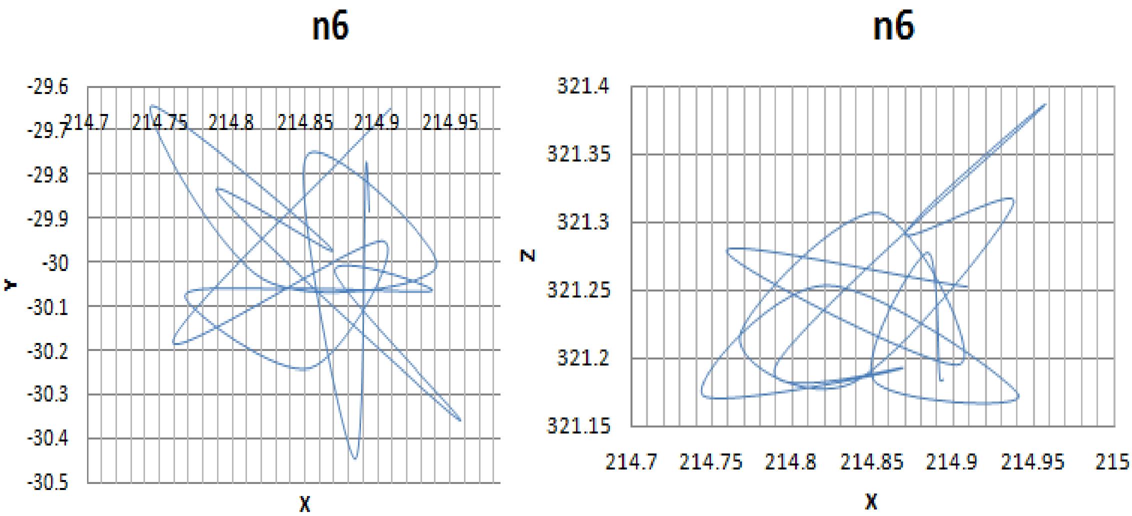

Figure122: X-Y and X-Z trajectories of point n6.

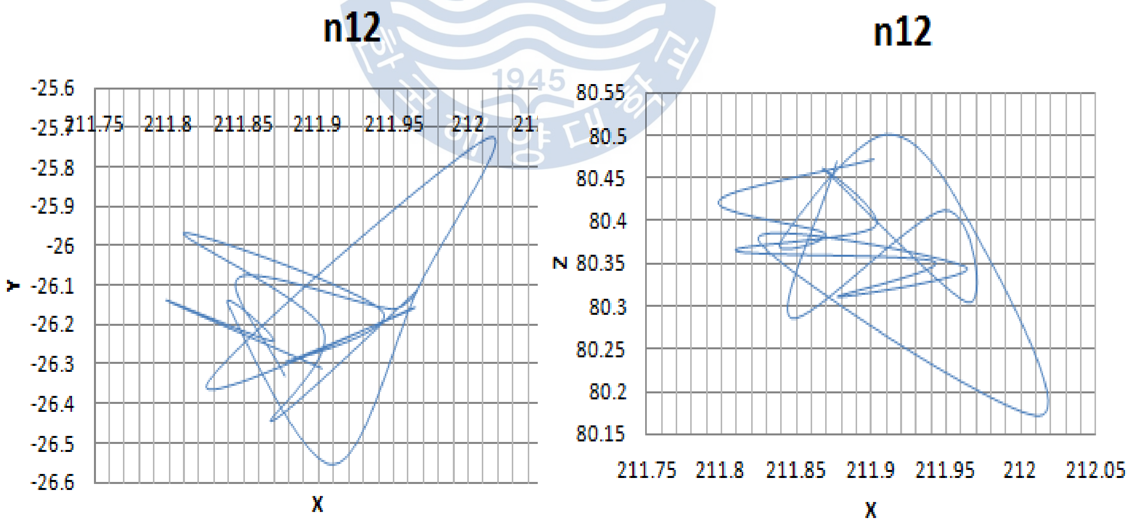

Figure 123: X-Y and X-Z trajectories of point n12.

5.40: EFFECTS OF WAVE HEIGHTS ON CROSS FLOW DISPLACEMENTS OF SLENDER CYLINDER.

From Table13 and Table 14 shown below, generally the magnitude of cross flow displacements depends on the magnitude of lift force, it is found that the cross flow displacements increases as the wave height increase, because the flow velocity increases as wave height increases as shown in equation (2.7) and magnitude of lift force depends on lift force coefficientC_L , square of flow velocity, length of a cylinder (l) and density of fluid (ρ). It is given by equation F_L=$\frac{1}{2}$ρ$C_L U^2$l. From Figure 124, the graph of cross flow displacement of Acryl model, the magnitude of cross flow at wave height H=10cm fluctuate very much at an interval between 0.1s and 0.15s, this is due to fact that shedding frequency can vary over a cycle of flow oscillations and resonance can be formed and broken over a cycle of single wave period.

Collection

Table 13: Inline and Cross flow displacements of Acryl model.

Displacements of Acryl model at wave height H=5cm,Period T=0.8s					Displacements of Acryl model at Wave height H=10cm,Period T=0.8s			
Time	n0(X)	n0(Y)	n1(X)	n1(Y)	n0(X)	n0(Y)	n1(X)	n1(Y)
0.016667	214.399	-33.3478	214.3761	-32.5146	214.3662	-33.5989	214.4105	-32.5173
0.033333	214.3844	-33.1943	214.3691	-32.5891	214.2676	-33.8424	214.4652	-32.4239
0.05	214.4507	-33.2429	214.3732	-32.5729	214.258	-33.8668	214.4485	-32.5771
0.066667	214.3802	-33.3575	214.3525	-32.5792	214.3065	-33.6771	214.4628	-32.6187
0.083333	214.3706	-33.3996	214.4053	-32.5488	214.3014	-33.7218	214.4447	-32.5229
0.1	214.3444	-33.3035	214.3691	-32.5891	214.4509	-33.487	214.442	-32.2723
0.116667	214.4063	-33.4692	214.3691	-32.5891	214.4216	-33.3614	214.4756	-32.4208
0.133333	214.4264	-33.2887	214.3691	-32.5891	214.3773	-33.5885	214.4288	-32.6204
0.15	214.3435	-33.4031	214.347	-32.5571	214.406	-33.42	214.4626	-32.5101

Table 14: Magnitude of cross flow displacement of Acryl model at Period T=0.8s and wave height H=5cm and H=10cm.

Time	n0(Y)-5cm	n0(Y)-10cm
0.016667	33.34776	33.598941
0.033333	33.19429	33.842423
0.05	33.24294	33.866765
0.066667	33.35752	33.677094
0.083333	33.39961	337211821
0.1	33.30354	33.487
0.116667	33.28868	33.361369
0.133333	33.28868	33.588518
0.15	33.40311	33.419962

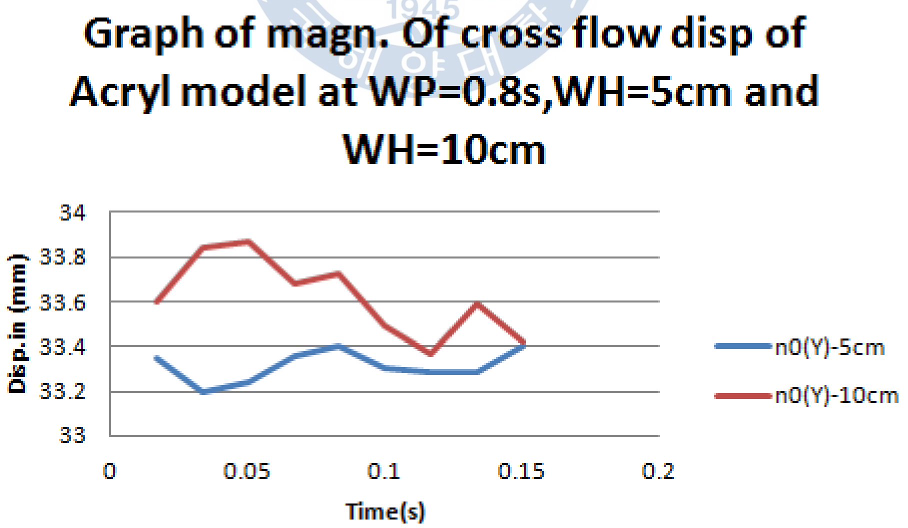

Figure 124: Magnitude of cross flow displacements of Acryl model at WP=0.8s, WH=5cm and WH=10cm.

Collection

6.0: Summary and Conclusions.

In this research the theoretical and experimental studies on the behavior of slender cylinder on both waves and currents are presented. The experimental studies performed using two flexible slender cylinder models (Acryl and Teflon models), the experiments showed various interesting results of cylinder motion. From the experimental results the following conclusions may be drawn:

(1) When slender cylinder oscillates in Vortex Induced Vibration mode, the magnitude of cross flow displacement is amplified, this is due to fact that the natural frequency of slender cylinder is locked in with exciting frequency of exciting source (shedding frequency).

(2) The hydrodynamic coefficients are not constant values, their value depends on Re, KC and β, all these three parameters depends on the flow conditions.

(3) From experimental studies it is found that the motion of a slender cylinder and behavior in both waves and currents are chaotic in nature.

(4) From experimental results it is found that as the mass ratio of the slender cylinder increases the magnitude of cross flow displacement increases, this is in agreement with observations made by (Blevins 1990)-As the mass ratio increases the potential of Vibrations increases.

(5) From experimental results it is found that when wave height increases the magnitude of cross flow displacement increases, this results can be easily seen in the analysis of Acryl model at wave

Collection

heights WH=5cm and WH=10cm. In WH=10cm the magnitude of cross flow displacement is higher than that of WH=5cm, this is due to fact that hydrodynamic forces increases as the flow velocity increases which depends entirely on wave height i.e. flow velocity increases as wave height increases.

Collection

ACKNOWLEDGEMENT

The work described in this thesis was performed at Korea Maritime University employing the facilities available within the department of Naval Architecture and Ocean System Engineering.

First and foremost, It is a pleasure to thank my supervisor Prof Hyo –Jae Jo whose broad knowledge and great effort s to explain everything clearly have been invaluable. It wouldn't possible to develop my ideas if it wasn't for his encouragement and I am grateful for his support. I would like also to thank Prof Seung Jae Lee and Prof Sohn of Korea Maritime University who has been very influential for me from the very beginning of my Master's degree Program and their insightful comments have made this research possible. Special thanks goes to my friends Hwang,Jae-Hyuk, Jiwon Park and Sung Hoon, Han who assisted me in my stay here, whenever I need help I turned to my friends, I was ever sure that they have a solution and they proved me right time and again. Thank you always. I would like to express my special thanks to my brother Mr John .S.Lendisa the CEO of Bishop Durning, Justine, Robert, Paul and Ferdinand all these people give moral support for my studies. Finally I would like to express my gratitude thanks to my wife Jema Lema and my daughter Lynchristine who always encouraged me in my studies and made everything much easier and possible to finish my research.

Collection

REFERENCES

Sarpkaya, T. and Isaacson M 1981. “Mechanics of Wave Forces on offshore structures” Van Nostrand Reinhold, New York.

Sarpkaya, T. and Storm, M1985. “In line force on a cylinder Translating oscillatory flow” Applied Ocean Research Vol 17, No4 pp188-196.

Sarpkaya T. 1985 “Forces on a circular cylinder in Viscous oscillating Flow at low Keulegan-Carpenter numbers. “Journal of Fluid Mechanics”, Vol 165 pp 61-71.

Buckingham, W.R 1982. “Forces on a cylinder due to waves and a collinear currents”, MAsc thesis British Columbia University.

Iwagaki Y and Ansano T 1984, “Hydrodynamic Forces on a circular cylinder placed in wave-current coexisting field, Memoirs of the Faculty of Engineering Kyoto University XLV pp 11-23.

Brian.R.Hughes 1988 “Inline force on a slender structure subjected to combined wave and currents, MAsc thesis British Columbia University.

B. Mutlu Sumer and Jorgen Fredsoe 2006. “Hydrodynamics around cylindrical structures” World Scientific.

Collection

S.K Chakrabati 2007 “Hydrodynamics of offshore structures, Springer Verlag.

Shin Da Rae 2012. “A study on behavior of slender bodies in waves, Msc thesis,Korea Maritime University

D.Jung, H.Lee, H.Kim and D.Moon, “Study of VIV in a riser under low Keulegan-Carpenter number” ISOPE June 17-22, 2012 pp 559-564.

M.Shafiee-far, W.W Massie and J.H Vugts “The Validity of Morison equation Extensions OTC 8064 pp331-340.

Robert.D.Blevins 1990 “Flow induced Vibrations”. Van Nostrand Reinhold.

Collection